Overexpression of DNA Polymerase Beta and its Effect on Genome Stability

A thesis submitted for the degree of Doctor of Philosophy

by

Katie Kin Ling CHAN

Biochemistry Group
Radiation and Genome Stability Unit
MRC Harwell

Department of Biochemistry
University of Oxford
&
Wolfson College, Oxford

August 2006

Supervisors: Dr Grigory L. Dianov (MRC Harwell)
Prof. David Sherratt (Oxford)

Acknowledgements

First and foremost I would like to thank the Medical Research Council (MRC) for funding my PhD studentship. I have really enjoyed my time at the Radiation and Genome Stability Unit (RAGSU), Harwell, and have developed so much, both academically and personally. I am grateful to my supervisor Dr Grigory Dianov for giving me this opportunity and thanks to his continued support and guidance I have come out of this experience smiling. It has been a pleasure to be part of the Biochemistry group and I would like to thank all members past and present. To my post-docs Sarah, Jason and Emma: thank you for your patience and valuable advice. You've all taught me so much and I really appreciate all your help. To Kate, Beth and Phill: it's been great sharing this experience with you, the highs and the lows, and I'll really miss our tea breaks. Last but definitely not least, I would like to say a special thank you to Irina for always being there to cheer me up.

A big heartfelt thank you goes to my family and friends (you know who you are!) who have supported and encouraged me throughout my PhD, with a special mention to my dear brother Andrew for his (many!) pearls of wisdom. You have all kept me sane and without you none of this would have been possible.

Finally, I'd like to thank Prof. Ian Hickson for providing the cell lines, Prof. David Sherratt my Oxford supervisor for insightful discussions and Wolfson College.

Overexpression of DNA Polymerase beta and its Effect on Genome Stability

Katie Kin Ling Chan
Wolfson College, Oxford

Submitted for the degree of Doctor of Philosophy
Trinity Term, 2006

Abstract

DNA polymerases play key roles in DNA synthesis by catalysing the polymerisation of deoxynucleotides opposite a parental (template) DNA strand to generate a new or repaired complementary daughter strand. Faithful replication by DNA polymerases is essential in maintaining genome integrity during cell division, DNA repair and DNA recombination. DNA polymerase beta (Pol β) plays a pivotal role in the base excision repair (BER) pathway by performing repair synthesis to fill single nucleotide gaps which arise during DNA repair. However, overexpression of Pol β is found in many human cancers and has been shown to promote a mutator phenotype. The aim of this study was therefore to investigate the effect of Pol β overexpression on BER. *In vitro* repair assays using whole cell extracts and DNA substrates containing site-specific BER lesions were conducted to compare two cell lines, one of which was derived from a cancer patient overexpressing Pol β. I found that overexpression of Pol β results in a 5 to 10-fold increased frequency of one nucleotide frameshift mutations and based on biochemical studies a mechanism is proposed to explain this phenomenon. I therefore conclude that an excess of Pol β can have potentially mutagenic consequences.

Table of Contents

List of Figures

Chapter V

List of Tables

Abbreviations

3-meA	3-methyladenine
7-meG	7-methylguanine
8-oxoG	8-oxoguanine; 7,8-dihydro-8-oxoguanine
(6-4)PP	(6-4) pyrimidine-pyrimidone photoproducts
A	adenine
AAG	alkylpurine-DNA-*N*-glycosylase
APE1	AP endonuclease 1
APE2	AP endonuclease 2
AP sites	apurinic/apyrimidinic sites; abasic sites
ATF/CRE	activating transcription factor/cAMP response element.
ATM	ataxia telangiectasia mutated
ATP	adenosine triphosphate
ATR	Rad 3-related protein
BER	base excision repair
bp	base pair
BSA	bovine serum albumin
C	cytosine
cAMP	cyclic adenosine monophosphate
CHO	Chinese hamster ovary
CPD	cyclobutane pyrimidine dimers
CREB	cAMP response element binding
C_t	cycle threshold
CTP	cytosine triphosphate
DEPC	diethylpyrocarbonate

DMSO	dimethyl sulfoxide
DNA	deoxyribonucleic acid
dNTP	deoxynucleotide triphosphate
ddNTP	dideoxynucleotide triphosphate
dRP	deoxyribosephosphate residue
dRPase	DNA deoxyribosephosphatase
DSB	double-strand breaks
DTT	dithiothreitol
EDTA	ethylene diamine tetra-acetic acid
EMS	ethyl methanesulphonate
Fe^{2+}	Iron
FEN1	flap endonuclease 1
fmol	femto mole
g	gram
G	guanine
GTP	guanosine triphosphate
HR	homologous recombination
h	human
MYH	MutY homolog
IPTG	isopropyl-β-D-thiogalactopyranoside
IR	ionising radiation
kb	kilo base
kDa	kilo Dalton
L	litre
LB	Luria-Bertani Media

M	molar
mL	millilitre
mM	millimolar
Mg^{2+}	magnesium
MGMT	O^6-methylguanine-DNA methyltransferase
MMR	mismatch repair
MMS	methyl methanesulphonate
mRNA	messenger RNA
NAD^+	nicotinamide adenine dinucleotide (oxidised form)
NEIL1	Endonuclease VIII (Nei)-like DNA glycosylase 1
NER	nucleotide excision repair
ng	nanogram
NHEJ	non-homologous end joining
nM	nanomolar
nt	nucleotide
OD	optical density
OGG1	7,8-dihydro-8-oxoguanine-DNA glycosylase
OH	hydroxyl
PARP-1	poly(ADP-ribose) polymerase 1
PBS	phosphate-buffered saline
PCNA	proliferating cell nuclear antigen
PCR	polymerase chain reaction
PCV	packed cell volume
Pol β	DNA polymerase β
Pol δ	DNA polymerase δ

Pol ε	DNA polymerase ε
pmol	picomole
PMSF	phenyl methyl sulphonyl fluoride
PNK	polynucleotide kinase
PVDF	polyvinylidene fluoride
RFC	replication factor C
rh	recombinant human
RNA	ribonucleic acid
RPA	replication protein A
ROS	reactive oxygen species
rpm	revolutions per minute
SAM	S-adenosylmethionine
SDS	sodium dodecylsulphate
SDS-PAGE	SDS-polyacrylamide gel electrophoresis
SSB	single-strand break
SSBR	single strand break repair
T	thymine
TAE	tris-acetate EDTA
TBE	tris-borate EDTA
Tg	5,6-dihydroxy-5,6-dihydrothymine (thymine glycol)
T_m	melting temperature
tRNA	transfer RNA
TTP	thymidine triphosphate
U	uracil
UDG	uracil-DNA glycosylase

UTP	uridine 5'-triphosphate
UV	ultraviolet
WCE	whole cell extract
XRCC1	X-ray cross complementing protein 1
μCi	microcurie
μg	microgram
μL	microlitre

Chapter I

Introduction

1.1 THE HUMAN GENOME

A genome describes an organism's complete set of deoxyribonucleic acid (DNA) which contains the information required to construct and maintain life. DNA is made of four structurally similar nucleotide units each comprising; a pentose sugar, a phosphate group and a base (adenine (A), guanine (G), cytosine (C) or thymine (T)) which are linked together by phosphodiester bonds to form long polynucleotide chains. DNA is double-stranded and helical in structure, formed by two anti-parallel polynucleotide chains held together via hydrogen bonds between bases on opposing strands (Watson and Crick 1953). The bases are always paired purine with a pyrimidine, thus A:T via two hydrogen bonds and G:C via three hydrogen bonds. Each human cell, with the exception of mature red blood cells, contains a complete genome of approximately 3 billion base pairs which are arranged into 23 pairs of distinct chromosomes. About 2% of the genome is specifically ordered into genes which encodes for proteins, whilst the remainder is non-coding. The human genome is estimated to contain 20,000 to 25,000 genes.

1.2 DNA DAMAGE

DNA is an inherently unstable molecule and is susceptible to degradation by a range of endogenous and exogenous factors (Lindahl 1993). For example, the aqueous environment of the cell can spontaneously hydrolyse the labile N-glycosidic bond of purines at a rate of approximately 10,000 per human genome per day (Lindahl and Andersson 1972), resulting in abasic (AP) sites. AP sites are highly cytotoxic and potentially lethal as they are non-coding and if left unrepaired, may generate single-strand breaks subsequently resulting in mutations or cell death (Loeb and Preston 1986; Guillet and Boiteux 2002). Hydrolytic deamination of cytosine, 5-methylcytosine,

adenine and guanine to uracil [Fig. 1.1], thymine, hypoxanthine and xanthine respectively may also introduce errors into the genome by altering coding properties, for example uracil can mispair with adenine leading to a C:G → T:A transition. Cellular metabolites such as reactive oxygen species (ROS) and lipid peroxidation products also pose a threat to genome integrity. The most commonly formed ROS are hydrogen peroxide (H_2O_2), singlet oxygen ($^1O_2$), and hydroxyl radicals (·OH), which cause pro-mutagenic DNA lesions such as 8-oxoguanine (8-oxoG) and thymine glycol (Tg) [Fig. 1.1]. 8-oxoG greatly increases the frequency of spontaneous G:C to T:A transversion mutations as it can base pair with A as well as C residues. Besides the generation of 8-oxoG lesions in DNA *in situ*, they are also generated in the deoxynucleotide pool, from which they could be incorporated into the nascent DNA strand during replication (Cheng et al. 1992). Current estimates of steady-state 8-oxoG levels are between 100 to 1000 residues in normal cells per day (Ames et al. 1993; Collins 1999; Klungland et al. 1999). Byproducts of lipid peroxidation can act as alkylating agents and generate exocyclic etheno modifications of DNA bases, such as etheno-A and etheno-C (Lindahl and Wood 1999). But the most widely studied source of endogenous DNA alkylation is S-adenosylmethionine (SAM). SAM is an efficient methyl group donor and is a co-factor in most transmethylation reactions. However, the high transfer potential of SAM also means that it spontaneously methylates DNA generating 7-methylguanine (7-meG) and 3-methyladenine (3-meA) at a low but significant rate (Rydberg and Lindahl 1982).

Other major environmental sources of DNA damage include ultraviolet (UV) light, ionising radiation and chemical mutagens, such as cigarette smoke. UV light induces bulky DNA adducts such as cyclobutane pyrimidine dimers and 6-4 photoproducts (Friedberg 1995) which distort the DNA helix. Ionising radiation (IR) can generate ROS, particularly hydroxyl radicals that attack DNA, but more importantly

can directly damage DNA creating single- or double-strand breaks. Direct DNA damage can produce a variety of DNA ends, and of particular importance are 3'-end blocking groups such as 3'-phosphate or 3'-phosphoglycolate, which must be 'cleaned up' before repair can occur. Random energy deposition by IR can often produce clustered DNA damages where two or more lesions of the same or different nature are produced within one or two helical turns of the DNA. Simultaneous repair of lesions located on opposite DNA strands may generate double-strand breaks and enhance genome instability (Dianov et al. 2001). Double-strand breaks can lead to loss of information because the correct DNA ends must be matched up and repaired through recombinational processes. It has been estimated using radical scavengers that 60% of cellular DNA damage produced by IR is caused by indirect effects (Ward 1988). To date, a range of chemical mutagens have been developed to target faster growing cancer cells, for example the bi-functional cross-linking agent cisplatin which creates intrastrand crosslinks in DNA (Friedberg 1995).

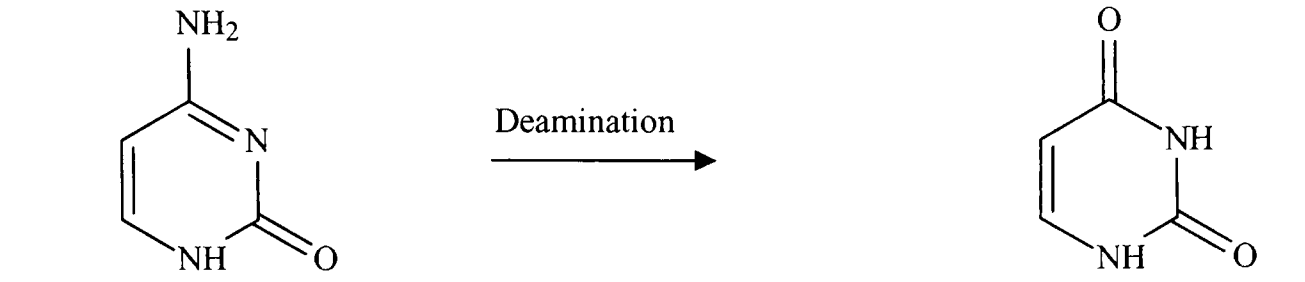

Cytosine

Uracil

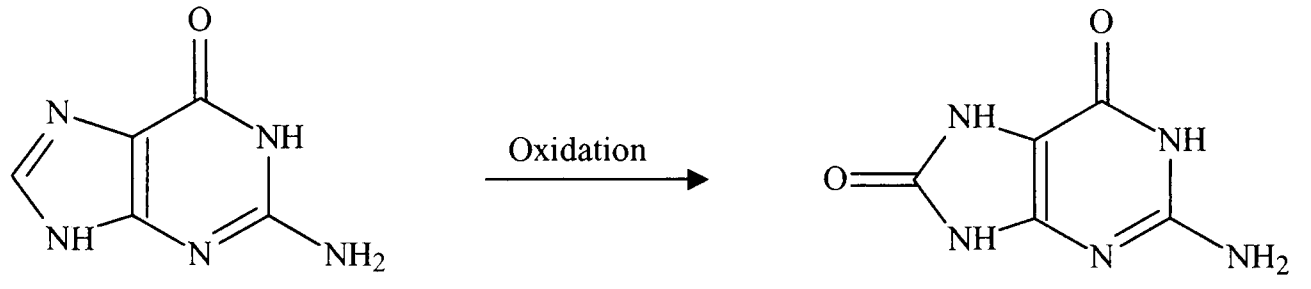

Guanine

8-oxoguanine

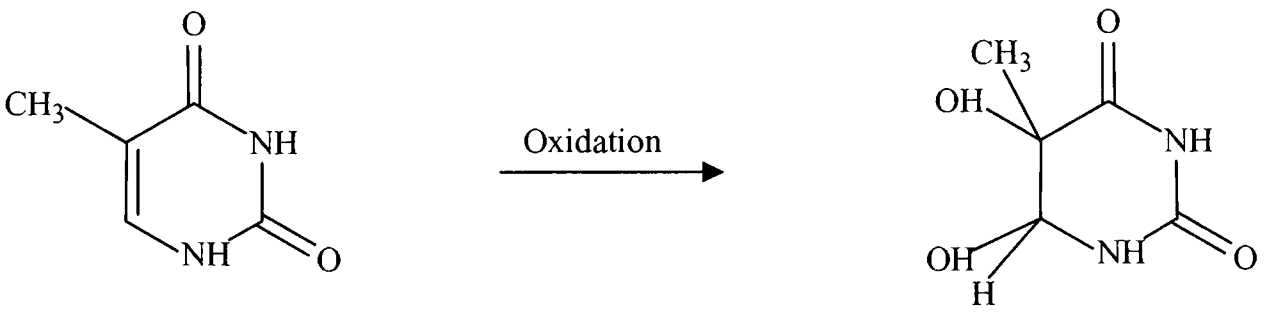

Thymine

Thymine glycol

Figure 1.1 Common BER lesions. Uracil can mispair with adenine leading to a C:G → T:A transition. 8-oxoguanine (8-oxoG) can mispair with adenine resulting in a G:C → T:A transversion. Thymine glycol (Tg) can also arise from oxidative deamination of 5-methyl cytosine and is then present as a Tg:G mispair.

1.3 DNA REPAIR

Faithful maintenance of the genome is crucial and DNA damage will ultimately have mutagenic consequences if left unrepaired. Not surprisingly, a variety of DNA repair mechanisms have evolved to handle different types of damage, which all vary in the enzymes and pathways utilised. In mammals, the majority of DNA repair is covered by two basic mechanisms: excision and recombination.

1.3.1 Excision repair pathways

'Cut and patch'-type excision pathways are used when only one DNA strand is affected, allowing the intact strand to be used as a template for gap-filling repair synthesis. Several common steps are involved in excision repair: recognition of the DNA damage, DNA incision, damage removal, nucleotide replacement and ligation of nicked DNA. The type of repair pathway employed is usually dictated by the type of damage. Small, non-bulky lesions are removed by base excision repair (BER) [Fig. 1.2], whereas nucleotide excision repair (NER) removes larger, bulky DNA adducts and DNA crosslinks that distort the DNA helix and subsequently block DNA synthesis. Less distortive lesions such as methylated bases can also be removed by NER. The mismatch repair (MMR) pathway is responsible for correcting errors generated during DNA replication such as base substitution mismatches and insertion-deletion mismatches. Direct single-strand breaks often require end-processing before repair is completed by gap filling and ligation, however indirect single-strand breaks also occur as intermediates during the excision step of BER, hence many of the BER enzymes are also involved in the single-strand break repair (SSBR) pathway.

1.3.2 Recombinational repair pathways

Recombinational pathways such as non-homologous end joining (NHEJ) or the homologous recombination (HR) pathway are primarily responsible for the repair of

double-strand breaks (DSB) and the efficiency and fidelity of each repair pathway differs. NHEJ is a fast repair pathway however it can delete DNA during the direct joining of broken DNA ends and mutations can frequently occur, whereas HR uses the homologous sister chromatid to ensure mostly error-free repair but HR is a slow repair pathway. Mammals primarily use NHEJ to repair DSB even though it is more error-prone. Through evolution mammalian genomes have accumulated a large proportion of non-coding 'junk' DNA, thus can afford to use a lower fidelity repair mechanism to keep the overall genome intact because the chances of encountering coding DNA is relatively low. Conversely, yeast have smaller genomes of which a higher proportion is comprised of essential coding DNA, therefore the high fidelity HR repair pathway is favoured to repair DSB in order to maintain the genome.

Double-strand breaks are recognised by a large number of nuclear proteins which initially bind to protect the lesion, and then signal the presence of the damage to the cell to initiate repair. In mammalian cells some of these proteins include the telomeric protein TRF2, the DNA-dependent protein kinase (DNA-PK), and its DNA binding Ku subunits, the three component exonuclease Mre11/RAD50/Nbs1 (MRN), ATM and ATR protein kinases, the DNA ligase IV-XRCC4 heterodimer, and the homologous recombination factor RAD52 (Baumann and West 1998; Critchlow and Jackson 1998; Bradshaw et al. 2005).

Although in higher mammalians NHEJ is the major pathway for DSB repair, HR is also used particularly in the late S and G2 phase of the cell cycle when a sister chromatid is present. The choice of which repair pathway is used is largely determined by the cell cycle stage but may also apparently be influenced by the relative amounts of Ku and RAD52 (Van Dyck et al. 1999).

1.3.2.1 Non-homologous end joining

NHEJ is the primary pathway for the repair of DSB in mammals and although it is a fast mechanism, NHEJ may result in the loss or change of genetic information. During the early stages of DSB recognition, the MRN complex localises to the site and cleans the DSB ends via its exonuclease and endonuclease activity (D'Amours and Jackson 2002). NHEJ is initiated by the binding of the Ku70-Ku80 heterodimers to the free DNA end, which then recruits the DNA-PK catalytic subunit (DNA-PKcs) to form the DNA-PK complex. DNA-PK catalyses the joining of the two DNA ends, which are trimmed by the nuclease Artemis before subsequent ligation by the DNA ligase IV-XRCC4 heterodimer (Helleday 2003).

1.3.2.2 Homologous recombination

HR utililses homologous DNA sequences so is accurate, however it is a slow DSB repair pathway. The initial step in HR is 5' to 3' resectioning of the 5' DNA end to produce a 3'-OH single-stranded DNA overhang. Various activities are required to perform this resectioning, and the exonuclease activity of the MRN complex is also thought to be involved (D'Amours and Jackson 2002). Prior to strand invasion, RPA molecules that protect the single-stranded ends are displaced by RAD51 (homologue of RecA in *E. coli*). RAD51 plays a key role in searching for homologous sequences, strand pairing and strand exchange usually with the sister chromatid during late S or G2 phase of the cell cycle. DNA synthesis is initiated at the 3' end by DNA Pol δ and a Holliday junction is formed at the site of invasion, which may branch migrate in either direction. Resolution of the Holliday junctions in mammalian cells generally yield 'non-crossover' gene conversion products, however, 'crossover' resolution of Holliday junctions are also possible. This is a simplified explanation of HR and it should be

noted that other proteins are also involved, see review by (Helleday 2003) for more details.

1.3.3 Direct damage reversal mechanisms

Direct damage reversal is the simplest method of repairing base damages. In contrast to the multi-step repair pathways mentioned above which involve multiple enzymes, direct reversal mechanisms are single-step reactions involving a single enzyme that can restore the damaged base back to its native state. However, direct damage reversal mechanisms are limited to the correction of DNA damaged by UV radiation and alkylating agents.

1.3.3.1 Reversal of UV radiation damaged bases

The most commonly formed lesions resulting from UV radiation at wavelengths (~260 nm) near the absorption maximum of DNA are cyclobutane pyrimidine dimers (CPD) and (6-4) pyrimidine-pyrimidone photoproducts ((6-4)PP). Interestingly, UV radiation is also required by DNA photolyase enzymes that can reverse these base damages by a process known as 'enzymatic photoreactivation'. CPD and (6-4)PP lesions are reversed by pyrimidine dimer-DNA photolyase and (6-4)PP-DNA photolyase respectively. Both types of DNA photolyases are structurally similar and the monomerisation of photodimers is mediated via two non-covalently bound chromophores that absorb light at a specific wavelength (>300 nm). One of these chromophores is a compound called flavin adenine dinucleotide (FAD), and the second non-essential chromophore can be a compound called 5,10-methenyltetrahydrofolyl polyglutamate (MTHF) or 8-hydroxy-5-deazaflavin (8-HDF). Thus, DNA photolyases can be further sub-divided into folate-type photolyases or deazaflavin-type photolyases respectively. Pyrimidine dimer-DNA photolyases are widely distributed across species however they are not found in placental mammals, and although a human (6-4)PP-DNA

photolyase orthologue has been found, it is non-functional against CPD or (6-4)PP reversal. DNA photolyases are important for the repair of UV lesions in plants and bacteria.

1.3.3.2 Reversal of alkylation damaged bases

Alkylation of guanine can yield O^6-methylguanine which can pair with both C and T, causing transition mutations. In humans, a specific repair protein encoded by the O^6-methylguanine-DNA methyltransferase (MGMT) gene removes the methyl group from G and transfers it to one of its own cysteine residues. However, the new methylated MGMT protein product is chemically very stable and is degraded by the ubiquitin pathway rather than being demethylated and re-used [reviewed by (Mishina et al. 2006)], and thus results in a suicidal mechanism of direct damage reversal. Recently though, two human DNA dioxygenase proteins called ABH2 and ABH3 were identified which can correct 1-methyladenine (1-meA) and 3-methylcytosine (3-meC) in DNA in a non-suicidal manner (Duncan et al. 2002; Aas et al. 2003). ABH2 and ABH3 are human homologues of bacterial AlkB protein which requires Fe^{2+} as a co-factor and 2-oxoglutarate (2OG; α-ketoglutarate) as a co-substrate (Aravind and Koonin 2001). The reaction proceeds by oxidative demethylation, whereby the methyl group bound to the nitrogenous base is hydroxylated by an oxy-ferryl intermediate. The reactive product decomposes and is then released as formaldehyde and the unmodified base is regenerated. Oxygen is consumed in this reaction, and the co-substrate 2OG is converted to succinate and CO_2 (Sedgwick 2004). ABH2 and ABH3 can act on 1-meA and 3-meA in double-stranded DNA, single-stranded DNA and RNA thus implicating a possible role for these DNA dioxygenases in RNA as well as DNA repair (Aas et al. 2003). The two direct alkylation damage reversal mechanisms described can only correct methylated bases which represent a subset of DNA base damage, moreover the

MGMT direct reversal mechanism is wasteful, and thus this may explain the evolution of DNA repair pathways which can repair a multitude of different DNA damage. This study will mainly focus on BER.

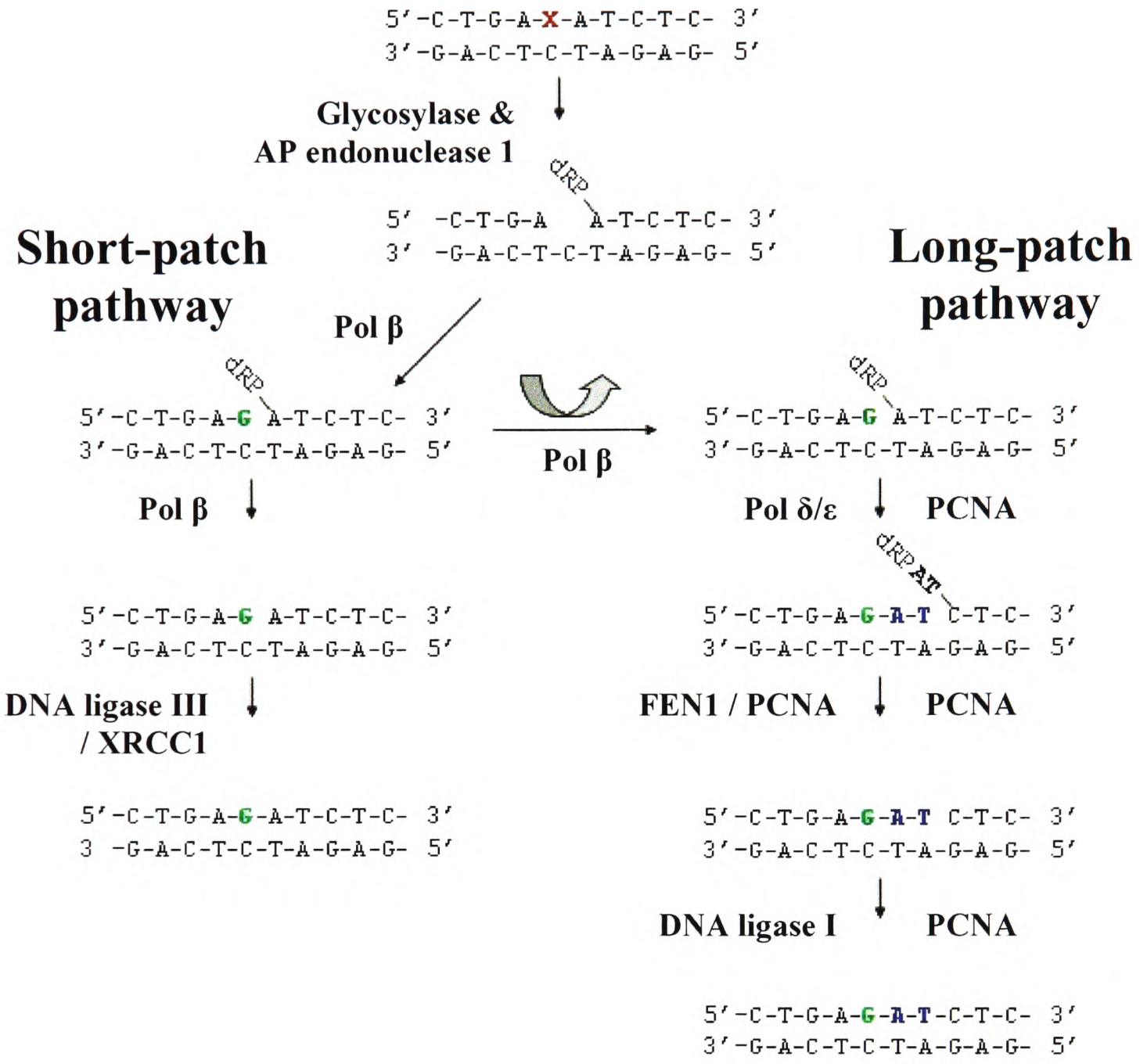

Figure 1.2 Current model of mammalian BER pathways. The damaged base (shown as X) is recognised and removed by a DNA glycosylase followed by APE1 incision, which generates a strand break 5' to the AP site. Pol β then adds one nucleotide to the 3' end of the nick and from this point Pol β plays a central role in determining the subpathway choice. Removal of the 5'-sugar phosphate by dRP lyase activity of Pol β directs BER to the short-patch repair pathway (removal and replacement of 1 nt). Alternatively, Pol δ/ε adds a few more nucleotides to the 3' end and generates a flap containing the 5'-sugar phosphate. This switches repair to the long-patch BER subpathway where the flap is removed by FEN1. In the short-patch pathway, DNA ligase III-XRCC1 completes DNA repair by sealing the strand break. In the long-patch pathway, PCNA serves as a processivity factor for Pol δ. PCNA also interacts with FEN1 and DNA ligase I and may stimulate both flap incision and ligation.

1.4 BASE EXCISION REPAIR (BER)

BER is the major repair pathway involved in the removal of oxidative base lesions or repair at sites of base loss. These small base damages do not necessarily block DNA synthesis or replication, but can however slow down replication or introduce mutations. The BER pathway has been highly conserved throughout evolution from bacteria to higher organisms, testimony to its importance for maintaining genome integrity (Lindahl and Wood 1999). Indeed, mouse knockout models of key BER enzymes proved to be embryonic lethal, further highlighting the importance of BER (Gu et al. 1994; Xanthoudakis et al. 1996; Tebbs et al. 1999; Puebla-Osorio et al. 2006).

Base excision repair (BER) is a highly co-ordinated multiprotein pathway [Fig 1.2] that is initiated by damage-specific DNA glycosylases which recognises and removes the damaged base by cleavage of the N-glycosidic bond leaving an AP site [Fig. 1.3]. Next AP endonuclease 1 (APE1) incises the DNA phosphodiester backbone 5' to the AP site, leaving a 3'-hydroxyl (OH) group and a 5'-deoxyribose phosphate (dRP) group flanking the nucleotide (nt) gap (Demple and Harrison 1994; Barzilay and Hickson 1995). Further repair can proceed via two sub-pathways that utilise different subsets of enzymes: (i) short-patch BER which involves replacement of 1-nt or (ii) long-patch BER which involves replacement of 2 to 6-nt (Klungland and Lindahl 1997). The majority of BER is accomplished through short-patch BER pathway, and both sub-pathways are initiated by DNA polymerase β (Pol β), the major BER DNA polymerase, which adds the first nucleotide into the repair gap (Podlutsky et al. 2001).

1.4.1 Short-patch BER

During short-patch BER Pol β adds 1-nt into the repair gap and simultaneously removes the 5'-dRP moiety by its intrinsic dRP lyase activity via a β-elimination

reaction (Matsumoto and Kim 1995) [Fig. 1.2]. Finally, the nick containing 3'-hydroxyl and 5'-phosphate ends are sealed by DNA ligase IIIα-XRCC1 heterodimer (Dianov et al. 2003).

1.4.2 Long-patch BER

Modification of AP sites either by oxidation (Nakamura et al. 2000) or reduction (Podlutsky et al. 2001) prevents β-elimination by Pol β, and repair must occur through the long-patch or 'PCNA-dependent BER' mechanism (Podlutsky et al. 2001). At this point, Pol β is replaced by Pol δ/ε which extends the repair patch and displaces several nucleotides to create a 5'-flap junction (Fortini et al. 1998). Flap endonuclease 1 (FEN1) cleaves the flap at the single-strand/double-strand DNA junction and the DNA ends are then sealed by DNA ligase I. All these reactions have been found to be stimulated by proliferating cell nuclear antigen (PCNA) (Klungland and Lindahl 1997).

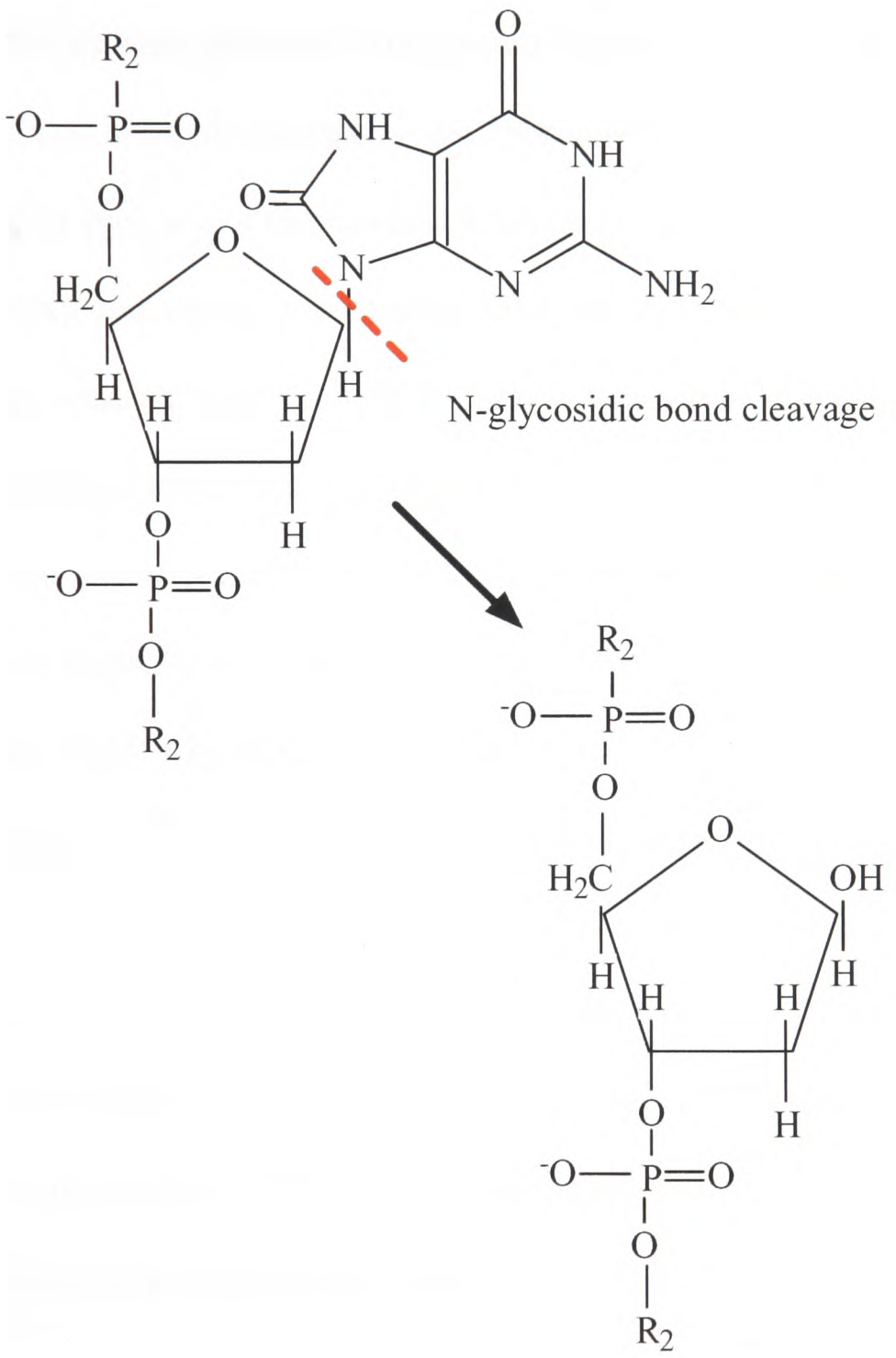

Figure 1.3 Formation of an abasic site. Structure of a nucleotide chain showing hydrolysis of the N-glycosidic bond linking the base to the sugar-phosphate backbone. In this example 8-oxoG is depicted and hydrolysis can occur spontaneously or through the action of OGG1 DNA glycosylase.

1.5 BER ENZYMES AND THEIR CO-ORDINATION

As previously mentioned, BER is a highly co-ordinated pathway involving multiple proteins. Paradoxically certain repair intermediates can be more cytotoxic to cells than the original base damage itself (Simonelli et al. 2005). Whereas base damage can be bypassed and repaired later by NER or SSBR, AP site intermediates are non-coding and APE1 incision generates single-strand breaks. The prolonged existence of repair intermediates is highly mutagenic and hence proteins within the BER pathway are co-ordinated in such a way to minimise these occurrences. This control is achieved through a 'passing the baton' mechanism (Wilson and Kunkel 2000), whereby the product-enzyme complex after each BER step is recognised and passed to the next enzyme in the pathway until repair has been achieved. Additionally, it is important that the levels of BER proteins are co-ordinated to prevent a bottle-neck effect where the pathway becomes stalled at one step.

1.5.1 Initiation of BER by DNA glycosylases

The majority of DNA base lesions are recognised and removed by DNA glycosylases. Presently, there are ten known DNA glycosylases with overlapping functions that can initiate BER [Table 1.1] (Wood et al. 2005). DNA glycosylases are relatively small monomeric proteins and the first DNA glycosylase to be discovered was uracil-DNA glycosylase (UDG) from *E. coli* (Lindahl 1974). UDG removes uracil lesions from DNA and is highly conserved between different species, such as bacteria, yeast, mouse, humans and several herpes viruses [reviewed by (Krokan et al. 1997). Extensive structural and functional studies of UDG revealed that uracil is specifically recognised and removed from DNA using a 'nucleotide-flipping mechanism' (Slupphaug et al. 1996); and further studies have established that this is a general strategy used by DNA glycosylases and other enzymes to gain better access to

nucleotides in DNA [reviewed by (Scharer and Jiricny 2001)]. DNA fits along a positively charged groove in the DNA glycosylase enzyme which can then scan along the DNA until the specific lesion is recognised by minor groove reading motifs. Nucleotide flipping is initiated through minor groove contacts and one or several amino acids are inserted into the DNA helix to occupy the place vacated by the flipped out nucleotide. Specific contacts between the enzyme and the sugar phosphate backbone adjacent to the lesion promotes DNA compression and enables the target nucleotide to be rotated by nearly 180° from its normal position into the active site cleft of the DNA glycosylase where the aberrant base is removed.

There are two mechanistic classes of DNA glycosylases: mono-functional (glycosylase activity only) such as UDG, and bi-functional (glycosylase/β-lyase activities) such as human 7,8-dihydro-8-oxoguanine-DNA glycosylase (hOGG1). Mono-functional DNA glycosylases create AP sites through cleavage of the C1'-N-glycosidic bond using an activated water molecule as an active site nucleophile (McCullough et al. 1999). Additionally, bi-functional glycosylases have an associated AP lyase activity which can further process the AP site by incising the DNA backbone 3' to the AP site. An amino group on the enzyme forms a transient Schiff base intermediate, and subsequently catalyses a β-elimination reaction which cleaves the DNA phosphodiester bond generating 3' α, β-unsaturated aldehyde and 5' phosphate products (McCullough et al. 1999).

Glycosylase	Substrates	Mechanism
UDG	U	Mono-functional
SMUG1	U, 5-OHU	Mono-functional
TDG	U:G, T:G or ethenoC:G	Mono-functional
MBD4	U:G or T:G in CpG sites	Mono-functional
AAG (MPG)	3-meA, 7-meG, ethenoA, ethenoG, hypoxanthine	Mono-functional
MYH	A:8-oxoG	Mono-functional
OGG1	8-oxoG:C, FapyA, Fapy G	Bi-functional
NTH1	Ring-saturated, oxidised or fragmented pyrimidines (e.g. DHU, Fapy, Tg)	Bi-functional
NEIL1 (NEH1)	DHU, FapyA, FapyG, Tg, 5-OHU/C	Bi-functional
NEIL2 (NEH2)	C oxidation products (5-OHU, DHU)	Bi-functional

Table 1.1 Mammalian DNA glycosylases.

5-OHU: 5-hydroxymethyl U; DHU: dihydroxyuracil; Fapy: formamidopyrimidine.
Adapted from (Dianov 2004) and (Wood et al. 2005).
(http://www.cgal.icnet.uk/DNA_Repair_Genes.html#DNA_glyco)

1.5.2 Damage removal by APE1 and Pol β dRP lyase activity

After base damage recognition and removal by DNA glycosylases, APE1 can bind with high affinity to AP sites on double-stranded DNA and induce pronounced kinking of the helical axis, thus displacing DNA glycosylases (Mol et al. 2000). The blocking unsaturated aldehyde residues produced during β-elimination reactions can also be excised by APE1 (Demple and Harrison 1994), thus verifying that DNA glycosylase products can be processed by APE1 during BER. The combined actions of DNA glycosylase and APE1 constitute the incision step in BER.

In humans, APE1 is the major AP endonuclease and is responsible for more than 95% of cellular AP site incision activity in a Mg^{2+}-dependent manner (Chen et al. 1991). Another AP endonuclease, APE2, also exists in mammals which contains a mitochondrial targeting sequence and localises in the nucleus and mitochondria, thus suggesting a possible role in mitochondrial BER (Tsuchimoto et al. 2001). APE1 processes approximately 9,000 AP sites per day in the human genome (Kunkel 1999) through cleavage of the DNA backbone 5' to the AP site leaving 3'-OH and 5'-dRP ends (Demple and Amabile-Cuevas 1991; Barzilay and Hickson 1995), and retains high affinity for this nicked product (Mol et al. 2000). Besides its AP endonuclease activity, APE1 possesses a weak 3'-phosphodiesterase activity capable of removing 3'-blocking groups occurring at single-strand breaks such as 3'-phosphate and 3'-phosphoglycolate (Chen et al. 1991; Demple and Harrison 1994; Parsons et al. 2004); and also 3' to 5' exonuclease activity on mismatched nucleotides at the 3'-termini of DNA (Chou and Cheng 2002). This latter activity implies that APE1 may have a proofreading role in BER by removing mismatched nucleotides arising from BER polymerases such as Pol β (Chou and Cheng 2002). Moreover, APE1 null mice were shown to be embryonic lethal, and heterozygotes were abnormally sensitive to oxidative stress (Meira et al.

2001), further emphasising the importance of APE1 in genome stability. Interestingly, APE1 physically interacts with various other BER enzymes such as Pol β, FEN1 and PCNA and thus may play a key role in the co-ordination of BER (Bennett et al. 1997; Dianova et al. 2001).

Following incision, APE1 passes its product to Pol β which has a higher affinity for the 5'-dRP containing nick. APE1 helps Pol β load onto incised AP sites, and also accelerates Pol β removal of the dRP group via its intrinsic dRP lyase activity (Bennett et al. 1997). As described previously [Fig. 1.2], Pol β plays a central role in BER and its ability to remove the 5'-dRP group determines whether BER is routed through the short-patch or long-patch 'PCNA-dependent sub-pathway. Indeed, APE1 may also facilitate long-patch BER by stimulating the removal of the 5'-flap through protein-protein interactions with FEN1 and PCNA (Dianova et al. 2001).

1.5.3 Short-patch BER co-ordination

Pol β is a 39 kDa monomeric protein comprising of two catalytic domains connected by a protease-sensitive hinge region: the N-terminal dRP lyase and DNA binding domain, and the C-terminal DNA polymerase domain (Wilson 1998). Pol β is the major BER DNA polymerase, and in order for short-patch BER to proceed the 5'-dRP residue must be removed [Fig. 1.2]. Bennett and colleagues showed that APE1 and Pol β have a dynamic protein interaction, where APE1 binding to AP sites helps to load Pol β onto the AP-DNA (Bennett et al. 1997). Following APE1 incision, Pol β exhibits a higher affinity for the substrate and simultaneously inserts the new nucleotide to the 3' end and removes the 5'-dRP group, resulting in a nick (Matsumoto and Kim 1995; Bennett et al. 1997; Prasad et al. 1998; Lindahl and Wood 1999). Ligation of the nick completes the final step of short-patch BER, and indeed, Pol β has been shown to interact with both DNA ligase IIIα-XRCC1 heterodimer (through XRCC1) (Caldecott et

al. 1996; Kubota et al. 1996) and DNA ligase I (Prasad et al. 1996; Dimitriadis et al. 1998). Moreover, *in vitro* studies demonstrated that DNA ligase I can substitute DNA ligase IIIα-XRCC1 complex during ligation of nicks in short-patch BER (Sleeth et al. 2004).

The interaction between XRCC1 and Pol β was shown to be essential for efficient short-patch BER (Marintchev et al. 2003; Dianova et al. 2004), and interestingly, XRCC1 acts as a scaffold protein with a multitude of protein-protein interactions but with no identified enzyme activity of its own (Kubota et al. 1996; Caldecott 2001). XRCC1 is often found in complex with DNA ligase IIIα and is thought to stabilise DNA ligase IIIα (Caldecott et al. 1994). Other XRCC1 interactions include PARP-1, Condensin I, polynucleotide kinase (PNK) and more recently it was implicated to have interactions with multiple DNA glycosylases, thus suggesting another way in which XRCC1 is recruited to sites of BER (Campalans et al. 2005).

1.5.4 Long-patch co-ordination

Modification of the dRP moiety by oxidation or reduction makes it refractory to β-elimination by the dRP lyase activity of Pol β and thus repair is routed through the long-patch BER sub-pathway (Podlutsky et al. 2001). During the 'PCNA-dependent' long-patch BER pathway [Fig. 1.2], the dRP is displaced at the head of an oligonucleotide flap that is subsequently removed by FEN1 (Klungland and Lindahl 1997; Kim et al. 1998) and the resulting nick is sealed by DNA ligase I.

As previously mentioned, Pol β is the major BER polymerase involved in short-patch BER (Sobol et al. 1996), and it has been established that Pol β also initiates long-patch BER by adding the first nucleotide into the repair gap (Podlutsky et al. 2001). Following this, a polymerase switch occurs and further strand-displacement DNA synthesis is conducted by Pol δ/ε which incorporate 2-10 more nucleotides (Klungland

and Lindahl 1997; Dianov et al. 2003). Pol δ/ε have similar roles in DNA replication and repair; however, their biochemical properties differ. Pol δ requires two other factors; PCNA and replication factor C (RF-C) for efficient DNA synthesis (Jonsson and Hubscher 1997). In contrast, Pol ε is highly processive in the absence of PCNA (Burgers 1991). Structurally, Pol δ is comprised of four subunits (125, 66, 50 and 12 kDa) (Podust et al. 2002) and Pol ε is a heterodimer with a 215 kDa catalytic subunit and 55 kDa subunit with unknown function (Kesti and Syvaoja 1991). Both Pol δ and ε contain 3' to 5' exonuclease proofreading activity and are able to remove misincorporated nucleotides (Weiser et al. 1991). The major function of Pol δ and Pol ε is in DNA replication, but they also play a role in NER [reviewed by (Hubscher et al. 2002)].

Pol β insertion of the first nucleotide in both short- and long-patch BER suggests that Pol β must also be able to co-ordinate long-patch BER enzymes. Indeed, Pol β has been shown to interact with PCNA and DNA ligase I (Prasad et al. 1996; Dimitriadis et al. 1998). Long-patch BER is PCNA dependent and PCNA has been shown to interact with and stimulate FEN1 (Li et al. 1995) and DNA ligase I (Montecucco et al. 1998; Tom et al. 2000). Therefore, Pol β can co-ordinate long-patch BER through its interaction with PCNA and the subsequent interaction of PCNA with other long-patch BER enzymes.

1.5.5 APE1-independent BER co-ordination

Recently, an APE1-independent DNA BER pathway was proposed (Wiederhold et al. 2004). Endonuclease VIII (Nei)-like (NEIL) DNA glycosylases generate DNA strand breaks with 3'-phosphate termini which are removed by PNK not APE1. Furthermore, NEIL1 stably interacts with Pol β and DNA ligase IIIα suggesting the formation of a BER complex including PNK, that removes the dirty ends that certain

glycosylases produce (Wiederhold et al. 2004). The physiological relevance of this recently suggested pathway is shown by the sensitivity to IR and MMS of PNK deficient A549 cells (Rasouli-Nia et al. 2004).

1.5.6 Importance of controlled BER enzyme expression

As previously mentioned, BER is a highly co-ordinated pathway mediated through protein-DNA and protein-protein interactions, and it has been reported that there is a fine balance between the concentrations of the enzymes involved in the BER pathway (Posnick and Samson 1999). Imbalances in DNA repair activities may have damaging effects, for example this may contribute to carcinogenesis during chronic inflammation (Hofseth et al. 2003).

Some of the DNA glycosylases which recognise DNA lesions and initiate BER have overlapping functions, thus there are backup mechanisms if the function of one DNA glycosylase is lost [Table 1.1]. Indeed, studies using DNA glycosylase knockout mouse models: AAG-/-, NEIL1-/-, NTH1-/-, OGG1-/- and NTH1,OGG1-/- double knockouts have shown little effect on the phenotype of the resulting knockout mice (see review (Parsons and Elder 2003)); and surprisingly only the OGG1-/- shows significant accumulation of oxidised bases in certain tissues of older animals compared to wild-type mice (Klungland et al. 1999; Minowa et al. 2000). So, whereas DNA glycosylases show functional redundancy, BER enzymes downstream of the glycosylase step play key roles in co-ordinating BER and are essential in embryonic development. Indeed, absence of APE1 (Xanthoudakis et al. 1996), Pol β (Gu et al. 1994), XRCC1 (Tebbs et al. 1999) and DNA ligase III (Puebla-Osorio et al. 2006) is embryonic lethal and these animals would not occur naturally, however, cells with imbalanced levels of BER enzymes can develop, for example in ulcerative colitis (Hofseth et al. 2003), and also

studies have shown that APE1 underexpression leads to apoptosis particularly in the brain (Meira et al. 2001).

It may be presumed that significant underexpression of a BER enzyme would result in attenuation of repair efficiency as the dynamics of the pathway would alter and the underexpressed enzyme would then become rate-limiting. If the repair capacity of BER lesions is reduced repair intermediates may accumulate in the genome resulting in genome stability or apoptosis. In the other extreme, overexpression of a BER enzyme may also have adverse effects on the cell. Overexpression is more commonly observed in tumour samples than underexpression, and overexpression of certain BER enzymes such as DNA glycosylases, APE1 and Pol β have been associated with genome instability [reviewed by (Frosina 2000)].

1.6 DNA POLYMERASE BETA (POL β)

Currently, over 19 different eukaryotic DNA polymerases, subdivided into 7 families (A, B, C, D, X, Y and RT) have been identified [Table 1.2, Table 1.3] [reviewed by (Hubscher et al. 2002)], including Pol β a member of the X-family which is the main BER DNA polymerase. Pol β is a relatively small monomeric protein (39 kDa) comprising of two catalytic domains connected by a protease-sensitive hinge region: the N-terminal 8 kDa dRP lyase and DNA binding domain, and the C-terminal 31 kDa DNA polymerase domain [reviewed by (Wilson 1998)]. The protein also consists of several subdomains necessary for catalysis; the fingers, the thumb and the palm ((Matsumoto and Kim 1995; Pelletier et al. 1996). In contrast to replicative DNA polymerases (Pol α, δ and ε), Pol β lacks any intrinsic 3' to 5' exonuclease activity and is incapable of proofreading.

The main role of Pol β is in gap-filling synthesis during DNA repair in mammalian cells (Singhal et al. 1995); primarily in short-patch BER (Sobol et al. 1996), but also in long-patch BER by adding the first nucleotide into the repair gap before a polymerase switch to Pol δ/ε. Pol β is also the rate-limiting enzyme in BER by providing vital dRP lyase function which releases the 5'-dRP moiety by β-elimination (Srivastava et al. 1998; Allinson et al. 2001). Pol β is constitutively expressed at low levels throughout the cell cycle (Zmudzka et al. 1988), and is inducible by some genotoxic treatments such as DNA alkylating agents (MNNG), oxidising agents (H_2O_2) and ionising radiation (Fornace et al. 1989; Canitrot et al. 1998; Frechet et al. 2001). Apart from its role in BER, Pol β is essential in neural development and Pol β null-mice are embryonic lethal (Gu et al. 1994). However, a regulatable transgenic mouse model has been developed by Sobol *et al.* which can overexpress Pol β and a cataract phenotype has been observed (Sobol et al. 2003).

DNA Pol	Human	Functional tasks	Family
Classical DNA polymerases and Pol lambda (λ)			
Pol α	Four subunits: 165 kDa catalytic, 67-86 kDa 3' to 5' exonuclease, 58 kDa primase and 48 kDa primase subunits.	DNA replication pol: initiates DNA synthesis. Participates in lagging strand synthesis.	B
Pol β	39 kDa: 31 kDa catalytic and 8 kDa dRPase domain	BER pol: short- and long-patch. Role in neurogenesis. Implicated in NER, meiosis, recombination and translesion synthesis.	X
Pol δ	Four subunits: 125 kDa catalytic, 66 kDa, 50 kDa regulatory and 12 kDa small subunits.	Main pol at the leading and lagging strand. Long-patch BER, NER, MMR, recombination and double-strand break repair.	B
Pol ε	Two subunits: 258 kDa catalytic, 59.5 kDa regulatory subunits.	Leading and lagging strand pol. Long-patch BER, NER, MMR and recombination.	B
Pol γ	140 kDa: a heterotrimer of catalytic subunit plus homodimer of accessory subunits.	Mitochondrial replication pol: DNA replication and BER in mitochondrial DNA.	A
Pol λ	39 kDa: 31 kDa catalytic and 8 kDa dRPase domain	Potentially functions in BER or meiotic recombination. Homologous to Pol β.	X

Table 1.2 Classical Mammalian DNA polymerases.

Adapted from (Dianov 2004), (Hubscher et al. 2002) and UniProt Knowledgebase (Swiss-Prot and TrEMBL) - Protein knowledgebase (http://www.expasy.org/sprot/)

DNA Pol	Human	Functional tasks	Family
Novel DNA polymerases and Telomerase			
Pol θ	198 kDa	Interstrand crosslink repair	A
Pol ζ	353 kDa	Lesion bypass extension	B
Pol σ	60 kDa	Role in sister chromatid cohesion?	B
Pol μ	55 kDa	Role in lymphoid formation. Somatic hypermutation pol? Homologous to TdT.	X
TdT	Terminal deoxynucleotidyl-transferase, 59 kDa	Template-independent DNA pol, catalyses random dNTP addition. Role in nt addition during maturation of B- and T- cells.	
Pol η (XPV) (RAD30 A)	78 kDa: Structural and functional homologue of yeast Pol η	Error-free bypass of thymine dimers, accurate mismatch pol. Xeroderma pigmentosum pol. Somatic hypermutation pol. Target Pol ι to replication foci.	Y, (UmuC /DinB super-family)
Pol ι, (RAD30 B)	80 kDa	Meiosis pol. Lesion bypass. Most error prone pol.	
Pol κ (DINB1)	99 kDa	Deletion and base substitution pol. Lesion bypass. Low fidelity.	
Rev1	138 kDa	Role in abasic site lesion bypass. Has deoxycytidyl transferase activity, can add C to 3'end of DNA primer in template-dependent reaction.	
Telomerase	127 kDa	Telomere maintenance, homologous to reverse transcriptase	RT

Table 1.3 Novel Mammalian DNA polymerases

Adapted from (Dianov 2004), (Hubscher et al. 2002) and UniProt Knowledgebase (Swiss-Prot and TrEMBL) - Protein knowledgebase (http://www.expasy.org/sprot/)

1.6.1 Pol β: fidelity and mutation rate

For many years, Pol β was considered to be a low fidelity DNA polymerase (Kunkel 1992) because both the efficiency and fidelity of Pol β synthesis was found to be reduced (average mutation frequency, 10^{-4}) compared to replicative DNA polymerases (average mutation frequency, 10^{-6} to 10^{-8}) (Kunkel and Bebenek 2000). Pol β has evolved as a distributive polymerase designed to fill 1-nt gaps containing 3'-hydroxyl and 5'-phosphate ends, and indeed several studies have shown that 5'-phosphorylated 1-nt gapped DNA is the preferred substrate for Pol β (Prasad et al. 1994; Chagovetz et al. 1997; Osheroff et al. 1999). Nucleotide misincorporation by Pol β is 10 to 100-fold lower on 5'-phosphorylated 1-nt gapped DNA compared with recessed, 6-nt gapped, 5'-phosphorylated 6-nt gapped and unphosphorylated 1-nt gapped substrates (Beard and Wilson 1998).

As Pol β has no proofreading activity, its incorporation accuracy results exclusively from the nucleotide selectivity of the enzyme. Unlike most replicative polymerases, which select the correct dNTP through an 'induced fit' mechanism, Pol β fidelity is determined through specific interactions between the enzyme and the template base at the active site. In the induced-fit mechanism, binding of the correct incoming nucleotide and two metal ions within the active site creates a substrate-induced conformational change from an open state to a closed state, which then activates the polymerase for catalysis and hence DNA extension (Beard and Wilson 1998). However, nucleotide discrimination by Pol β appears to be determined by steric exclusion against the incorrect substrate, the precise positioning of the DNA duplex terminus, templating and incoming nucleotides and the catalytic residues within the active site of Pol β (Sweasy 2003). Imprecise positioning of active site residues on DNA can result in misincorporation of nucleotides into DNA. Amino acid residues

both distant and near to the Pol β active site influence its geometry, suggesting that the movements and positioning of sub-domains of Pol β have a significant impact upon its fidelity and consequently its catalytic efficiency (Sweasy 2003).

Presently, it is not clear which DNA polymerase, Pol δ or Pol ε is contributing more to long-patch BER, since both enzymes can catalyse strand-displacement synthesis which is required for this pathway (Turchi et al. 1992; Podust and Hubscher 1993; Stucki et al. 1998). However, both Pol δ and Pol ε show very high fidelity DNA synthesis in the *in vitro* systems (Kunkel and Bebenek 2000).

1.6.2 Biological consequences of Pol β imbalance

As mentioned previously Pol β is essential during embryonic development, and Pol β null mice die immediately after birth (Gu et al. 1994). Interestingly, Pol β null embryos display a tissue-specific reduction of 1-nt frameshift mutations as well as increased apoptosis compared to wild type embryos (Sweasy et al. 2005). Various studies have shown that underexpression of Pol β increases the rate of chromosomal aberrations by reducing BER activity (Matsuzaki et al. 1996; Dalal et al. 2005), and ultimately the accumulation of DNA damages results in mutagenesis or apoptosis. Indeed, Albertella and colleagues observed reduced levels of Pol β mRNA and protein in approximately one fifth of all tumours sampled, particularly in breast and colon cancers using expression arrays (Albertella et al. 2005). Furthermore, Pol β underexpression seems to correlate with underexpression of other DNA polymerases as well (Albertella et al. 2005).

Early observations indicated that Pol β is overexpressed in some cancer cells (Canitrot et al. 1999; Srivastava et al. 1999; Bergoglio et al. 2001; Tan et al. 2005). Indeed, overexpression of Pol β by 2 to 4-fold in mammalian cells can increase mutation rate (Canitrot et al. 1998) and promote tumourigenesis as a consequence.

Recently Albertella and colleagues used expression arrays to systematically study the expression patterns of BER DNA polymerases (Pol β, λ, δ, ε) in cancer cells (Albertella et al. 2005). They found that Pol β was overexpressed at the mRNA and protein level in approximately one third of all tumours sampled and Pol β was most frequently overexpressed in uterus, ovary, prostate and stomach cancer samples. Pol λ was also overexpressed in a range of tumours, but to a lesser extent than Pol β. The long-patch BER DNA polymerases (Pol δ and ε) were not commonly overexpressed (Albertella et al. 2005).

1.7 RESEARCH OBJECTIVES

This research project is a collaboration between the Radiation and Genome Stability Unit (RAGSU) (Medical Research Council, Harwell) and Professor Ian Hickson (Weatherall Institute of Molecular Medicine, Oxford). Prof. Hickson kindly provided lymphoblastoid cells from cancer patients that demonstrated sensitivity to radiotherapy treatment. Patients had a variety of different cancers and lymphoblast cells from patients and wild-type controls were transformed with Epstein-Barr virus to created immortalised lymphoblastoid cell lines. Preliminary data by Dr. Irina Dianova (RAGSU, Medical Research Council, Harwell) demonstrated that the 'Ha' cell line overexpressed the BER enzyme Pol β, and this cell line was selected for further investigation. Thus, the aims of my project were to investigate the Pol β expressing cell line, Ha, and to determine whether Pol β overexpression affects the repair capacity or fidelity of lesions associated with BER.

Chapter II

Materials & Methods

2.1 MATERIALS

2.1.1 General reagents

All laboratory chemicals were from Sigma Aldrich (Poole, UK), except where otherwise stated. Protease inhibitors; aprotinin, chymostatin, leupeptin, pepstatin were from Roche Diagnostics Ltd (Lewes, UK). Synthetic oligonucleotides purified by high-performance liquid chromatography were obtained from MWG-Biotech (Ebersberg, Germany). [γ-^{32}P]ATP and [α-^{32}P]UTP (3,000 Ci/mmol) were purchased from Perkin-Elmer Life and Analytical Sciences (Boston, MA, USA).

2.1.2 Bacteriological reagents and bacterial strains

Bacto-agar, bacto-tryptone, bacto-yeast extract, peptone and LB-bouillon were from MERCK Biosciences (Nottingham, UK). Tetracycline was from Duchefa Biochemie BV (Haarlem, The Netherlands) and carbenicillin, disodium salt from Melford Laboratories Ltd (Ipswich, UK). X-gal and IPTG were from VWR International Ltd (Poole, UK). The XL-1 Blue bacterial strain was from Stratagene (La Jolla, CA, USA) and the JM109 strain was from Promega (Southampton, UK).

2.1.3 Proteins

Histidine-tagged Pol β and APE1 were purified on Ni-NTA agarose (Qiagen, Crawley, UK) as recommended by the manufacturer. Recombinant human uracil-DNA glycosylase (UDG) with 84 amino acids deleted from the amino terminus was purified as described previously (Slupphaug et al. 1995).

2.1.4 Cells

Immortalised Epstein-Barr virus (EBV) transformed human lymphoblastoid cells derived from normal (Jb) and head-neck cancer patient (Ha) were obtained from the Cancer Research UK Cell Services (Clare Hall Laboratories, Potters Bar, UK). The normal Jb cell line will be referred to as wild-type (Wt) from here onwards. The Ha cell

line was derived from a 53 year old man with stage 1, high grade, B-cell lymphoma located at the back of the throat. During the first phase of radiotherapy (15 fractions, 2 Gy each) he exhibited a severe oral reaction necessitating the introduction of nasogastric feeding. 6 months later, spinal cord damage was evident which was succeeded by apical pulmonary fibrosis. The Wt cell line was isolated from a normal, healthy, male volunteer with no history of cancer. Both cell lines were grown in suspension culture and maintained in RMPI 1640 medium (Invitrogen, Paisley, UK) supplemented with 10% (v/v) foetal bovine serum, 1% (v/v) L-glutamine and 1% (v/v) penicillin/streptomycin antibiotic mix at 37°C in the presence of 5% CO_2 in air.

2.2 WHOLE CELL EXTRACT PREPARATION

Whole cell extracts (WCE) for both cell lines were prepared by the method of Tanaka (Tanaka et al. 1992) as modified by Vodenicharov (Vodenicharov et al. 2000). Briefly, suspension cells were pelleted, resuspended in 10 ml of phosphate-buffered saline (PBS) [Section 2.18.1] and re-pelleted at 1,200 rpm, for 15 min at 4°C using Eppendorf Refrigerated Multipurpose Centrifuge 5804 R (Eppendorf AG, Hamburg, Germany). The packed cell volume (PCV) was measured and the cells were resuspended thoroughly in one PCV of Buffer I [Section 2.18.1] before two PCVs of Buffer II [Section 2.18.1] was added, then the cell suspension was rocked at 4°C for 2 h and centrifuged at 40,000 rpm, for 20 minutes at 4°C using Beckman Coulter TL-100 Ultracentrifuge TLA 45 (Beckman Coulter, Inc. Fullerton, CA, USA). Supernatants were carefully collected avoiding the cell pellet. The protein concentration of the WCE was determined by the Bradford protein assay (Bio-Rad Laboratories, Hercules, CA, USA) (Bradford 1976). Extracts were aliquoted and stored at –80°C.

2.3 GENOMIC DNA EXTRACTION

Genomic DNA was extracted from 3 x 10^7 lymphoblastoid cells (Wt and Ha) using 500 µl of DNA Lysis Buffer [Section 2.18.1] and contaminating RNA was removed using 10 µg of DNase-free RNase A. Proteins and other cellular debris were removed by phenol-chloroform extraction method, as follows (Kirby 1956). An equal volume of phenol:chloroform:isoamyl alcohol (25:24:1) was mixed thoroughly with the DNA sample and centrifuged at 13,000 rpm for 1 min at room temperature (Eppendorf Microcentrifuge 5415 D). The upper aqueous layer was then mixed with an equal volume of chloroform and centrifuged as before to remove traces of phenol. Genomic DNA was precipitated using one-tenth volume of 3M sodium acetate, pH 5.2, and three volumes of chilled absolute ethanol by incubation at -20°C for 1 h. The precipitated DNA was transferred into a fresh tube and washed several times with 70% (v/v) ethanol before being vacuum dried and resuspended in sterile TE [Section 2.18.1]. DNA concentration was measured using a spectrophotometer at OD_{260}. One optical unit of double-stranded DNA solution, in a 1 cm quartz cuvette, was estimated as 50 µg of DNA per ml. DNA was aliquoted and stored at –20°C.

2.4 RNA EXTRACTION

2.4.1 Total RNA

Total RNA was extracted from 1 x 10^7 cells (Wt and Ha) using TRIzol® reagent (Invitrogen) by the guanidinium thiocyanate method (Chomczynski and Sacchi 1987), following the manufacturers instructions. Cells were pelleted and lysed using 1 ml of TRIzol® reagent by repetitive pipetting, then incubated at room temperature for 5 min. 0.2 ml of chloroform was added to aid phase separation and mixed vigorously by hand for 15 sec and further incubated at room temperature for 2-3 min, before centrifugation

at 10,000 rpm for 15 min at 4°C (Eppendorf Microcentrifuge 5415 D). The upper aqueous phase containing the RNA was transferred to a fresh tube and precipitated by adding 0.5 ml of isopropanol. Samples were incubated for 10 min at room temperature, then centrifuged at 10,000 rpm for 10 min at 4°C (Eppendorf Microcentrifuge 5415 D). The RNA pellet was then washed by vortexing in 1 ml of 75% (v/v) RNase-free ethanol, followed by centrifugation at 8,000 rpm for 5 min at 4°C (Eppendorf Microcentrifuge 5415 D). Finally, the RNA was allowed to air-dry for 10 min, before dissolving in RNase-free water. Concentration of total RNA was measured using a spectrophotometer at OD_{260}. One optical unit of RNA solution, in a 1 cm quartz cuvette, was estimated as 40 µg of RNA per ml. RNA was aliquoted and stored at –20°C.

2.4.2 Messenger RNA

Messenger RNA (mRNA) was extracted from total RNA using GenElute™ mRNA Miniprep Kit (Sigma) following the manufacturers instructions. A known amount of total RNA was adjusted with RNase-free water to 250 µl, then an equal volume of 2X Binding Solution (Kit) was added before incubating with 15 µl of oligo $(dT)_{30}$-polystyrene beads for 3 min at 70°C, followed by cooling for 10 min at room temperature. The oligo (dT)-beads : mRNA complexes were pelleted then applied to a GenElute™ spin-filter column and washed with a low salt Wash Solution (Kit) to remove contaminants. Messenger RNA was eluted at 70°C in a suitable volume (50-100 µl) of RNase-free water and used immediately or aliquoted and stored at –80°C. mRNA only constitutes 1-5% of total RNA, so the final mRNA concentration was estimated based on several parameters: (i) known input amount of total RNA, (ii) assume same mRNA isolation efficiency with each preparation, (iii) assume 1% yield of

mRNA from total RNA, (iv) elute with known volume to get desired concentration of mRNA, and calculated as follows:

Amount of mRNA extracted = Input amount of total RNA X 0.01

$$\textit{Elution volume} = \frac{\text{Amount of mRNA extracted}}{\text{Desired mRNA concentration}}$$

2.5 REVERSE TRANSCRIPTION-POLYMERASE CHAIN REACTION (RT-PCR)

First-strand cDNA was synthesised using the SuperScript™ II first-strand synthesis system for RT-PCR kit (Invitrogen) using oligo $(dT)_{12-18}$ primers following the manufacturer's protocol. Briefly, 1 µg of total RNA was reverse transcribed in each 20 µl reaction to generate 1 µg of cDNA templates, at a concentration of 50 ng/µl. Initially, 500 ng of oligo (dT) primers and 0.5 mM each dNTPs were annealed to 1 µg of total RNA in the presence of RNase-free water at 65°C for 5 min and then chilled on ice for at least 1 min. Next, 10X RT Buffer (Kit) [Section 2.18.1], 5 mM $MgCl_2$, 10 mM DTT and 40 units of RNase OUT™ recombinant ribonuclease inhibitor was added to the reaction and incubated at 42°C for 2 min, before 50 units of SuperScript™ II reverse-transcriptase was added to complete the final 20 µl reaction. The reaction was further incubated at 42°C for 50 min, before termination by heating at 70°C for 15 min and chilling on ice. 2 units of *E. coli* RNase H were added later to each tube to remove RNA templates and samples incubated at 37°C for 20 min. Each sample was set up in duplicate in the presence or absence of reverse transcriptase to check for genomic contamination. The first-strand cDNA was stored at –20°C until use. An aliquot of the RT reaction equivalent to 50 ng RNA (1 µl) was amplified by PCR as described in [Section 2.6], using gene-specific primers.

2.6 POLYMERASE CHAIN REACTION (PCR)

2.6.1. Primers

Primer sequences, annealing temperatures and number of cycles used are listed in [Table 2.1]. Human DNA Pol β promoter (J04201) and mRNA (NM_002690) primers were designed using Primer CGI software and were obtained from MWG-Biotech AG (Ebersberg, Germany).

2.6.2 PCR conditions

Each 50 µl PCR reaction mixture comprised of 1X PCR Reaction Buffer (Abgene) [Section 2.18.1] with 1.5 mM $MgCl_2$, 0.2 mM dNTPs, 2.5 units of Thermoprime Plus *Taq* DNA Polymerase (ABgene, Epsom, UK) and 0.2 µM of each forward and reverse primer [see Table 2.1]. 100 ng of genomic DNA or 1 µl cDNA template was used for each PCR. 2% (v/v) DMSO was added to the reactions using genomic DNA to reduce secondary structure formation in the template. Deionised water was added to give a final reaction volume of 50 µl. Cycling conditions included an initial 2 min denaturation step at 95°C, followed by 95°C for 30 sec / χ°C for 30 sec annealing / 72°C for 90 sec for *n* cycles and a final extension step at 72°C for 10 min [see Table 2.1]. PCR products were electrophoresed on a 1% (w/v) agarose gel in 1X TAE buffer [Section 2.18.1] in the presence of 5 µg/ml ethidium bromide and subsequently visualised under UV light. 1 kb ladder (0.25 - 10 kb) (Promega) was used as a size marker.

Pol β template (Accession no.)	Region of homology to sequence (nt position)	Description & Primer Sequence 5' – 3'		PCR Product Length (bp)	Annealing Temp (χ °C)	PCR Cycles (*n*)
Promoter (J04201) 1866 bp	5 - 9	A	F: CTA CCA GAT TAG TAA CAA ACT ACC C	AR (1344)	53	35
	387 - 407	B	F: ATA TGA ACC CAG GAG TTA CGC	BR (962)	53	35
	644 - 661	C	F: TTC CTG TTC TCG GCA TTG	CR (705)	53	35
	1039 - 1058	D	F: CCG AGT TCT CTC TCC TCA CC	DR (310)	53	35
	1348 - 1325	R	R: AAC CTG TGA GCA TGT CGG TGA TTC		53	35
	267 - 247	Prom rev-1	R: TGA TCT CAC CCT ACA GCT GAA			
mRNA (NM_002690) 1259 bp	19 - 37	a	F: TGC TCC CGT CTC CAA GTC C	ar (1146)	55	30
	444 - 466	b	F: GCA AGG AAG TTT GTA GAT GAA GG	br (715)	55	30
	802 - 822	c	F: AGG GTG AGA CAA AGT TCA TGG	cr (357)	55	30
	1158 - 1140	d	R: CCA TTG GGT TGT GTC TGC G		55	30
	737 - 718	mRNA rev-1	R: CCA TTC GCT GAT GAT GGT TC			
	528 - 509	mRNA rev-2	R: TGG CTG TTT GGT TGA TTC TG			

Table 2.1 Primers used for PCR and DNA sequencing of human DNA Polymerase beta (β) promoter and mRNA gene.

2.7 DNA SEQUENCING

ABI PRISM® BigDye® Terminators v3.1 Cycle Sequencing Kit (Applied Biosystems, Warrington, UK) was used for automated sequencing according to the manufacturer's instructions and is based on the Sanger method of dideoxy chain termination (Sanger et al. 1977). In each 10 µl reaction, PCR templates or single-stranded DNA [see Table 2.2, for amounts], 4 µl of BigDye® terminator ready reaction mix that contains dRhodamine dye terminators, 2 µM primer and deionised water were mixed together and cycled at 96°C for 10 sec / 50°C for 5 sec / 60°C for 4 min for 25 cycles then held at 4°C. Reactions were prepared for sequencing by incubating for 20 min at room temperature with 90 µl of 67% (v/v) isopropanol, and then centrifuged at 13,000 rpm for 20 min at room temperature (Eppendorf Microcentrifuge 5415 D) to pellet DNA and remove excess fluorescent dye terminators. The DNA pellet was washed with 75% (v/v) isopropanol and centrifuged again for 5 min, then allowed to air-dry. The ABI PRISM® 3100 Capillary Genetic Analyzer (Applied Biosystems) was used to sequence the DNA by members of the Genotyping, Mutation detection and Sequencing (GEMS) core facility at MRC Harwell. Sequences were analysed for similarity to known sequences using the BLAST tool (http://www.ncbi.nlm.nih.gov/BLAST).

2.7.1 Single-stranded DNA preparation

Single-stranded M13 DNA was extracted from an exponentially growing LB culture of infected JM109 *E. coli* cells using a QIAprep® Spin M13 Kit (Qiagen) according to the manufacturer's protocol. This was based on an initial high-speed centrifugation step to remove bacterial cells, followed by precipitation of M13 phage particles using a precipitation buffer (Buffer MP, Kit). Intact phage particles were applied to a QIAprep® spin column, where they were retained on a specially adapted

silica-gel membrane. Addition of a high salt containing M13 lysis and binding buffer (Buffer MLB, Kit) lyses the phage particles and adsorbs the single-stranded DNA to the membrane. Contaminants and impurities were removed by a high salt wash and residual salt was removed by washing with an ethanol-containing buffer (Buffer PE, Kit). Single-stranded M13 DNA was finally eluted in 50 µl of elution buffer containing 10 mM Tris-Cl, pH 8.5 (Buffer EB, Kit), and concentration was measured using a spectrophotometer at OD_{260}. One optical unit of single-stranded DNA solution, in a 1 cm quartz cuvette, was estimated as 33 µg of single-stranded DNA per ml. Single-stranded DNA was aliquoted and stored at –20°C.

Template	Quantity (ng)
PCR Product	
200 – 500 bp	3 – 10
500 – 1,000 bp	5 – 20
1,000 – 2,000 bp	10 – 40
Single-stranded DNA	25 – 50
Double-stranded DNA	150 – 300

Table 2.2 Amount of template used for DNA sequencing.

Protein	Size (kDa)	Dilution	Source	Details
APE1	34	1 : 50,000	Rabbit, polyclonal In-house	0.38 mg/ml
β-actin	29	1 : 50,000	Mouse,	
Pol β	39	1 : 10,000	Rabbit, polyclonal In-house	1 mg/ml
PARP-1 (C- 2-10)	113	1 : 10,000	Mouse, monoclonal Axxora (UK) Ltd, Nottingham, UK	
PCNA	29	1 : 5,000	Mouse, monoclonal Santa Cruz	
XRCC1	69	1 : 10,000	Rabbit, polyclonal Abcam	
CREB	43	1 : 200	Rabbit, polyclonal Abcam	1 mg/ml
pCREB to Ser133	43	1 : 500	Rabbit, polyclonal Abcam	1 mg/ml

Table 2.3 Antibodies and dilutions used for Western blotting.

2.8 WESTERN BLOT ANALYSIS

Western blots were performed by a standard procedure as recommended by the vendor (Invitrogen). Briefly, samples were diluted 1:1 in 2X SDS-PAGE Sample Loading Buffer [Section 2.18.1], and heated for 5 min at 90°C. Samples were then spun briefly in an Eppendorf Microcentrifuge 5415 D, 1,300 rpm, 10 sec before loading on a 10% (w/v) Novex® Tris-Glycine Gel (SDS-PAGE) (Invitrogen). A protein size marker (10 - 250 kDa) was always loaded (Precision Plus Protein™ Standards, Bio-Rad). The gel was electrophoresed in SDS-PAGE Running Buffer [Section 2.18.1] for 2 h at a constant 125 Volts.

2.8.1 Odyssey detection method

The proteins were transferred onto polyvinylidene fluoride (PVDF) Immobilon-FL membrane, 0.45 μm pore size (Millipore, Billerica, MA, USA) for 1.5 h at a constant 25 Volts in SDS-PAGE Transfer Buffer [Section 2.18.1]. The membrane was rinsed thoroughly in PBS before blocking in 50% (v/v) Odyssey® Blocking Buffer (LI-COR® Biosciences) [Section 2.18.1] diluted in PBS (Blocker:PBS), for 1 h at room temperature. All primary and secondary antibodies were diluted in Odyssey® Blocker:PBS, containing 0.1% (v/v) Tween-20®. See [Table 2.3] for dilutions used and antibody details. Western blots were incubated with primary antibodies overnight at 4°C and then washed three times for 5 min in PBS, containing 0.1% (v/v) Tween-20® (PBST). Blots were then probed with goat anti-mouse or goat anti-rabbit secondary antibodies conjugated to Alexa Fluor 680 (Molecular Probes™, Invitrogen) or IRdye 800 (Rockland Immunochemicals, Gilbertsville, PA, USA) for 1 h at room temperature and then washed three times for 5 min in PBST. Blots were rinsed for a further 5 min in PBS to remove excess Tween-20®. Blotted proteins were detected and quantified using

the Odyssey® infrared imaging system (LI-COR® Biosciences). All Western blots were repeated, and representative blots are shown where appropriate.

2.8.2 ECL detection method

The proteins were transferred onto a polyvinylidene fluoride (PVDF) membrane, 0.2 µm pore size (Invitrogen) for 2 h at a constant 25 Volts in SDS-PAGE Transfer Buffer [Section 2.18.1]. The membrane was then blocked for 1 h in 5% (w/v) dried milk solution in 1X TBS Buffer [Section 2.18.1] containing 0.1% (v/v) Tween-20® (TBST). See [Table 2.3] for dilutions used and antibody details. Western blots were incubated with the primary antibody (in milk) overnight at 4°C, and then washed three times for 5 min in TBST. Blots were then incubated with the secondary anti-mouse or anti-rabbit antibody (in milk) for 1 h followed by three 20 min washes with TBST. Blots were visualised using the ECL plus system (Amersham). All Western blots were repeated, and representative blots are shown where appropriate.

2.9 NORTHERN BLOT ANALYSIS

2.9.1 Northern Blotting

Northern blots were performed by a standard procedure as recommended by the vendor (Ambion, Inc., Austin, TX, USA). Briefly, mRNA samples were diluted 1:1 in NorthernMax®-Gly Sample Loading Dye (Ambion) [Section 2.18.1] and heated for 30 min at 50°C. Samples were then spun briefly in an Eppendorf Microcentrifuge 5415 D, 1,300 rpm, 10 seconds before loading on a 1% (w/v) agarose gel containing 1X NorthernMax®-Gly Gel Prep/Running Buffer (Ambion) [Section 2.18.1]. A single-stranded RNA size marker (0.24 - 9.5 kb) was always loaded (Invitrogen). The gel was electrophoresed in 1X NorthernMax®-Gly Gel Prep/Running Buffer [Section 2.18.1] for 2 h at a constant 60 Volts, then photographed alongside a ruler under UV light to

locate size markers (Invitrogen). The mRNA samples were transferred to BrightStar®-Plus positively charged nylon membrane (Ambion) for 2 h by downward capillary transfer in NorthernMax®-Gly Transfer Buffer (Ambion). The membrane was rinsed in transfer buffer before the mRNA was UV-crosslinked (120,000 mJ/cm^2, for 30 – 45 s) onto the membrane using Stratalinker® UV crosslinker 1800 (Stratagene, La Jolla, CA, USA). Membranes were stored at –20°C until required, or probed immediately.

2.9.2 RNA probes

Labelled riboprobes were synthesised using the Strip-EZ® RNA labelling kit (Ambion) following the manufacturer's instructions. Template DNA containing the mRNA-complementary (antisense) transcript sequence downstream of a T7 RNA polymerase promoter site was generated for *in vitro* transcription. Briefly, each 20 µl reaction containing 1 µg of DNA template, 1X Transcription Buffer (kit) with DTT, 0.5 mM each of ATP and GTP solution, 0.1 mM of modified CTP solution, 3.125 µM (50 µCi) of [α-^{32}P]UTP (10 mCi/ml) and 2 µl of T7 enzyme mix was mixed together by gentle pipetting, then incubated at room temperature for 1 h. The DNA template was then removed by addition of 1 µl of DNase I and incubation at 37°C for 15 min. The Strip-EZ RNA labelling kit was chosen as a modified CTP nucleotide (supplied in the kit) is incorporated into the probe. The probe is stable for hybridisation, washing and signal detection but the presence of the modified nucleotide facilitates probe removal from the membrane. Treating the membrane with Probe Degradation Buffer (kit) reduces the full-length probe to short oligonucleotides which are subsequently washed away.

2.9.3 Hybridisation

Northern blots were prehybridised in UltraHyb® Ultrasensitive Hybridisation Buffer (Ambion) at 68°C for 1 h prior to addition of the riboprobe. The probe was

hybridised overnight at 68°C followed by two 5 min washes at 68°C in NorthernMax® Low Stringency Wash Buffer (Ambion) [Section 2.18.1] and two 10 min washes at 68°C in NorthernMax® High Stringency Wash Buffer (Ambion) [Section 2.18.1]. The blots were exposed to X-ray film for the appropriate amount of time.

2.9.4 Removal of RNA probe from Northern blots

Following detection of hybridised probe, blots were incubated at 68°C for 10 min in 1X Probe Degradation Buffer (Ambion) (kit) / 0.1% (w/v) SDS, followed by a 10 min wash at 68°C in a 1X Blot Constitution Buffer (Ambion) (kit) / 0.1% (w/v) SDS and a final wash for 10 min at 68°C in 0.1% (w/v) SDS. Blots were stored at –20°C until required.

2.10 REAL-TIME QUANTITATIVE PCR

A two-step real-time quantitative PCR (qPCR) method based on SYBR® Green I detection chemistry was used to measure gene expression levels. First-strand cDNA templates were used [see Section 2.5] and all primers were designed with PrimerExpress 1.0 software (Applied Biosytems) using the default parameters (Primer T_m: min/max = 58/60°C; Primer GC%: min/max = 30/80%; Primer Length: min/max = 9/40 bases, optimal = 20 bases; Amplicon Length: min/max = 50/150 bases, max T_m = 85 °C). An additional requirement was a maximum GC content of 40% for the five last 3'-end nucleotides

2.10.1 Initial optimisation

To determine the optimal primer concentration giving the lowest threshold cycle (C_t) and maximum amplification efficiency while minimising non-specific amplification, nine different combinations of reverse and forward primer concentrations (100, 300, or 900 nM) were titrated. A range of cDNA (50 ng/µl) volumes (0.25, 0.5, 1,

and 2 µl) were also tested to ensure that amplification was within the linear range. For each combination, a no-template control (NTC) was included. The primer concentrations giving the lowest C_t, and a suitable cDNA volume within the linear range was selected for further use in real-time qPCR analysis.

2.10.2 PCR conditions

Each 50 µl qPCR reaction mixture contained 1X qPCR MasterMix Plus for SYBR® Green I Reaction Buffer (containing dNTP/dUTP, HotGoldStar DNA polymerase, 5 mM $MgCl_2$, Uracil N-glycosylase (UNG), SYBR® Green I, stabilisers and ROX passive reference) (Eurogentec, Seraing, Belgium), forward and reverse primer (100-900 nM), 1 µl of cDNA template (50 ng/µl) and deionised water to give a final 50 µl reaction volume. Reactions were analysed using the ABI PRISM® 7000 Sequence Detection System (Applied Biosystems). The cycling conditions comprised of an initial UNG step at 50°C for 2 min, then a polymerase activation / UNG inactivation step at 95°C for 10 min. This was followed by 40 cycles at 95°C for 15 sec for denaturation / 60°C for 1 min for annealing and polymerisation reactions were held at 50°C or a Dissociation Curve Profile was created for each sample. Amplicons were denaturated at 95°C for 15 sec, then re-annealed at 60°C for 20 sec. The temperature was gradually increased from 60°C to 95°C over a 20 min ramp time and dissociation curve profile and T_m of the amplicon was determined. Primer dimers and non-specific products could also be detected.

2.10.3 Analysis

The standard curve method for absolute quantitation of gene expression levels was used. Firstly, the absolute quantities of the standards must first be known by some independent means. Refer to 'Absolute Quantitation using Standard Curve Guide' from Applied Biosystems (http://docs.appliedbiosystems.com/pebiodocs/04364014.pdf).

2.11 PROTEIN DEGRADATION ASSAY USING CYCLOHEXIMIDE

Suspension cells were freshly seeded at 1 x 10^6 cells/ml density 16 h prior to the start of the experiment. 50 µg/ml of cycloheximide in DMSO was added to the cells and then incubated for various time points. A DMSO only control was also used and for time = 0, no cycloheximide was added. For each time point 5 x 10^6 cells (5 ml) were harvested, WCEs made [Section 2.2] and samples were analysed by Western blotting [Section 2.8].

2.12 GEL PURIFICATION OF OLIGONUCLEOTIDES

Oligonucleotides used for repair assays were purified on a 20% (w/v) native polyacrylamide gel [Section 2.19]. 100 µg of oligonucleotide and 100 µl of Native-PAGE Sample Loading Buffer [Section 2.18.1] was heated at 95°C for 2-3 min, before being loaded onto a pre-warmed gel (containing one well) and electrophoresed in 1X TBE [Section 2.18.1] at 15 W for about 1.5 h or until the lower dye front (bromophenol blue) reached the bottom. Strips of the gel from either side of the well were excised and stained in 1X TBE [Section 2.18.1] containing ~1 µg/ml of ethidium bromide for 10-15 min at 4°C and subsequently visualised under UV light. The major oligonucleotide band was located, notches in the strips were excised and the strips were re-aligned with the gel to determine the position of the oligonucleotide. The gel containing the oligonucleotide was cut out, crushed and incubated in deionised water overnight at 37°C. The DNA-containing solution was recovered through a 0.2 µM Corning® Spin-X® microcentrifuge filter (Sigma) and concentrated by passing through Centricon®-10 filters (Millipore) (Eppendorf Refrigerated Multipurpose Centrifuge 5804 R, 2,000 rpm, 30 min, 20°C) and buffer exchanged with TE [Section 2.18.1]. The oligonucleotide concentration was measured using a spectrophotometer at OD_{260}. One optical unit of

oligonucleotide solution, in a 1 cm quartz cuvette, was estimated as 33 μg of DNA per ml. Oligonucleotides were aliquoted and stored at –20°C.

2.13 PREPARATION OF CLOSED-CIRCULAR PLASMID SUBSTRATES

Briefly, a synthetic oligonucleotide containing a single lesion was 5'-end radiolabelled with [γ-^{32}P]ATP, then annealed to complementary M13In (Dianov et al. 1998) single-stranded circular DNA, followed by primer extension to re-circularise the plasmid. Closed-circular double-stranded substrate was collected on a CsCl gradient (ρ = 1.55 g/ml). This method was previously described by Dianov and colleagues (Dianov et al. 1998), who generated M13In, by cloning the synthetic DNA duplex corresponding to the sequence 5'-ATATACCGCGGCCGGCCGATCAAGCTTATT-3' into the *Sma*I site of M13mp18 DNA (Accession number, M77815).

2.13.1 8-oxoguanine containing DNA substrate

The oligonucleotide 5′-ATATACCGCG[**8-oxoG**]CCGATCAAGCTTATT-3′ was 5′-end radiolabelled using T4 polynucleotide kinase (PNK) (NEB, Hitchin, UK) and [γ-^{32}P]ATP (6000 Ci/mmol). Briefly, 30 pmol of oligonucleotide was incubated with 100 μCi (16.7 pmol) of [γ-^{32}P]ATP and 20 units of T4 PNK for 2 h at 37°C in 1X T4 PNK Reaction Buffer (NEB) [Section 2.18.1]. Any unincorporated [γ-^{32}P]ATP was removed using a Micro Bio-Spin® P-6 chromatography column (Bio-Rad) pre-equilibrated with 10 mM Tris-HCl, pH 8.0. Substrate DNA was constructed by annealing 30 μg (12.5 pmol) of single-stranded M13In (Dianov et al. 1998) DNA with a 2.4-fold molar excess of the phosphorylated oligonucleotide in the presence of 1X Annealing Buffer [Section 2.18.1], by incubating at 90°C for 5 min, then slow cooling to room temperature. The extension reaction was performed for 4 h at 37°C in a 250 μl reaction mixture containing the annealed oligonucleotide-DNA, 500 μM dNTPs, 100

μM ATP, 100 μg T4 gene 32 protein (Roche), 35 units T4 DNA ligase (Roche) and 40 units T4 DNA polymerase (Roche) in 1X T4 DNA Polymerase Buffer (Roche) [Section 2.18.1]. The unincorporated primers were then removed by passing through a Centricon®-30 filter (Millipore) four times (Eppendorf Refrigerated Multipurpose Centrifuge 5804 R, 2,000 rpm, 30 min, 20°C). The substrate was then purified on a CsCl gradient (ρ= 1.55 g/ml, 55,000 rpm, 16 h, 20°C, Beckman Coulter Optima™ L-100 XP Ultracentrifuge VTI 65.1 (Fullerton, CA, USA)) before being fractionated. 2 μl of each fraction was analysed on a 1% (w/v) agarose gel by electrophoresis, then was exposed to a PhosphorImager screen (Bio-Rad) and analysed using Quantity One software (Bio-Rad). The closed-circular DNA containing fractions were then pooled and substrate DNA was butanol extracted to remove the ethidium bromide, then desalted and concentrated by passing through Centricon®-30 filter (Millipore) four times (as previously described), with buffer exchange into TE [Section 2.18.1]. Finally, the 8-oxoG containing DNA substrate was washed from filters using 400 μl of TE and stored at –20°C.

2.13.2 Abasic site containing DNA substrate

The 8-oxoguanine containing substrate [Section 2.13.1] was converted to an abasic site containing substrate by incubating 2 nM (20 μl) 8-oxoguanine containing substrate with 25 nM OGG1 enzyme at 37°C for 20 min in 1X BER Buffer [Section 2.18.1]. Mono-nucleotides were removed by passing through a Micro Bio-Spin® P-6 chromatography column (Bio-Rad) pre-equilibriated with 10 mM Tris-HCl, pH 8.0. Due to the instability of the abasic site containing DNA, the substrates were freshly prepared just before performing the BER reactions.

2.14 PREPARATION OF OLIGONUCLEOTIDE SUBSTRATES

Oligonucleotide substrates containing a nick or 1-nt gap lesion were constructed using 3 oligonucleotides; Top1(5'):Top2(3'):Bottom together in a 1:1:2 molar ratio [Fig 4.2A]. Oligonucleotides were gel purified before used [see Section 2.12]. 30 pmol of Top 1 oligonucleotide [Fig. 4.2B] was 5'-end radiolabelled by incubating with 20 μCi (3.3 pmol) of [γ-^{32}P]ATP and 5 units of T4 PNK for 1 h at 37°C in 1X T4 PNK Reaction Buffer (NEB) [Section 2.18.1]. Any unincorporated [γ-^{32}P]ATP was removed using a Micro Bio-Spin® P-6 chromatography column (Bio-Rad) pre-equilibrated with 10 mM Tris-HCl, pH 8.0. Phosphorylated Top1 (30 pmol) : Top2 (30 pmol) : Bottom oligonucleotides (60 pmol) [see Fig. 4.2B] were annealed in a 100 μl reaction containing 0.3 M NaCl and TE by incubating at 90°C for 5 min, then slow cooling to room temperature. The annealed substrates were electrophoresed at 5W, 4°C for 2 h on a 12% (w/v) native polyacrylamide gel [Section 2.19] in 0.5X TBE Buffer [Section 2.18.1] to check integrity.

2.15 *IN VITRO* BER REACTIONS USING WCE

2.15.1 Closed-circular DNA substrates

Each 50 μl BER reaction mixture contained 100 ng (20 fmol) of ^{32}P-labelled DNA substrate [see Section 2.13], 20 μM of each of the indicated dNTPs or ddNTPs, 1X BER buffer [Section 2.18.1], 0.5X RWDB buffer [Section 2.18.1], 2 mM ATP, 0.2 mM NAD^+, 0.4 mg/ml bovine serum albumin (BSA), 25 mM phosphocreatine (di-Tris salt, Sigma), 2.5 μg creatine phosphokinase (type I, Sigma) and 400 ng of carrier plasmid DNA (pUC18). Reactions were initiated by the addition of WCEs [see Section 2.2] at the indicated concentrations and incubated for the indicated times at 37°C. BER reactions were quenched by adding 2 μl of 0.5 mM EDTA, 2 μl of 10% (w/v) SDS and

2 µl of Proteinase K (5 mg/ml) and then further incubated for 30 min at 37°C. Substrate DNA was purified from the reaction mixture by phenol-chloroform extraction and filtered through a Micro Bio-Spin® P-6 chromatography column (Bio-Rad) equilibriated with 10 mM Tris-HCl, pH 8.0. Samples were evaporated (Eppendorf Concentrator 5301, 45°C, 1 h or to completion), then treated with *Hin*dIII (20 units) or *Hae*III (10 units) restriction endonuclease(s) (NEB) for 1 h at 37°C in buffers supplied by the manufacturer. An equal volume of Denaturing-PAGE Sample Loading Buffer [Section 2.18.1] was added and incubated at 90°C for 2–5 min to denature the DNA. Products were separated by electrophoresis on a 10% (w/v) denaturing polyacrylamide gel [Section 2.19] containing 7M urea in 1X TBE Buffer [Section 2.18.1] at 42W for the indicated time and then fixed in 10% (v/v) acetic acid for 10 min, before being vacuum-dried and exposed to storage phosphor screens. Images were scanned in a phosphorimager (Bio-rad) and bands were analysed using Quantity One software (Bio-Rad).

2.15.2 Oligonucleotide substrates

Each 20 µl BER reaction mixture contained 300 fmol of ^{32}P-labelled DNA substrate [see Section 2.14], 20 µM of each of the indicated dNTPs (unless otherwise stated), 1X BER Buffer [Section 2.18.1], 0.5X RWDB buffer [Section 2.18.1], 2 mM ATP, 250 µM NAD^+, 50 ng/µl BSA, 25 mM phosphocreatine (di-Tris salt, Sigma), 50 ng/µl creatine phosphokinase (type I, Sigma) and 20 ng/µl of carrier DNA (5'-AATAAGCTTGATCGGCCGGCCGCGGTATAT-3'). Reactions were initiated by the addition of WCEs [see Section 2.2] at the indicated concentrations and incubated for 20 min at 37°C. BER reactions were stopped by adding an equal volume of denaturing-PAGE Sample Loading Buffer [Section 2.18.1], then incubated at 90°C for 2–5 min. Products were separated by electrophoresis in a 20% (w/v) denaturing polyacrylamide

gel containing 7M urea in 1X TBE at 42W for 2 h, then exposed to storage phosphor screens and analysed using a phosphorimager and Quantity One software (Bio-Rad).

2.16 RECONSTITUTED BER REACTIONS

2.16.1 Oligonucleotide substrates

Each 10 µl BER mixture was reconstituted with purified enzymes and comprised of 300 fmol of ^{32}P-labelled oligonucleotide DNA substrate [see Section 2.14], 20 µM of each of the indicated dNTPs or ddNTPs (unless otherwise stated), 1X BER Buffer [Section 2.18.1], 1X RWDB Buffer [Section 2.18.1] and 0.1 µg/µl BSA. Reactions were initiated by the addition of recombinant human Pol β enzyme [see Section 2.1.3] at the indicated amounts and incubated for 20 min at 37°C. BER reactions were stopped by adding an equal volume of Denaturing-PAGE Sample Loading Buffer [Section 2.18.1] then incubated at 90°C for 2–5 min. Products were separated by electrophoresis on a 20% (w/v) denaturing polyacrylamide gel [Section 2.19] containing 7M urea in 1X TBE at 42W for 2 h, then exposed to storage phosphor screens and analysed using a phosphorimager and Quantity One software (Bio-Rad).

2.17 *IN VITRO* MUTAGENESIS ASSAY

2.17.1 Preparation of 1-nt gap containing M13 DNA substrate

Single-stranded M13mp18 DNA (Accession number: M77815) was isolated from *E. coli* JM109 and purified according to Kunkel *et al.* (Kunkel et al. 1987). The 5'-GCCTGCAGGTCGACT[**U**]TAGAGGATCCCCGGGTA-3' (33mer) oligonucleotide was used to construct a substrate containing a single uracil in closed-circular double-stranded M13mp18 DNA, as previously described (Dianov et al. 1998; Zhang and Dianov 2005). Briefly, single-stranded M13mp18 DNA was annealed with a

10-fold molar excess of the above uracil-containing oligonucleotide. The annealed oligonucleotide was extended using dNTPs, ATP, T4 gene 32 protein (Roche), T4 DNA ligase (Roche) and T4 DNA polymerase (Roche). Any unincorporated primer or incompletely synthesised DNA molecules were separated using isopycnic caesium chloride/ethidium bromide gradient (ρ= 1.55 g/ml) centrifugation. Fractions containing closed-circular DNA molecules were pooled together; butanol extracted to remove ethidium bromide, then desalted and concentrated using a Centricon®-10 filters (Millipore). Finally, the DNA substrate was washed from filters using 150 µl of TE and the concentration was estimated against DNA standards prior to aliquoting and storing at –80°C.

The 1-nt gap containing substrate was freshly prepared on the day of the experiment by incubating 200 ng of uracil-containing substrate with 30 ng human UDG at 37°C, for 20 min in 1X BER Buffer [Section 2.18.1]. 100 ng of human APE1 and 50 ng of human Pol β were added and the reaction was further incubated at 37°C for 20 min. The 1-nt gap substrate was purified from the reaction mixture by phenol-chloroform extraction before passing through a Micro Bio-Spin® P-6 chromatography column (Bio-Rad) pre-equilibirated with 10 mM Tris-HCl, pH 8.0. The sample was divided equally into 2 tubes (one for each extract used) and evaporated using Eppendorf Vacufuge Concentrator 5301, at 45°C for 1 h or until completion before resuspending in the desired volume of water.

2.17.2 BER reaction supplemented with Pol β

The BER reactions were carried out in a 50 µl reaction mixture containing 100 ng of 1-nt gap DNA substrate, 20 µM each of the dNTPs, 1X BER Buffer [Section 2.18.1], 0.5X RWDB buffer [Section 2.18.1], 2 mM ATP, 200 µM NAD^+, 0.4 mg/ml BSA, 25 mM phosphocreatine (di–Tris salt, Sigma) and 2.5 µg creatine phosphokinase

(type I, Sigma). Reactions were initiated by the addition of 100 μg WCE, or WCE extract supplemented with 40 ng Pol β, then incubated at 37°C for 30 min and stopped by the addition of 2 μl of 0.5 M EDTA, 2 μl of 10% (w/v) SDS and 2μl of proteinase K (5 mg/ml). After incubation for a further 30 min at 37°C, the substrate DNA was purified from the reaction mixture by phenol–chloroform extraction and filtered through a Micro Bio-Spin® P-6 chromatography column (Bio-Rad) pre-equilibrated with 10 mM Tris–HCl, pH 8.0. Each sample was divided equally between two tubes. To select 'mutant DNA', *in vitro* repaired DNA was treated overnight at 37°C with or without 40–60 units of *Xba*I restriction endonuclease and used for bacterial cell transformation. The reaction products were analysed by agarose gel electrophoresis.

2.17.3 Measuring mutation frequency

An equal amount (1 ng) of restriction endonuclease digested or undigested *in vitro* repaired DNA was introduced into *E. coli* XL-1 Blue by the calcium chloride method (Sambrook 1989). The transformed cells were diluted in SOB medium [Section 2.18.1] and were plated on LB agar [Section 2.18.1] containing 0.2 mM of IPTG and 40 μg/ml of X-gal, then incubated at 37°C for 16 h. After scoring the plaques as either colourless or blue, the mutation frequency was calculated as the ratio of the number of colourless plaques obtained from digested DNA, to the total number of plaques obtained from undigested DNA. Colourless plaques were picked, transferred into 1 ml of LB [Section 2.18.1] and were stored at 4°C overnight. The extracted phages were diluted in LB media and titrated against *E. coli* XL-1 Blue on LB agar plates containing IPTG and Xbal. An individual colourless plaque after secondary screening was used to isolate phage DNA for nucleotide sequence analysis.

2.17.4 Determination of mutation spectrum

Colourless plaques obtained from the secondary screening were used to isolate M13mp18 derived single-stranded DNA according to the manufacturer's protocol (QIAprep Spin M13 Kit, Qiagen) [see Section 2.7.1]. The DNA sequence was determined on an ABI 3100 Genetic Analyser with sequencing primers M13mp18-100 or M13mp 18-200 using an ABI PRISM BigDye Terminator (v3.1) Cycle Sequencing Kit (Applied Biosystems).

2.18 SOLUTIONS AND MEDIA

2.18.1 General Solutions

Annealing Buffer (10X):

500 mM Tris-HCl, pH 8.0, 200 mM KCl, 70 mM $MgCl_2$, 1mM EDTA.

BER Buffer (20X):

0.8 M HEPES-KOH, pH 7.8, 100 mM $MgCl_2$, 2 mM EDTA, 10 mM DTT.

Buffer I (for WCE preparation):

10 mM Tris-HCl, pH 7.8, 200 mM KCl, 1 µg/ml leupeptin, 1 µg/ml chemostatin, 1 µg/ml pepstatin, 4 µg/ml phenyl methyl sulfonyl fluoride (PMSF).

Buffer II (for WCE preparation):

10 mM Tris-HCl, pH 7.8, 600 mM KCl, 2 mM EDTA, 40% (v/v) glycerol, 0.2% (v/v) Nonidet P-40.

Denaturing-PAGE sample loading buffer:

95% (v/v) formamide, 20 mM EDTA, 0.02% (w/v) bromophenol blue, 0.02% (w/v) xylene cyanol.

DNA Lysis Buffer:

10 mM Tris-HCl, pH 8.0, 5 mM EDTA, 0.2% (w/v) SDS.

Native-PAGE Sample Loading Buffer (5X):

30% (v/v) glycerol, 0.25% (w/v) bromophenol blue, 0.25% (w/v) xylene cyanol.

NorthernMax® High Stringency Wash Solution (Ambion):

Equivalent to 0.1X SSC or SSPE, but with additional reagents.

NorthernMax® Low Stringency Wash Solution (Ambion):

Equivalent to 2X SSC or SSPE, but with additional reagents.

NorthernMax®-Gly Gel Prep/Running Buffer (1X) (Ambion):

25 mM Tris-HCl, pH 8.3, 192 mM glycine, 0.1% (w/v) SDS.

NorthernMax®-Gly Sample Loading Dye (Ambion):

Glyoxal-based sample load dye containing bromophenol blue and 10 µg/ml ethidium bromide.

Odyssey® Blocking Buffer (LI-COR® Biosciences):

PBS buffer containing 0.01% (w/v) sodium azide.

PCR Reaction Buffer (10X)(Thermoprime Plus DNA pol, Abgene):

750 mM Tris-HCl, pH8.8, 200 mM $(NH_4)_2SO_4$, 0.1% (v/v) Tween 20®.

Phosphate-buffered Saline (PBS):

0.1 M phosphate buffer, pH 7.4, 0.15 M NaCl.

RT Buffer (10X) (cDNA kit, Invitrogen):

200 mM Tris-HCl, pH 8.4, 500 mM KCl.

RWDB Buffer (1X):

25 mM HEPES-KOH, pH 7.8, 100 mM KCl, 12 mM $MgCl_2$, 1 mM EDTA, 2 mM DTT, 17% (v/v) glycerol.

SDS-PAGE Running Buffer (1X) (1X TGS, Bio-rad):

25 mM Tris-HCl, pH 8.3, 192 mM glycine, 0.1% (w/v) SDS.

SDS-PAGE Sample Loading Buffer (2X):

50 mM Tris-HCl, pH 6.8, 2% (w/v) SDS, 2 mM EDTA, 10% (v/v) glycerol, 5% (w/v) β-mercaptoethanol, 0.02% (w/v) bromophenol blue.

SDS-PAGE Transfer Buffer (1X) (1X TG(Bio-Rad) plus methanol):

25 mM Tris-HCl, pH 8.3, 192 mM glycine, 20% (v/v) methanol (VWR International Ltd, Poole, UK).

T4 DNA Polymerase Buffer (1X) (Roche):

50 mM Tris-HCl, pH 8.8, 15 mM $(NH_4)SO_4$, 7 mM $MgCl_2$, 100 µM EDTA, 10 mM 2-mercaptoethanol, 20 µg/ml bovine serum albumin (BSA).

T4 PNK Reaction Buffer (1X) (NEB):

70 mM Tris-HCl, pH 7.6, 10 mM $MgCl_2$, 5 mM dithiothreitol (DTT).

TAE Buffer (1X):

40 mM Tris-HCl, pH 8.0, 20 mM acetic acid, 1 mM EDTA.

TBE Buffer (1X):

89 mM Tris-HCl, pH 8.0, 89 mM boric acid, 2 mM EDTA.

TBS Buffer (1X):

20 mM Tris-HCl, pH 7.4, 0.5 M NaCl.

Tris-EDTA buffer (TE):

10 mM Tris-HCl, pH 8.0, 1 mM EDTA.

2.18.2 Media

LB Agar (per Litre):

15 g of Bacto-agar per 1 L of LB medium. Autoclave.

LB Medium (per Litre), pH 7.0:

10 g Bacto-tryptone, 5 g bacto-yeast extract, 10 g NaCl.

Autoclave.

SOB Medium (per Litre), pH 7.0

20 g Bacto-tryptone, 5 g bacto-yeast extract, 0.5 g NaCl, 2.5 mM KCl.

Autoclave, then add 10 mM $MgCl_2$.

2.19 POLYACRYLAMIDE GEL RECIPES

10% (w/v) Denaturing polyacrylamide gel containing 1X TBE:

7 M Urea, 10% (w/v) acrylamide:bis-acrylamide (19:1), 1X TBE, pH 8.0, 0.07% (w/v) ammonium persulfate (APS), 0.035% (v/v) N,N,N′,N′-Tetramethylethylenediamine (TEMED).

12% (w/v) Native polyacrylamide gel containing 0.5X TBE:

12% (w/v) Acrylamide:bis-acrylamide (19:1), 0.5X TBE, 0.07% (w/v) APS, 0.035% (v/v) TEMED.

10% / 20% (w/v) Native polyacrylamide gel containing 1X TBE:

10 / 20% (w/v) Acrylamide:bis-acrylamide (19:1), 1X TBE, 0.07% (w/v) APS, 0.035% (v/v) TEMED.

Chapter III

Results

CHARACTERISATION OF POL β OVEREXPRESSING CELL LINE (Ha)

3.1 INTRODUCTION

The patient lymphoblastoid cell line Ha [see Section 2.1.4], was initially selected for further analysis based on its two-fold increased sensitivity to ionising radiation (personal communication with Prof. I. Hickson) and was compared to a control, wild-type lymphoblastoid cell line Wt [see Section 2.1.4]. Preliminary investigations demonstrated that the Ha cells did respond differently to ionising radiation [Appendix A], and cells were indeed abnormal. A higher basal level of DNA damage was observed in Ha cells [Appendix B, Dr I. Dianova], and solid metaphase staining demonstrated aneuploidy in Ha cells, where Ha cells are tetraploid and Wt cells are diploid [Appendix C]. Initial biochemical characterisation of the two cell lines confirmed that the Wt cells were comparable to other known wild-type cells (AG09387) when repairing an 8-oxoguanine (8-oxoG) lesion [Appendix D, Dr S. Allinson], whereas the Ha cells were less efficient in repair [Appendix D, Dr S. Allinson]. Interestingly, preliminary data suggested that the BER protein, Pol β, was also overexpressed in Ha cells [Appendix E, Dr I. Dianova].

Ionising radiation can react directly with DNA causing strand breaks, or indirectly with oxygen molecules to generate reactive oxygen species (ROS), which consequently damage DNA by causing mutagenic and cytotoxic base damages (Ward 1988). Simple base damages are efficiently removed and repaired by the BER pathway (Friedberg 1995), which is a well co-ordinated series of enzymatic reactions, where it has been proposed that the lesion or substrate passes from one enzyme to the next enzyme in a sequential manner (Wilson and Kunkel 2000). Any imbalance of BER proteins will disturb the equilibrium of the pathway and may consequently affect the repair efficiency and capacity (Allinson et al. 2004). Pol β is the major DNA polymerase involved in BER, and the ability of Pol β to remove the dRP group

generated by AP endonuclease incision via its dRP lyase domain is recognised as the rate-limiting step in BER (Srivastava et al. 1998). The key step controlling BER fidelity is the polymerisation step, which depends on the ability of the polymerase to correctly insert the new nucleotide and continue DNA synthesis from it [reviewed by (Kunkel and Bebenek 2000)].

Pol β has been found to be overexpressed in about 30% of cancers, ranging from breast, prostate, ovarian, gastric, colorectal, bladder, lung, oesophageal, melanoma and stomach (Srivastava et al. 1999; Bergoglio et al. 2001; Albertella et al. 2005; Tan et al. 2005). Overexpression has been observed using both mRNA and protein microarrays where matched normal and tumour samples were compared (Albertella et al. 2005). Proteins are translated from mRNA, so protein overexpression is likely to be coupled to mRNA transcript overexpression. If however, mRNA levels are not elevated then protein overexpression could be attributed to higher rates of protein translation from the mRNA transcript or due to decreased protein degradation at the post-translational level.

The aim of the work presented in this chapter was to characterise the Pol β overexpressing Ha cells by confirming Pol β overexpression and then trying to elucidate the mechanism behind this phenomenon. The nature of the Pol β mRNA transcript in Ha cells was further assessed and Pol β protein stability was examined.

3.2 RESULTS

3.2.1 Characterisation of BER protein levels in Ha and Wt WCE

Preliminary Western blotting data at the start of this project suggested that Pol β protein was about 6-fold overexpressed in Ha cells compared to Wt control [Appendix E, Dr I. Dianova]. To confirm and expand upon this initial data, Western blot analysis using the Odyssey® infrared imaging system was further used to determine the levels of

various BER proteins in Ha whole cell extracts (WCE) compared to Wt that may suggest whether the highly coordinated BER pathway is disturbed in Ha cells. A sample of WCE (10 μg) was loaded in each lane and BER protein levels were normalised against β-actin as a loading control [Fig. 3.1F]. Similar levels of APE1 [Fig. 3.1A], XRCC1 [Fig. 3.1C] and PCNA [Fig. 3.1D] protein were observed in both the Ha and Wt WCE, although the levels of Pol β [Fig. 3.1B] protein in Ha WCE was determined as 5-fold elevated compared to Wt WCE. This result is comparable to the 6-fold Pol β overexpression observed using the ECL™ detection system (Amerhsam) [Appendix E, Dr I. Dianova]. This slight difference may be explained by variations during the multiple steps involved before quantification, such as; substrate reaction, exposure to film, length of exposure, background and the scanning step.

XRCC1 is found in a stable complex with DNA ligase III (Caldecott et al. 1994) and it is known that cells lacking XRCC1 have reduced levels of DNA ligase III (Caldecott et al. 1995). Thus XRCC1 serves as a stability factor for DNA ligase III and subsequently the levels of XRCC1 also reflects the levels of DNA ligase III in cells. However, as XRCC1 levels between the Ha and Wt cells are equivalent, it may be presumed that DNA ligase III levels are also equivalent. Interestingly, PARP-1 [Fig. 3.1E] expression in Ha WCE showed more 85 kDa caspase cleavage fragments, which is a hallmark of apoptosis (Kaufmann et al. 1993; Affar et al. 2001). These results give an early indication that BER may be perturbed due to a misbalance of BER enzymes.

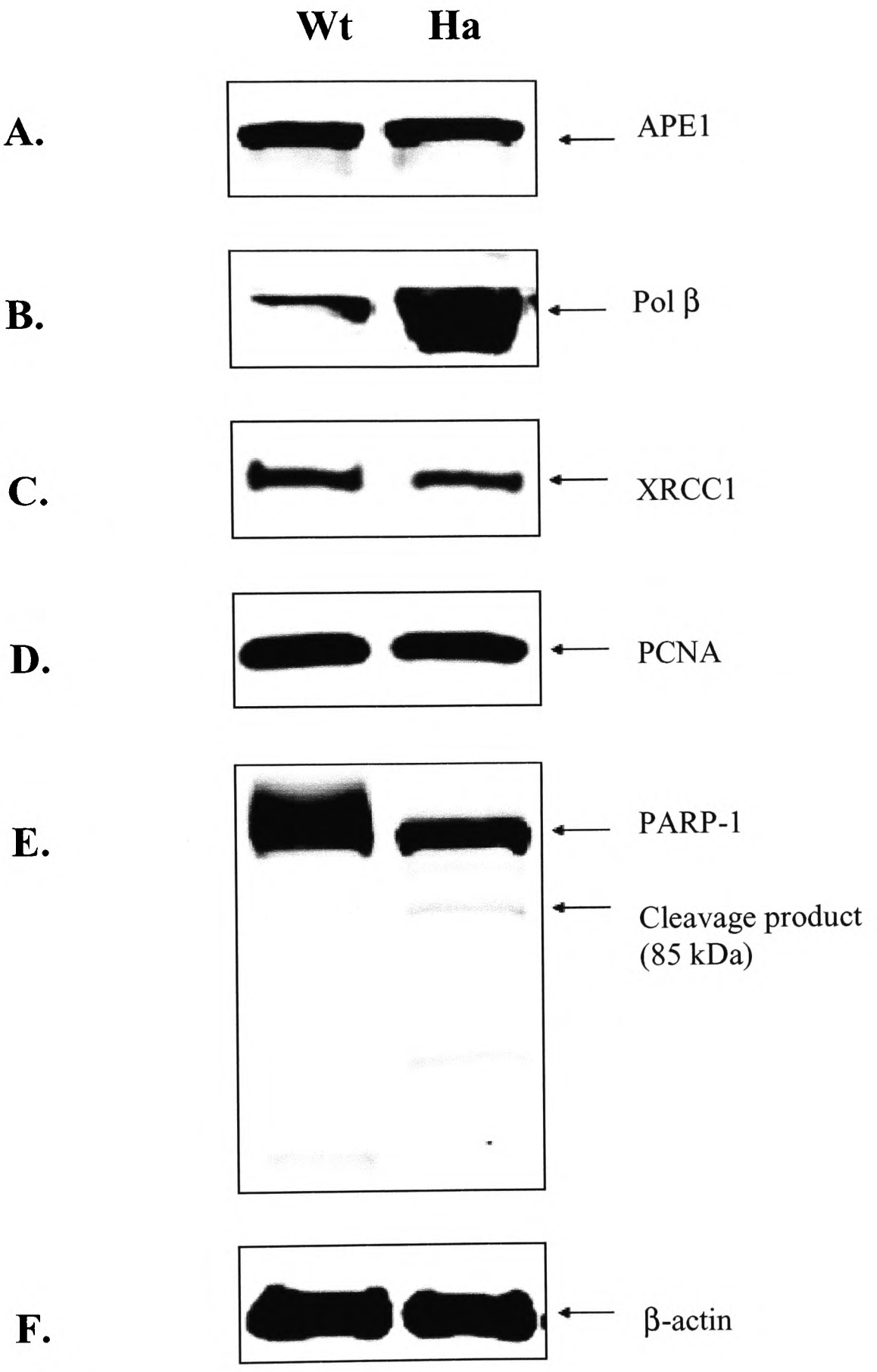

Figure 3.1 Western blot analysis of BER proteins in Ha and Wt WCE. 10 μg of WCE was separated by 10% (w/v) SDS-PAGE, transferred onto a PVDF membrane and immunoblotted with the indicated antibodies using the Odyssey® immunofluorescence method [see Section 2.8.1]. **(A)** anti-APE1, 34 kDa band. **(B)** anti-Pol β, 39 kDa band. **(C)** anti-XRCC1, 69 kDa band. **(D)** anti-PCNA, 29 kDa band. **(E)** anti-PARP-1, 113 kDa band. **(F)** anti-β-actin, 42 kDa band. Each experiment was repeated 3 times and representative blots are shown.

3.2.2 Increased Pol β mRNA levels in Ha cells

Proteins are translated from messenger RNA (mRNA) transcripts within the ribosomes by transfer RNA (tRNA) molecules, therefore an increased protein level of Pol β observed in Ha cells may be due to increased mRNA levels which can translate into increased amounts of protein. Various methods have been successfully used to determine levels of mRNA transcripts. Even though highly-sensitive, high-throughput real-time PCR based methods have been developed, the more traditional Northern blotting method is still commonly used for gene quantitation because it provides a direct relative comparison of mRNA abundance between samples on a single membrane. Information about transcript size and alternatively spliced transcripts can also be determined, however, high quality RNA samples are essential.

A two-step, SYBR® Green I based real-time quantitative PCR method was used to confirm mRNA levels in Ha and Wt, where the reverse-transcription reaction is separate from the real-time PCR step. SYBR® Green I dye emits fluorescence when bound to double-stranded DNA and specific amplicon detection is monitored by measuring the increase in fluorescence throughout each PCR cycle (excitation and emission maxima: 494 nm and 521 nm, respectively) [Appendix Fi]. DNA binding by SYBR® Green I is non-specific, so care was taken to design specific primers [see Section 2.10] yielding a specific PCR product, which could be verified using a dissociation curve analysis [Appendix Fii]. During PCR amplification a point is reached in which a sufficient number of amplicons have accumulated above the background, and the cycle number at which the fluorescence generated within a reaction crosses the threshold is termed the threshold cycle (C_t). The C_t value is a useful indicator and can be inversely correlated to the logarithm of the initial copy number. PCR conditions were optimised [see Section 2.10.1], initially by independently varying

forward and reverse primer concentrations to find the optimal primer concentrations for each gene of interest. The best primer concentrations yielding the lowest C_t values for Pol β were 300 nM forward and 900 nM reverse primer [Fig. 3.2Ai], and for β-actin endogenous control, 300 nM forward and 300 nM reverse primer [Fig. 3.2Aii]. Secondly, a suitable amount of cDNA template within the linear range (0.1 – 1 µl) of PCR amplification was used for the qPCR reactions. cDNA (50 ng/µl) was synthesised from 1 µg of total RNA in a 20 µl reaction, and the assumption was made that the reverse transcriptase amplification efficiency for Ha and Wt sample was equivalent. A standard curve method for relative quantification of gene expression levels was used. The quantity of Pol β for each experimental sample; Ha and Wt, was first determined using a standard curve, log input vs. C_t [Fig. 3.2Bi], and then expressed relative to a single calibrator sample, in this case, Wt, which was designated as 1-fold (Livak 1997). The same cDNA was used to find the relative amounts of β-actin for each sample, Ha and Wt, using a standard curve [Fig. 3.2Bii], and Pol β samples were normalised against β-actin housekeeping gene. Ha was found to be 1.4-fold overexpressed compared to Wt, after normalisation against β-actin.

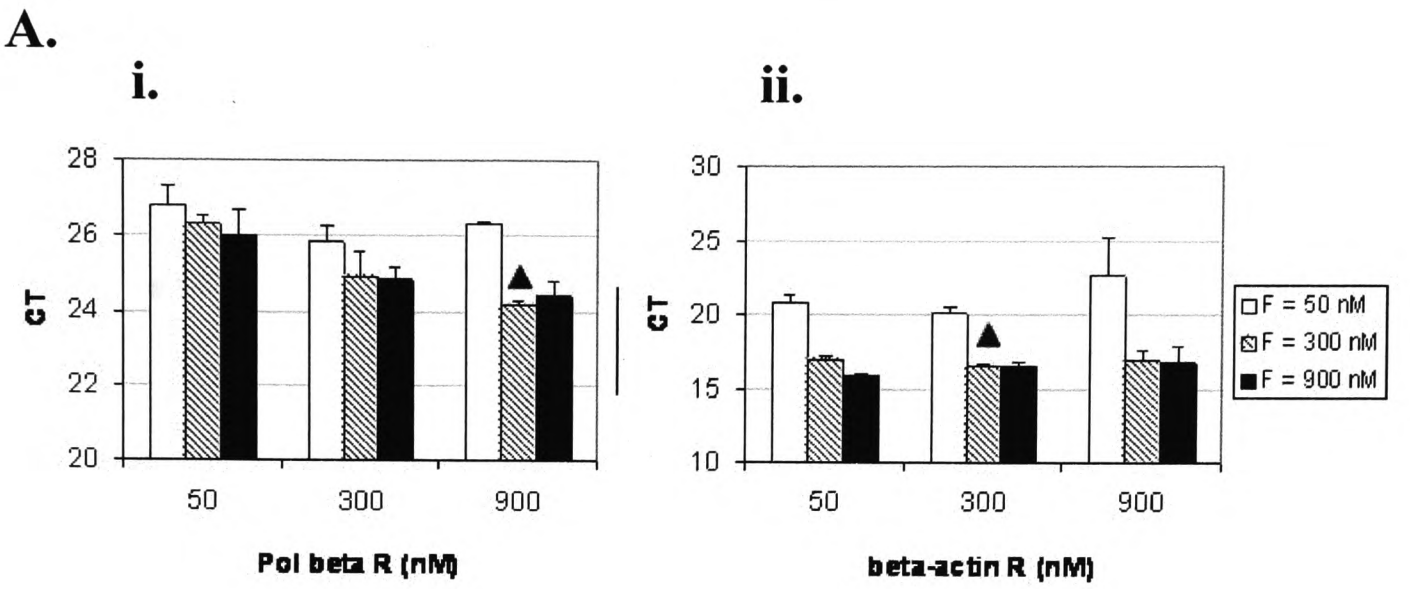

Figure 3.2 Real-time quantitative PCR primer concentration and template optimisation. **(A)** Primer concentration optimisation for **(i)** Pol β and **(ii)** β-actin. F; forward primer, R; reverse primer, ▲; optimal primer concentration. **(B)** Standard curve plots: log of input vs. C_t value for **(i)** Pol β and **(ii)** β-actin.

Northern blotting allows the RNA sample to be monitored at each experimental step. Messenger RNA makes up about 1-5% of total RNA, so samples are hard to visualise when separated on an agarose gel and stained with ethidium bromide [Fig. 3.3A], however, it is important to visualise the RNA size ladder in order to calculate the migration distances of RNA. Messenger RNA samples were enriched from total RNA to allow the detection of rare transcripts. Riboprobes were designed specifically for Pol β mRNA (based on Genbank sequence NM_002690), and hybridised to Northern membranes [Fig. 3.3B]. The Pol β transcript is 1.25 kb in size, and a corresponding band of this size was observed. A 5 kb band was also observed, which coincides with the size of 28S ribosomal RNA. Ribosomal RNAs should have been removed with the GenElute™ kit (Sigma) and indeed no rRNA was visible on the agarose gel [Fig. 3.3A], however, some residual rRNA must have been present in the mRNA sample. This band could be completely eliminated by making hybridisation conditions more stringent, either by increasing temperature or using lower salt concentration washes. An increasing amount of Wt mRNA was loaded in lanes 1 to 3 [Fig 3.3], and a linear signal intensity was observed. Equivalent amounts of Ha and Wt mRNA were loaded in lanes 3 and 4 respectively, and the Pol β signal observed in the Ha lane was significantly stronger compared to the Wt [Fig 3.3B]. However, a loading control was needed, before quantification could be done. Pol β [Fig. 3.3Cii] and β-actin [Fig. 3.3Ciii] X-ray film images were captured using the Bio-Rad GS-710 imaging densitometer and then mRNA levels were quantified using the Quantity One® image analysis software (Bio-Rad). After normalisation of results against β-actin housekeeping gene, Pol β was found to be 1.4-fold overexpressed at the mRNA level in Ha cells compared to Wt [Fig. 3.3Ci], which matched exactly with the qPCR result.

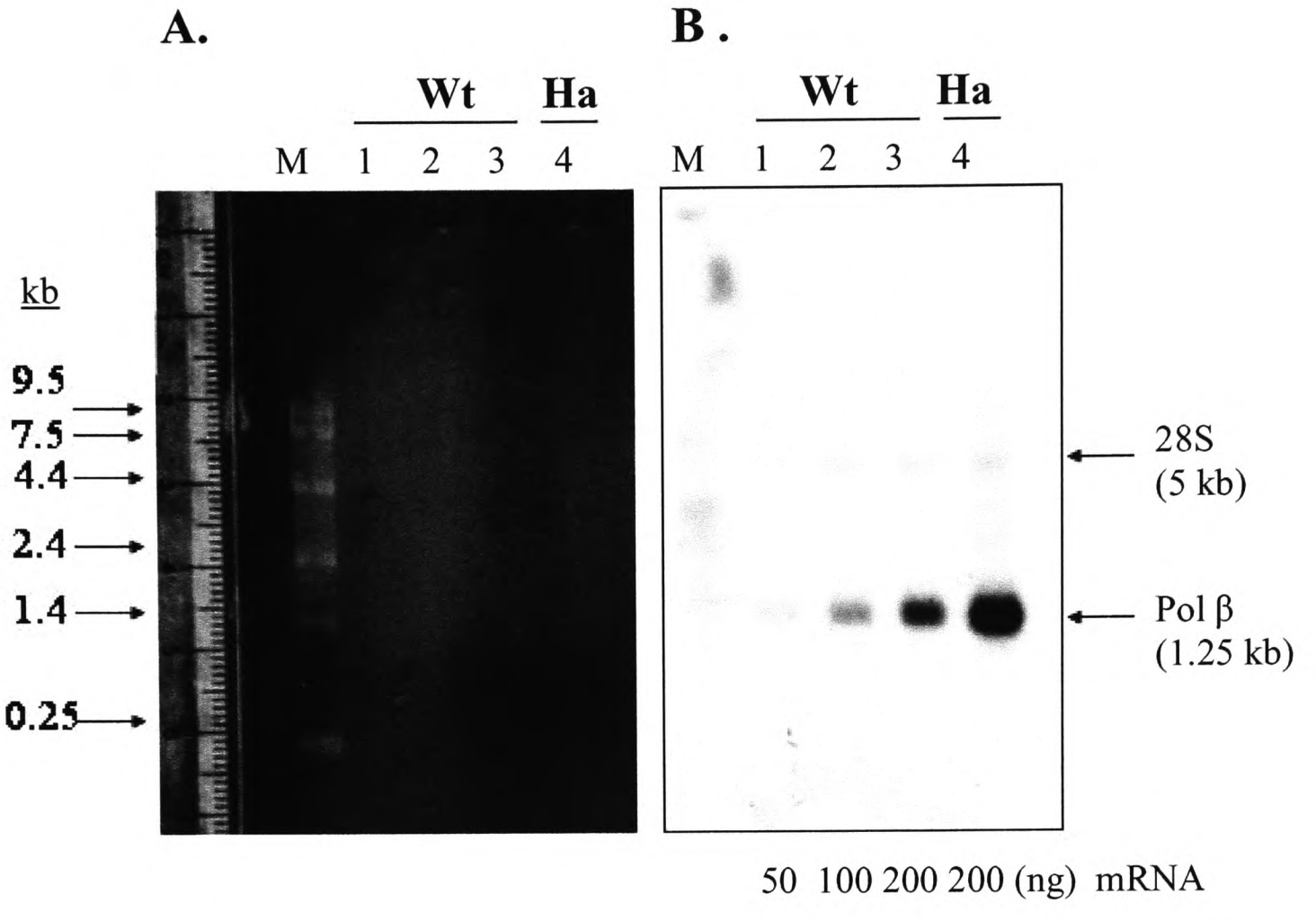

Figure 3.3 Northern blot analysis of Pol β mRNA levels in Ha and Wt cells. 50, 100, 200 ng of Wt mRNA was loaded in lanes 1, 2 and 3 respectively. 200 ng of Ha mRNA was loaded in lane 4. M; RNA ladder (NEB). **(A)** mRNA was separated on a 1% (w/v) agarose gel. RNA ladder is shown. **(B)** mRNA was transferred onto a nylon filter and probed with Pol β riboprobe. **(C) (i)** Graphical representation of Pol β mRNA expression, normalised against β-actin. **(ii)** Expression of sense Pol β transcripts in Ha and Wt mRNA. **(iii)** Filters were stripped and re-probed with β-actin to establish mRNA loading levels and confirm mRNA integrity.

3.2.3 Pol β *cis*-acting promoter and mRNA coding sequences

Protein expression levels can be regulated by the quality and quantity of mRNA transcripts, and also by the amount of protein translation. Northern blotting [Fig. 3.3] and real-time qPCR [Fig. 3.2] showed a 1.4-fold greater expression of Pol β mRNA and Western blotting demonstrated a 5 to 6-fold greater expression of Pol β protein in Ha cells compared to the Wt control cells [see Fig. 3.1B].

Ha and Wt cells DNA were prepared for sequencing using the dideoxy-mediated chain terminating method with fluorescent labels. Sequencing data were displayed in chromatograms where each DNA base was represented by a specifically coloured peak (A = green, C = blue, G = black, T = red). From each chromatogram, the section of good quality sequencing data of at least 200 bases was selected and aligned using BLAST 2 Sequences program (http://www.ncbi.nlm.nih.gov/blast/bl2seq/wblast2.cgi) against the Pol β mRNA (NM_002690) or the Pol β promoter (J04201) sequences in Genbank. The anti-sense sequences obtained using the reverse primers (R and r) were converted to the sense strand prior to alignment, using BCM Search Launcher Sequence Utilities; Reverse Complement program (http://searchlauncher.bcm.tmc.edu/seq-util/seq-util.html).

To compare the Ha and Wt mRNA gene transcripts, first-strand cDNA was synthesised from total RNA, before being amplified using the polymerase chain reaction and sequenced using a capillary genetic analyser. Forward primers a, b, and c, and the reverse primer r were used for sequencing [Table 2.1, Fig. 3.4A]. The specificity of sequencing primers a, b, and c were tested to see if the expected size PCR products were produced when the forward primers were paired with the reverse primer r [Fig. 3.4A]. The ar (1146 bp), br (715 bp) and cr (357 bp) PCR bands correlated well with the expected band sizes [Fig. 3.4C]. A complete sequence of the Pol β mRNA was

obtained for both Ha and Wt, using the overlapping sequences produced by each primer a, b, c and r [see Fig. 3.4A]. Both the Ha and Wt showed 100% sequence identity against the published Pol β mRNA (Genbank sequence: Homo sapiens polymerase (DNA directed), beta (POLB), mRNA (NM_002690)) (SenGupta et al. 1986). Therefore, the Ha and Wt mRNA transcripts are normal at the nucleotide level.

To compare the promoter region of Ha and Wt samples, genomic DNA was isolated from cells using a phenol-chloroform extraction method, before amplification using PCR and sequencing with forward primers A, B, C and D and the reverse primer R [Table 2.1, Fig. 3.4A]. Sequencing primers were designed against the Human Pol β gene, exons 1 and 2 (J04201). Specificities of sequencing primers were verified by PCR product sizes and indeed, primer pairs AR (1344 bp), BR (962 bp), CR (705 bp) and DR (310 bp) did produce bands of the expected sizes [Fig. 3.4B]. A complete Pol β promoter sequence for both the wild-type control (Wt) and Pol β overexpressor (Ha) was obtained from the overlapping sequences produced by each primer A, B, C, D and R [see Fig. 3.4A].

Alignments between the Ha and Wt sequence showed 100% homology, so no differences were found between the Ha and Wt Pol β promoter region at the nucleotide level. However, both Ha and Wt only showed 99% sequence similarity when compared to the database Pol β promoter region (Genbank sequence: Human beta-polymerase gene, exons 1 and 2, (J04201)) (Widen et al. 1988). An additional guanine residue was found in both Ha and Wt sequences situated between bases -34 and -35 downstream to the Pol β transcription start site, and is flanked by a region of dyad symmetry (ATF/CRE) and the third high affinity Sp1 binding domain [Fig. 3.5A]. This result represents a variation to the first published sequence of the Pol β promoter region (J04201) by Widen and colleagues in 1988 (Widen et al. 1988). The sequenced Pol β

promoter region was submitted to the nucleotide-nucleotide BLAST (blastn) program (http://www.ncbi.nlm.nih.gov/blast/) to search for other homologues in the public genome databases. A full length Pol β gene sequence from the National Institute of Environmental and Health Sciences (NIEHS) Environmental Genome Project was identified (Genbank sequence: Homo sapiens DNA polymerase beta (POLB) gene, complete cds. (AF491812)) (NIEHS-SNPs, Environmental Genome Project, NIEHS ES15478, Department of Genome Sciences, Seattle, WA (http://egp.gs.washington.edu). This Pol β sequence also shows the same additional guanine that I observed in both Ha and Wt samples, therefore indicating that the original Human beta-polymerase gene, exons 1 and 2 (J04201) sequence was incorrect.

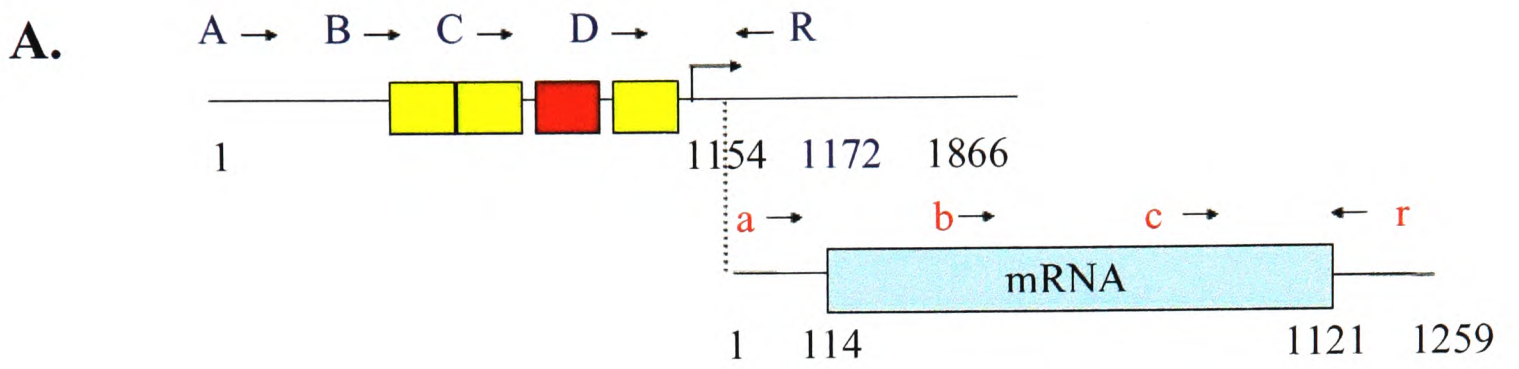

Pol β promoter
(J04201)

B.

M AR BR CR DR

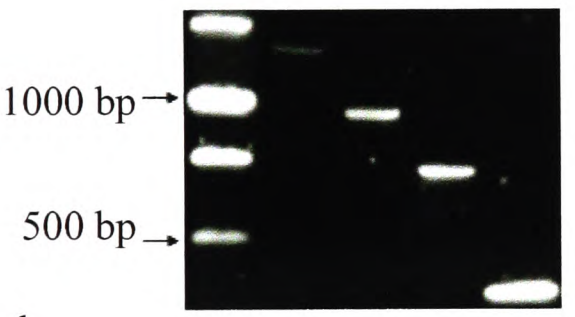

Expected product size	1344	962	705	310 bp

Pol β mRNA
(NM_002690)

C.

M ar br cr Primer pair

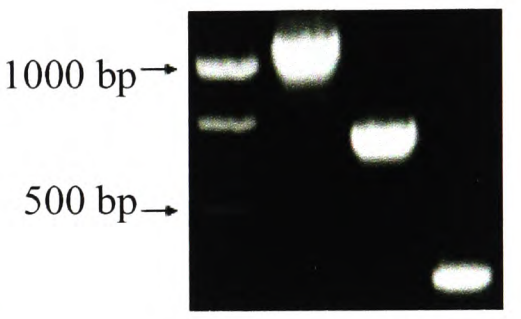

1146	715	357 bp

Figure 3.4 A schematic representation of the overlapping human DNA Pol β promoter (J04201) and Pol β mRNA (NM_002690) Genbank sequences illustrating sequencing primers. **(A)** Pol β promoter contains three high affinity Sp1 transcription factor binding domains (yellow boxes) and one decanucleotide region with perfect dyad symmetry (red box). Base +1 of the Pol β mRNA corresponds to base +1154 on the Pol β promoter sequence. Positioning of PCR/sequencing primers along each template are shown. **(B)** Validity of Pol β promoter sequencing primers were confirmed based on the expected size of PCR products for each illustrated primer pairs [Fig. 3.4A]. **(C)** Validity of Pol β mRNA sequencing primers were confirmed based on the expected size of PCR products for each illustrated primer pairs [Fig. 3.4A]. PCR products were analysed on a 1% (w/v) agarose gel and visualised under UV by ethidium bromide staining. M; 1 kb DNA ladder (Promega). The full-length PCR products AR (Pol β promoter) and ar (Pol β mRNA) were used as templates for sequencing reactions. See Table 2.1 for primer details and cycling conditions.

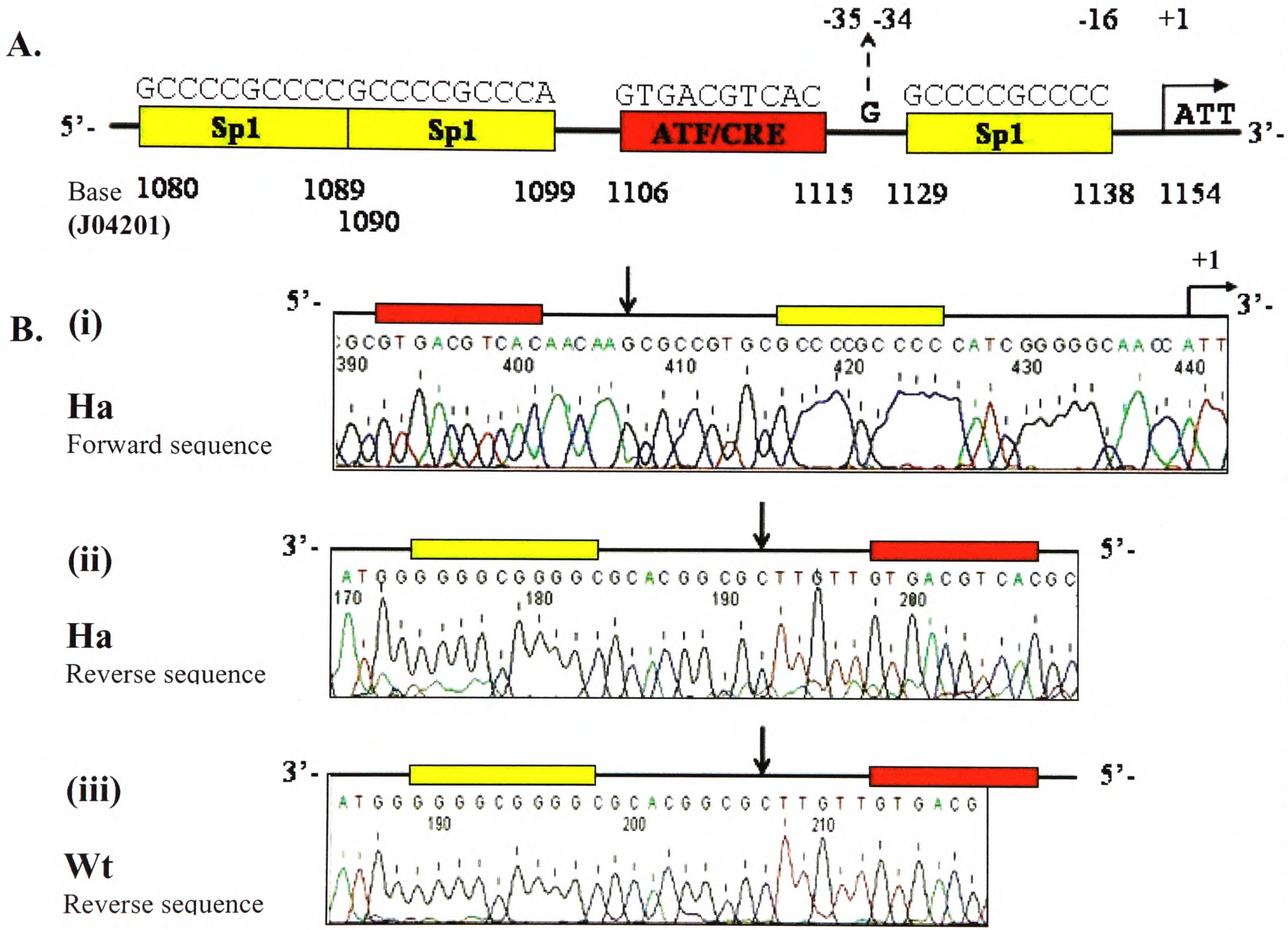

Figure 3.5 Insertion of a guanine residue in human DNA Pol β promoter sequence (J04201).
(A) The *cis*-acting promoter sequence contains three GC-rich Sp1 binding domains and one ATF/CRE sequence with perfect dyad symmetry. An additional guanine residue located between position -34 and -35 of the Pol β gene was found in both the Ha patient and Wt control promoters. **(B)** Sequencing chromatograms illustrating additional guanine in **(i)** Ha forward strand, **(ii)** Ha reverse strand, **(iii)** Wt reverse strand. Nucleotide residues are numbered based on the Genbank sequence. The major transcription start site is designated as +1.
ATF/CRE; activating transcription factor/cAMP response element.

3.2.4 CREB transcription initiation/levels

So far, I have deduced that the Ha mRNA transcript is normal but more abundant which may partially explain the increase in Pol β protein levels. In eukaryotes, gene expression is regulated through *cis*-elements in promoters and their cognate DNA-binding elements. The human Pol β core promoter [Fig. 3.5A] comprises of approximately 100 bp 5'-upstream of the transcription start site. In addition to the three Sp1 boxes and ATF/CRE sequence located -48 to -41 bp upstream of the transcription start site, there is also an Inr (initiator) element that binds TFII-I, a RNA polymerase II accessory protein. The ATF/CRE element is recognised by ATF/CREB family members that includes CREB1, ATF-α1, ATF-1 and ATF-2. Wilson and colleagues previously demonstrated that phosphorylated CREB-1 stimulates the Pol β promoter by recruiting more pre-initiation complex at the promoter and by stimulation of promoter clearance after open complex formation (Narayan et al. 1996).

Therefore, the levels of CREB-1 (inactive) and phosphorylated CREB-1 (pCREB-1) (active) were investigated in Ha and Wt cells in order to elucidate whether the increase in Pol β transcription in Ha cells is mediated through pCREB-1 activation of the CRE element. 10 μg of WCE was separated on SDS-PAGE and immunoblotted with either CREB-1 or pCREB-1 antibodies (Abcam) [Fig. 3.6A]. The CREB antibodies are mutually exclusive, so CREB-1 antibodies do not detect pCREB-1 and vice versa. Bands were also normalised against a β-actin loading control. Interestingly, approximately 2-fold more CREB-1 and pCREB-1 protein was observed in Wt WCE compared to Ha [Fig. 3.6B], possibly indicating more CRE activation in Wt cells. However, the proportion of pCREB-1 to total CREB-1 is equivalent between the Wt and WCE [Fig. 3.6C].

A.

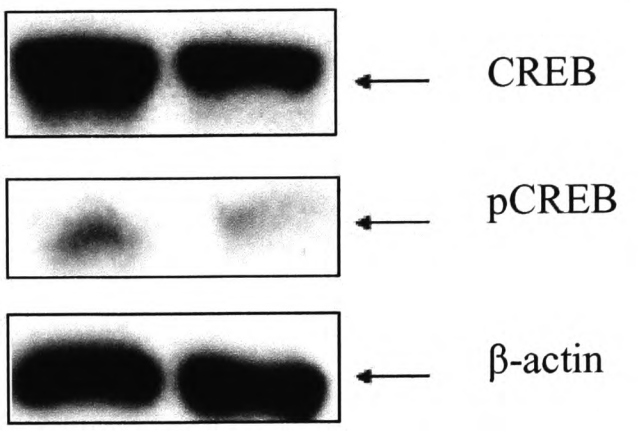

B.

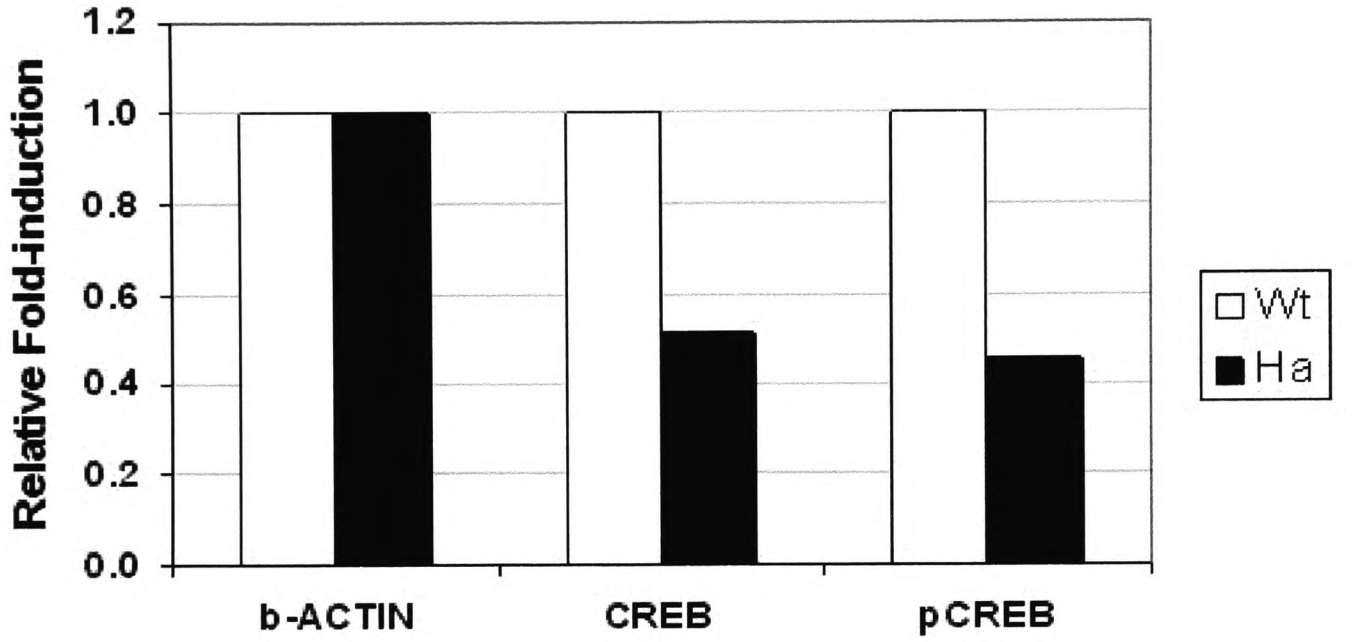

C.

	Wt	Ha
CREB	17.77 ± 0.90	9.14 ± 1.25
pCREB	1.52 ± 0.97	0.80 ± 0.26
β-actin	16.78 ± 2.11	16.78 ± 2.09
$\frac{\text{pCREB}}{\text{CREB}}$	7.9 %	8.0 %

Figure 3.6 Western blot analysis of CREB transcription factor levels in Ha and Wt cells. 10 µg of WCE was separated on SDS-PAGE, transferred onto a PVDF membrane and immunoblotted with the indicated antibodies. Experiment was performed in duplicate **(A)** Western blot with indicated antibodies, anti-CREB, 43 kDa, anti-pCREB, 43 kDa, anti-β-actin, 29 kDa. **(B)** Relative fold-induction normalised against β-actin. **(C)** Average expression levels based on arbitrary intensity values, and standard deviations. Each experiment was repeated 3 times and representative blots are shown.

3.2.5 Pol β protein stability

Levels of Pol β protein were approximately 5 to 6-fold higher in Ha versus Wt cells but only a 1.4-fold difference in mRNA was observed, this discrepancy could indicate that Pol β protein turnover is perturbed. This implies that either more Pol β protein is being translated in Ha cells, or Pol β protein is being degraded less in Ha, thus resulting in an overall higher Pol β protein level. Northern blotting data and sequencing data did not indicate any differences between the Ha and Wt mRNA transcripts in terms of sequence, size, or splice variants. Translation of proteins is controlled by the ribosomes, so it is more likely that post-translational differences may occur between Ha and Wt cells. We looked at Pol β protein stability by treating cells with cycloheximide, a protein synthesis inhibitor. Cycloheximide is diluted in DMSO, and so a DMSO diluent control [Fig. 3.7, Lanes 7 and 14] was also incorporated to ensure that it had no effect on cells. Cells were treated with cycloheximide for up to 24 h, after each time point WCEs were generated [see section 2.11] and equivalent amounts of WCE protein (20 μg) were analysed by SDS-PAGE and immunoblotting. IκBα was used as a positive control to test that cycloheximide treatment of cells was effective as it has an estimated half-life of around 1-2 h (Rice and Ernst 1993). It is noteworthy that significantly more Pol β was observed in Ha cells compared to Wt [Fig. 3.7A, Lanes 7 and 14], correlating well with previous Western blotting data [Fig. 3.1], although equivalent amounts of IκBα were observed between Ha and Wt cells, serving as a loading control [Fig. 3.7B, Lanes 7 and 14]. Pol β protein was stable even after 24 h in both Ha and Wt cells [Fig. 3.7A], whereas degradation of IκBα was clearly observed within 1-2 h [Fig. 3.7B]. The half-life of IκBα was estimated to be between 2-4 h and 1-2 h for Ha and Wt respectively [Fig. 3.7B].

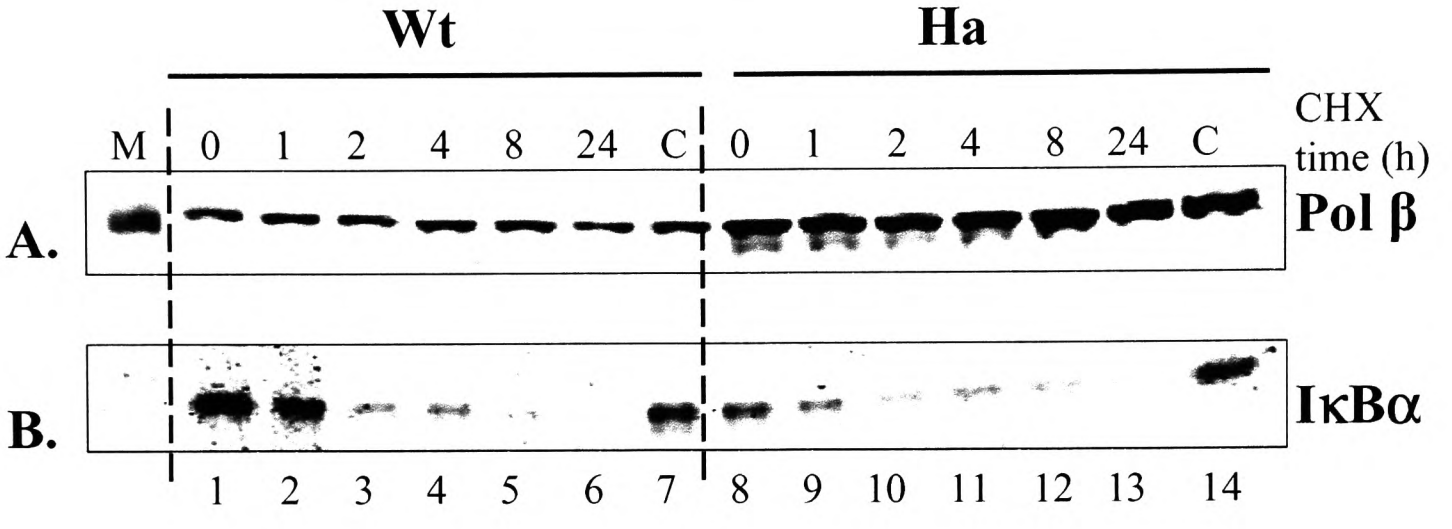

Figure 3.7 Analysis of Pol β protein stability following cycloheximide treatment. Ha and Wt cells were treated with 50 μg/ml cycloheximide for the indicated times and harvested. 20 μg of WCE was separated on SDS-PAGE, transferred onto a PVDF membrane and immunoblotted with the indicated antibodies. **(A)** anti-Pol β, 39 kDa band. **(B)** anti-IκBα, 37 kDa band. C; DMSO only control, M; Protein marker (Bio-rad). (Note, the 0 h time-point represents a sample that has not been treated with cycloheximide). Each experiment was repeated 3 times and representative blots are shown.

3.3 CONCLUSIONS

In this chapter, I have confirmed that Pol β protein is overexpressed in Ha cells compared to Wt, and tried to elucidate the mechanisms governing this by investigating Pol β mRNA levels and transcriptional control. I found the Pol β promoter and mRNA gene sequence in Ha cells to be normal and I also characterised Pol β protein stability. Western blot analysis showed that Pol β protein was 5 to 6-fold overexpressed in Ha cells compared to Wt. Northern blotting and a SYBR® Green I based real-time qPCR method confirmed that Pol β mRNA was also slightly overexpressed in Ha cells. Thus, it can be concluded that Pol β protein overexpression may partially be explained by Pol β mRNA overexpression.

Interestingly, Pol β mRNA was only 1.4-fold overexpressed in Ha cells, this equates to ~4-fold more Pol β protein than mRNA overexpression in Ha cells. All results were normalised against the β-actin housekeeping gene. Although technological advances have allowed increasingly accurate analyses of mRNA and protein expression levels, it is still difficult to correlate protein abundance with mRNA levels in a cell. These quantification methods may still have significant error noise in both the protein and mRNA experiments. There are a multitude of complex post-transcriptional mechanisms involved in converting mRNA into protein, which are still not fully understood. Protein turnover also needs to be considered, rates of degradation or synthesis govern a protein's half-life *in vivo* and these factors may be altered under different cellular conditions to vary overall protein expression levels.

In this study, a fairly crude Western blot method was used to measure protein levels. However, mRNA abundance was quantified using two different methods; real-time qPCR and Northern blotting. Real-time qPCR is a highly sensitive technique whereas Northern blotting technique is comparable to Western blotting in terms of

'crudeness'. Regardless, both methods of mRNA level detection gave the same result (1.4-fold Pol β overexpression in Ha).

I checked the integrity of the Pol β mRNA gene transcript. No variations were found between Ha and Wt by sequencing and Northern blot analysis also showed mRNA transcripts to be of the same size. Ha and Wt Pol β proteins were also the same size as demonstrated by Western blot analysis, so splice variants were ruled out. The mRNA transcripts were thus determined to be normal.

To elucidate why more mRNA is expressed in Ha cells, we investigated the possible regulation of the Pol β promoter. Firstly the *cis*-acting promoter was sequenced, and again no variations were found between Ha and Wt cells. An additional guanine residue was observed between bases -34 and -35 from the transcription start site of Ha and Wt Pol β sequences when compared to the DNA promoter sequence (Genbank, J04201) (Widen et al. 1988). However, comparison with a more recent complete Pol β sequence (Genbank, AF491812) showed the guanine to be normal and part of the Pol β sequence.

The Pol β promoter contains an 8 bp palindromic CRE sequence, which members of the ATF/CREB family of proteins can bind to, for example, CREB-1, ATF-α1, ATF-1 and ATF-2 [reviewed by (Roesler et al. 1998)]. The exact mechanism of Pol β promoter activation is still not fully understood. Several studies have suggested that Pol β expression is upregulated by phosphorylated CREB-1 (pCREB-1) acting on the CRE element, where CREB-1 is phosphorylated at serine 133 by cellular protein kinase A activity (Sheng et al. 1991; Wang et al. 2001). And so, we investigated levels of CREB-1 and pCREB-1, and found a lower total amount of CREB-1 in Ha, compared to Wt, but the proportion of pCREB-1 to CREB-1 in Ha and Wt cells were equivalent. Nevertheless, this result indicates a lower amount of pCREB-1 in Ha cells, so in order

for mRNA to be overexpressed in Ha cells, there must be other mechanisms involved in Pol β transcription. Indeed, recently TEIF (telomerase elongation initiation factor) has been found to activate the Pol β promoter at the GC-rich Sp-1 elements (Zhao et al. 2005), and ATF-α and ATF-2 variants have been implicated as negative regulators of the Pol β promoter (Pescini et al. 1994; Chyan et al. 2003).

Another interesting finding was that there was ~4-fold more protein overexpressed compared to mRNA overexpressed. This discrepancy between levels of mRNA and protein expression could be attributed to protein turnover. Rates of degradation or synthesis govern a protein's half-life *in vivo*. More protein translation and less protein degradation, leads to an overall abundance of protein. I had already confirmed that the mRNA gene transcript in Ha cells was normal, so therefore the protein should be normal too. Proteins are translated using ribosomes and translation machinery. I investigated the stability of Pol β protein using a protein synthesis inhibitor, cycloheximide, and found Pol β protein was still stable after 24 h.

To summarise, Ha lymphoblastoid cell line overexpresses Pol β protein and this is likely in part to be a consequence of Pol β mRNA overexpression in Ha cells compared to Wt. Overexpression of mRNA in Ha cells is likely to be a result of altered Pol β promoter activation. Indeed, analysis of one activator (CREB-1) did produce a variation in protein levels between Ha and Wt and although this was not able to explain the activation of Pol β expression, it does suggest a variation between the two cell lines. Further investigation into levels of possible Pol β promoter regulators, such as TEIF and ATF proteins, may help to elucidate how Pol β mRNA in Ha cells are overexpressed. Pol β protein is a stable protein with a half-life greater than 24 h. The actual half-life would need to be determined by using longer time points.

Chapter IV

Results

EFFECT OF POL β OVEREXPRESSION ON BER

4.1 INTRODUCTION

Ha cells were confirmed by Western blot analysis to overexpress Pol β protein by approximately 5 to 6-fold, whereas the levels of other BER proteins (APE1, PCNA, XRCC1) were equivalent compared to Wt cells. Thus Ha cells are a good cell line for investigating the effects of Pol β overexpression on BER. Pol β is the major BER DNA polymerase and determines whether repair is routed through the short-patch or long-patch BER sub-pathway (Podlutsky et al. 2001). As BER is highly co-ordinated, we may expect variations in the expression levels of BER proteins to perturb the efficiency and capacity of repair. Whereas underexpression of BER enzymes is likely to attenuate repair and prolong the existence of lesions or repair intermediates (Cabelof et al. 2003), overexpression of various BER proteins may be associated with cancer and disease by compromising fidelity or making a repair intermediate which can not be repaired by the next enzyme in chain. To investigate BER activity, *in vitro* assays were employed to monitor the repair of certain lesions using cell extracts. Oxidative base damages are the main lesions dealt with by the BER pathway, and during repair of these yield abasic site and single-strand break repair intermediates. Ha and Wt WCE were used to find out whether Pol β overexpression might affect the repair capacity of abasic site and 1-nt gap BER lesions.

The aim of this chapter is to elucidate whether Pol β overexpression has any effect on the repair capacity of lesions commonly dealt with by the BER pathway.

4.2 OVERVIEW OF BASE EXCISION REPAIR ASSAY

In this chapter, I describe the repair of certain lesions and intermediates associated with the BER pathway, such as abasic sites and 1-nt gaps. Two types of DNA substrates containing a single lesion at a defined position and an upstream ^{32}P label were utilised in the repair assays; closed-circular double-stranded DNA and double-stranded oligonucleotide substrates. After repair in WCE, products were separated and analysed on 10% (w/v) denaturing polyacrylamide gels. To examine whether an excess of Pol β has any effect on BER, extracts from Pol β overexpressing (Ha) and control (Wt) human lymphoblastoid cells were used in these *in vitro* BER assays.

4.2.1 Closed-circular DNA substrate characterisation

An 8-oxoG lesion-containing M13-based DNA substrate [Fig. 4.1A] was constructed [see Section 2.13] and the lesion was converted to an abasic site by hOGG1 treatment. The abasic site was then repaired in Ha or Wt WCE.

A majority (~60%) of abasic sites are processed through short-patch BER (Dianov et al. 1992), therefore using an abasic site allows the investigation of short-patch BER. The ^{32}P radiolabelled lesion-containing DNA strand is flanked by two *Hin*dIII sites and following restriction digest results in a 59-mer containing the damaged site. Within this fragment are two *Hae*III cleavage sites, and the abasic site lesion is situated within the upstream *Hae*III site, effectively blocking cleavage at this site until the lesion has been repaired [Fig. 4.1A]. Thus, digestion with both *Hin*dIII and *Hae*III will create two different sized fragments depending on repair of the lesion; an unrepaired 52-mer containing the damage, and a repaired 48-mer fragment. See Fig. 4.1Bi for the possible short-patch BER digestion products. Incised, but unrepaired lesions can also be observed as a 47-mer band [Fig. 4.1Bi].

Abasic sites can also be repaired using the long-patch BER pathway. In order to measure second nucleotide addition chain-terminating ddNTPs are used. A dNTP pool comprising of dGTP, to fill the repair gap, and ddATP, ddCTP, ddTTP were used in these BER reactions. Any attempts to repair the abasic site via long-patch BER results in the addition of a second chain terminating nucleotide and yields a 2-nt-added 49-mer product [Fig 4.1Bii], which is resistant to *Hae*III cleavage, therefore only *Hind*III digests are necessary to measure long-patch repair products. Digestion with *Hind*III would also give rise to an incised but unrepaired 47-mer, a 1-nt added unligated 48-mer and a repaired 59-mer band [Fig 4.1Bii]. It is noteworthy that some residual unrepaired substrates could be in the 59-mer band, however, this is unlikely as abasic sites are generally unstable and are easily converted to single-strand breaks.

4.2.2 Double-stranded oligonucleotide substrate characterisation

A 36-mer double-stranded DNA substrate containing a centrally positioned 1-nt gap or nick with 3'-hydroxyl and 5'-phosphate ends was constructed by annealing the indicated oligonucleotides together [see Section 2.14] [Fig. 4.2]. The T1 strands are ^{32}P labelled. Both lesions were repaired in HeLa WCE supplemented with recombinant human Pol β (rhPol β), or Ha and Wt WCE. Nick substrates require ligation; unrepaired nicks are represented as 17-mers and repaired nicks are 36-mers. The 1-nt gap (16-mer) requires nucleotide insertion (17-mer) then ligation (36mer) [Fig. 4.2].

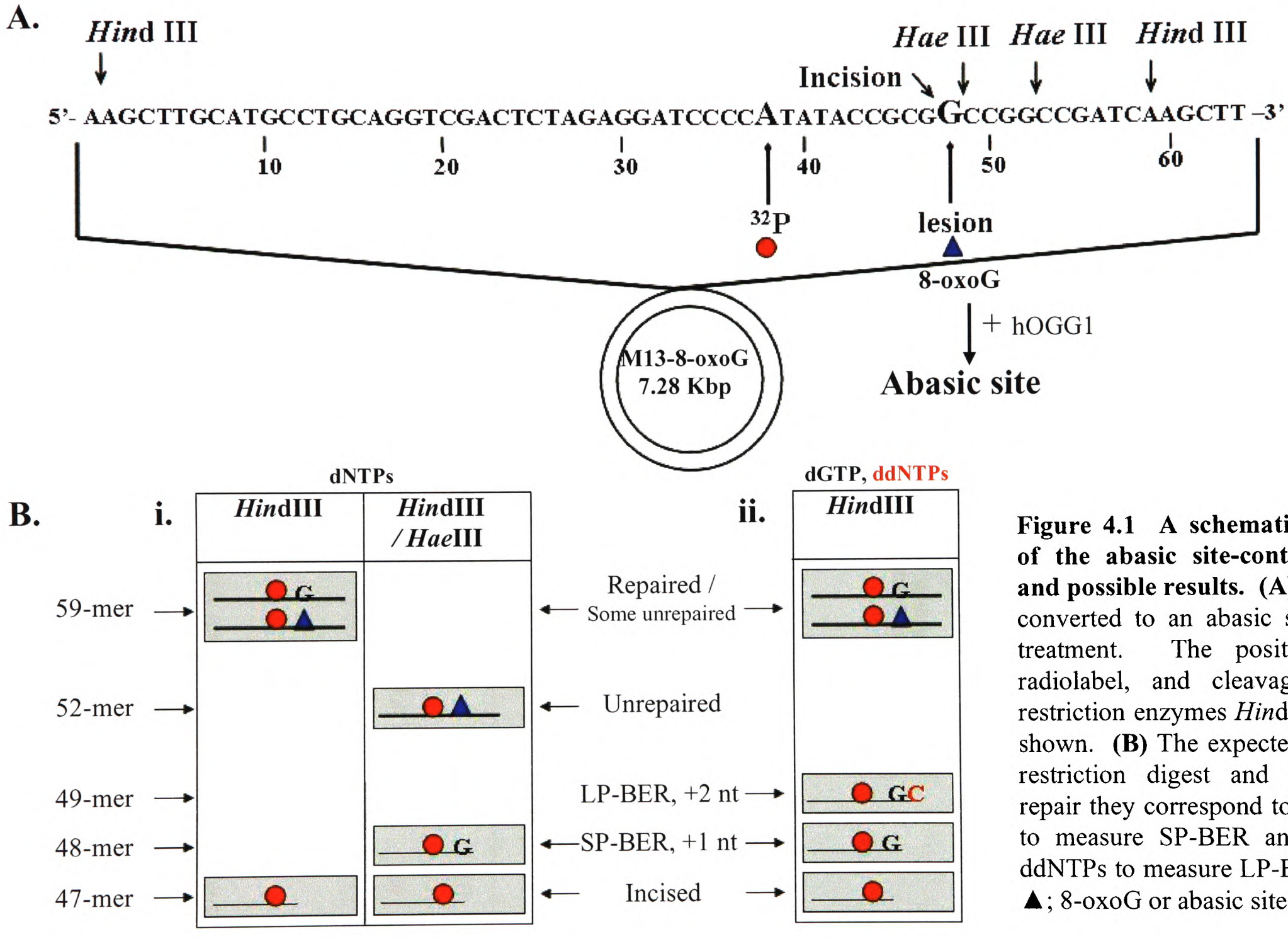

Figure 4.1 A schematic representation of the abasic site-containing substrate and possible results. (A) 8-oxoG lesion is converted to an abasic site after hOGG1 treatment. The position of the ^{32}P radiolabel, and cleavage sites for the restriction enzymes *Hin*dIII and *Hae*III are shown. **(B)** The expected band sizes after restriction digest and which stages of repair they correspond to using: **(i)** dNTPs to measure SP-BER and **(ii)** dGTP and ddNTPs to measure LP-BER. ●; ^{32}P label, ▲; 8-oxoG or abasic site lesion.

A.

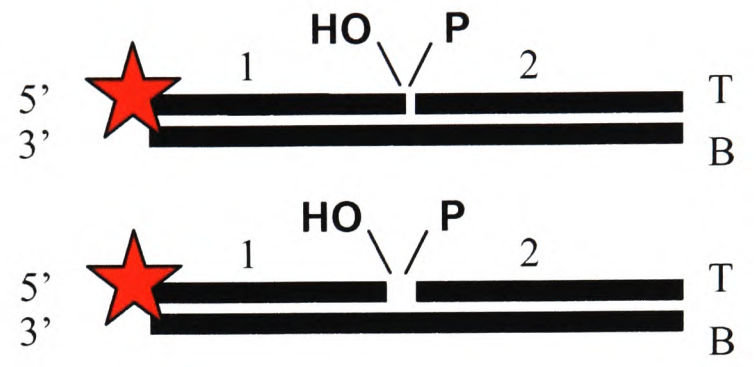

B.

Sequence Name	5' to 3'	Length
Nick – T1 5'- radiolabelled	CAA TAG AGT AAC ACG GC	17
Gap – T1 5'- radiolabelled	CAA TAG AGT AAC ACG G	16
Nick/Gap – T2 5'- phosphate	pCGA CCA GTC CCT GCC AAT C	19
Nick/Gap – B	GAT TGG CAG GGA CTG GTC GGC CGT GTT ACT CTA TTG	36

Figure 4.2 A schematic representation of the nick and 1-nt gap oligonucleotide substrates. (A) 36-mer double-stranded substrates with a centrally positioned nick or 1-nt gap with 3'-hydroxyl (OH) and 5'-phosphate (P) ends. **(B)** Oligonucleotide strands which are used to construct the double-stranded nick or 1-nt gap oligonucleotide substrates. T; top strand, B; bottom strand, 1; downstream (5') top strand with ^{32}P radiolabel represented by star, 2; upstream (3') top strand.

4.3 RESULTS

4.3.1 Ha cells show faster initial binding of abasic sites

Abasic sites can be generated by spontaneous or enzymatic N-glycosidic bond cleavage and are highly unstable because APE1 incision of the DNA backbone 5' to the lesion results in a nick or single-strand break (Demple and Harrison 1994; Barzilay and Hickson 1995). Studying an abasic site lesion allows the DNA glycosylase step of the BER pathway to be bypassed, thus eliminating the need for DNA glycosylases to initiate BER. Previously, Western blot analysis demonstrated that APE1 levels in Ha and Wt cells are equivalent [see. Fig. 3.1A], suggesting that the capacity of DNA backbone incision by APE1 should also be equivalent. Therefore, any differences in repair capacity between the two cell lines can now be attributed to steps after DNA backbone incision, i.e. polymerase, 5' dRP-removal and ligation steps.

Repair of abasic sites are represented by increasing 59-mer (repaired) band intensity with time (1, 2, 4, 15 and 30 min) [Fig. 4.3A] in the Wt (Lanes 1-3, 13, 14) and Ha (Lanes 7-9, 15, 16) WCE. Bands were quantified and percentages of total repaired products were calculated from the *Hin*dIII only digested bands as:

$$\frac{\text{Repaired (59mer)}}{\text{Total bands (59mer, 48mer, 47mer)}} \times 100\% = \text{Complete repair (\%)}$$

A maximal 90% of abasic sites were repaired in both Wt and Ha WCE after 30 min, however, repair had already began to plateau after 20 min [Fig. 4.3B]. The repair profiles for Ha and Wt are similar, however, the initial binding and recognition of the abasic sites differ. The graph indicates that Ha WCE recognise the abasic site lesion more quickly than the Wt WCE.

A.

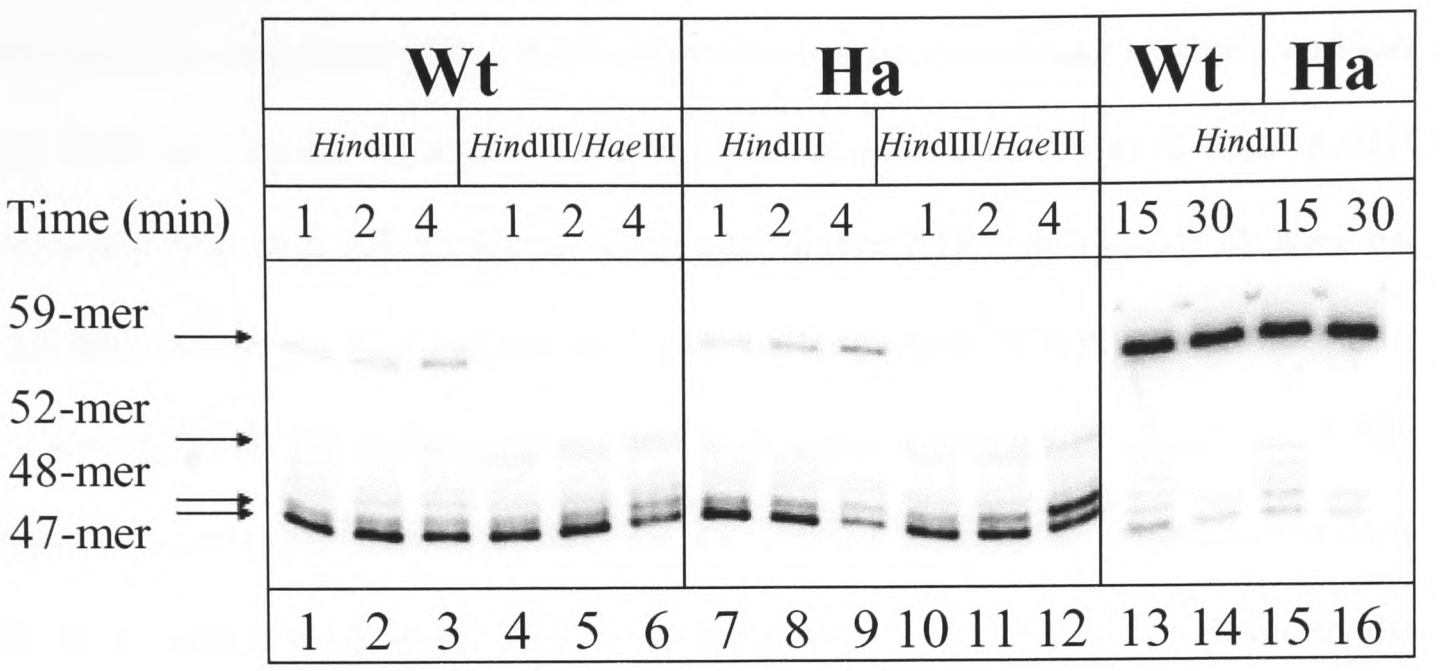

B.

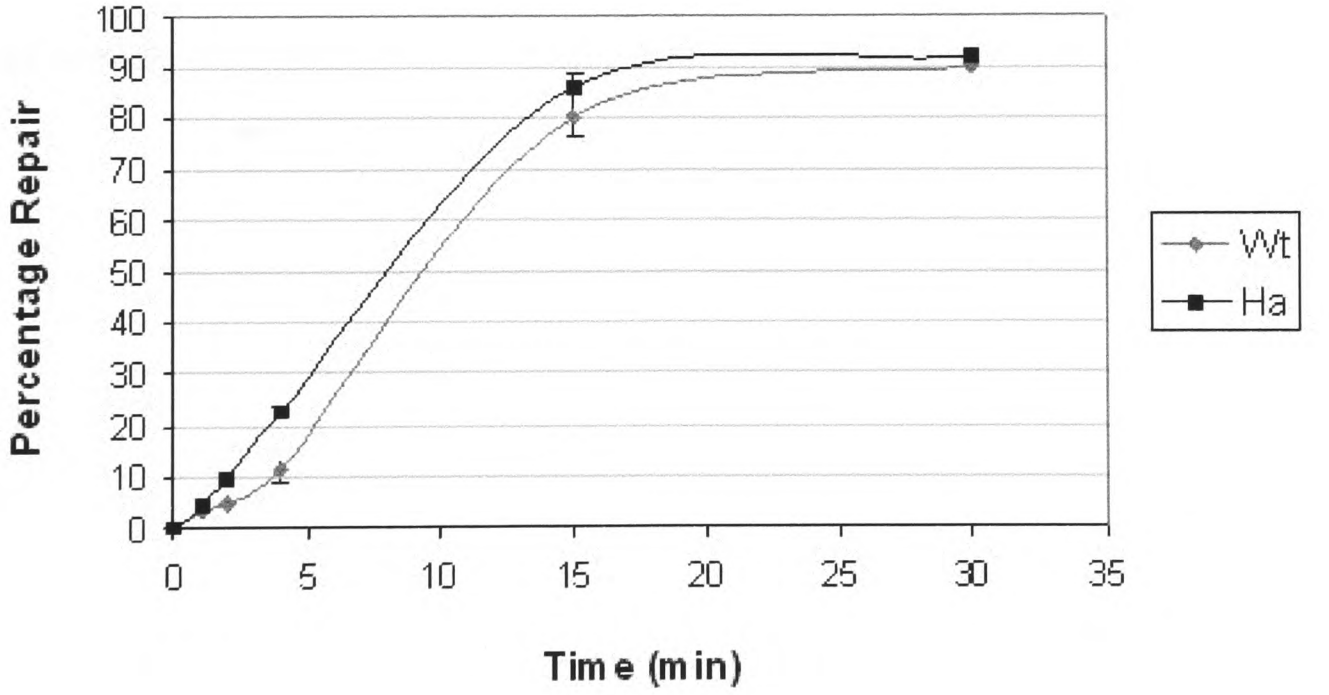

Figure 4.3 BER repair of an abasic site-containing substrate using Ha and Wt WCE. (A) Restriction digest of substrate incubated with 25 µg of Ha or Wt WCE and dNTPs at 37°C for indicated times. Reaction products were analysed on a 10% (w/v) denaturing polyacrylamide gel. **(B)** Graphical representation showing the percentage repair of an abasic site by Ha (■) and Wt (♦) WCE at 37°C for indicated times and a representative gel is shown. Each experiment was repeated 3 times. Error bars show the standard deviation.

4.3.2 Ha cells show faster addition of second nucleotide during repair of abasic sites

A majority of BER is routed through the short-patch pathway, but Pol β also participates in long-patch BER. So in order to compare the amount of short- and long-patch BER between the Ha and Wt cells chain terminating ddNTPs were used. A dNTP pool comprising of dGTP, to fill the repair gap, and ddATP, ddCTP, ddTTP were used in the BER reactions. Any attempts to repair via long-patch BER results in the addition of a second chain terminating nucleotide and yields a 49-mer product [Fig. 4.1Bii]. Abasic sites were repaired to completion for 20 min, then bands were analysed on a 10% (w/v) polyacrylamide gel [Fig. 4.4]. Interestingly, the 48-mer repair intermediate bands (1 nt added, unligated) are more pronounced in the Wt samples compared to the Ha samples. This suggests that Ha cells are adding the second nucleotide faster, thus forming the long-patch (49-mer) (2 nt added) BER product more quickly than Wt cells. This result may be indicative of more strand displacement synthesis by Ha cells.

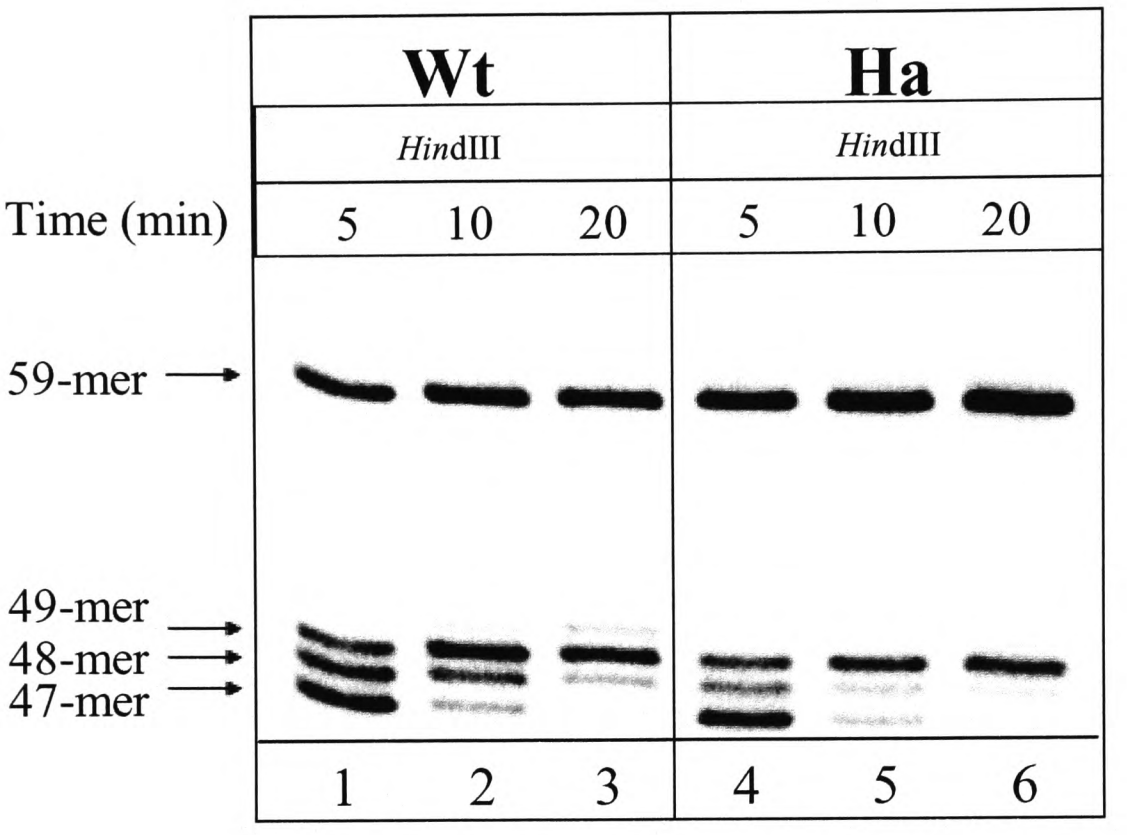

Figure 4.4 Ha cells add second nucleotide faster to an abasic site containing substrate. Restriction digest of substrate incubated with 25 μg of Ha or Wt WCE and dGTP, ddATP, ddCTP, ddTTP at 37°C for indicated times. Reaction products were analysed on a 10% (w/v) denaturing polyacrylamide gel. Each experiment was repeated 3 times and a representative gel is shown.

4.3.3 Excess Pol β enhances strand displacement during repair of 1-nt gaps using HeLa WCE

As mentioned previously, Pol β is involved in both BER pathways by inserting the first nucleotide into a repair gap. Various *in vitro* studies have shown that 1-nt gapped DNA is the preferred substrate for Pol β, and the 5'-phosphate is required for efficient gap filling (Prasad et al. 1994; Chagovetz et al. 1997; Osheroff et al. 1999). Using an *in vitro* repair assay and oligonucleotide substrates [Fig. 4.2], I investigated the effect of excess Pol β on the repair of 1-nt gapped DNA (3'-hydroxyl, 5'-phosphate) compared to a nick, the latter lesion testing for DNA ligase function. Human HeLa WCE were used, and varying amounts of rhPol β was added to the extracts to mimic protein overexpression.

Firstly, the amount of HeLa WCE to be used in the repair assay was titrated [Fig. 4.5A]. The indicated amounts of WCE and 20 μM each dNTP were used to repair the nick [Fig. 4.5A, Lanes 1-7] or 1-nt gap [Fig. 4.5, Lanes 8 – 14] substrate. 8 μg of WCE was sufficient to repair a majority of the substrates, and so this optimal HeLa WCE concentration was used in further experiments.

Next, rhPol β protein was titrated to investigate whether excess Pol β has any effect on repair of these lesions [Fig. 4.5B]. Because the same amount of substrate was loaded in each lane, the proportion of total substrates repaired can be estimated by comparing the 36-mer (repaired) bands for each HeLa WCE repaired sample to the 16-mer (unrepaired) band in sample X for each lesion [Fig. 4.5B]. The nick substrate simply requires ligation, so as may be expected, addition of rhPol β did not affect repair of this lesion, as it is a substrate for DNA ligase, rather than Pol β. All HeLa extract repaired samples showed >90% repair of the nick [Fig. 4.5B, Lanes 2-6]. The 1-nt gap substrate only requires the polymerase activity of Pol β, followed by ligation. A

majority (>90%) of 1-nt gaps were repaired by HeLa extracts alone [Fig. 4.5B, Lane 8], thus the repair reactions are already 'near maximal' and subsequently increases in repair rate would not be seen by adding more rhPol β. However, more repair intermediates are observed [Fig. 4.5B, Lanes 9-12]. This may indicate more strand displacement and processive DNA synthesis.

Pol β is usually a distributive polymerase which dissociates from the template after insertion of 1-nt (Osheroff et al. 1999). These repair intermediates indicate that 1-nt gap repair could be conducted by Pol β in a processive manner, whereby Pol β continues DNA synthesis past the gap through to the end of the oligonucleotide. To deduce further the nature of these repair intermediates, the gap filling nucleotide dCTP was used in the repair reaction [Fig. 4.6]. A mono-nucleotide dCTP pool should limit processive DNA synthesis because only two cytosines can be correctly inserted; opposite the gap and one nucleotide downstream. Indeed, only +1, and +2 nucleotide repair intermediates can be observed [Fig. 4.6, Lanes 9-14], with accumulation of the latter when more rhPol β was added. Interestingly, repair of a 1-nt gap by HeLa extracts alone using a mono-nucleotide dCTP pool (<20% repair) [Fig. 4.6. Lane 8] was reduced compared to when a full dNTP pool (>90% repair) [Fig. 4.5B, Lane 8] was used. Additionally, more 36-mer (repaired) products were observed as increasing amounts of rhPol β was added [Fig. 4.6, Lanes 9-14], with >80% repair achieved when 16ng rhPol β was added [Fig. 4.6, Lane 14]. These results may simply reflect the inhibition of strand displacement DNA synthesis by the dCTP pool which only allows the 1-nt gap to be repaired through the short-patch BER mechanism (addition of 1-nt and ligation). Whereas using a full dNTP pool, 1-nt gap repair can be achieved through strand displacement and processive DNA synthesis as well as short-patch BER.

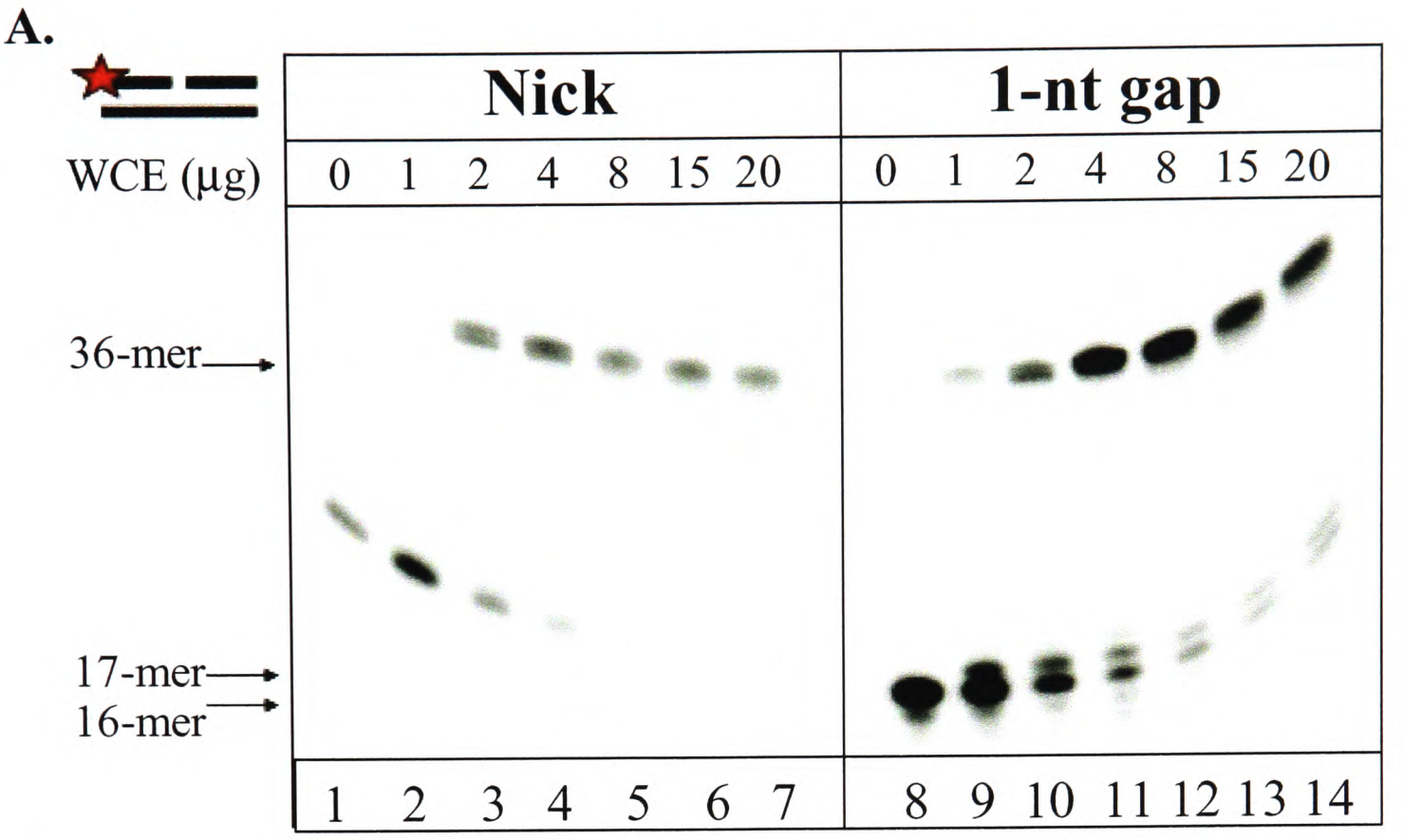

Figure 4.5 ***In vitro*** **repair of a nick and 1-nt gap containing oligonucleotide substrate using HeLa WCE.** BER reactions were incubated at 37°C for 20 min. **(A)** WCE titration using indicated amounts of HeLa WCE. **(B)** Recombinant human Pol β protein titration using 8 µg of WCE. Reaction products were analysed on a 10% (w/v) denaturing polyacrylamide gel. Each experiment was repeated 3 times and a representative gel is shown. X; substrate only control.

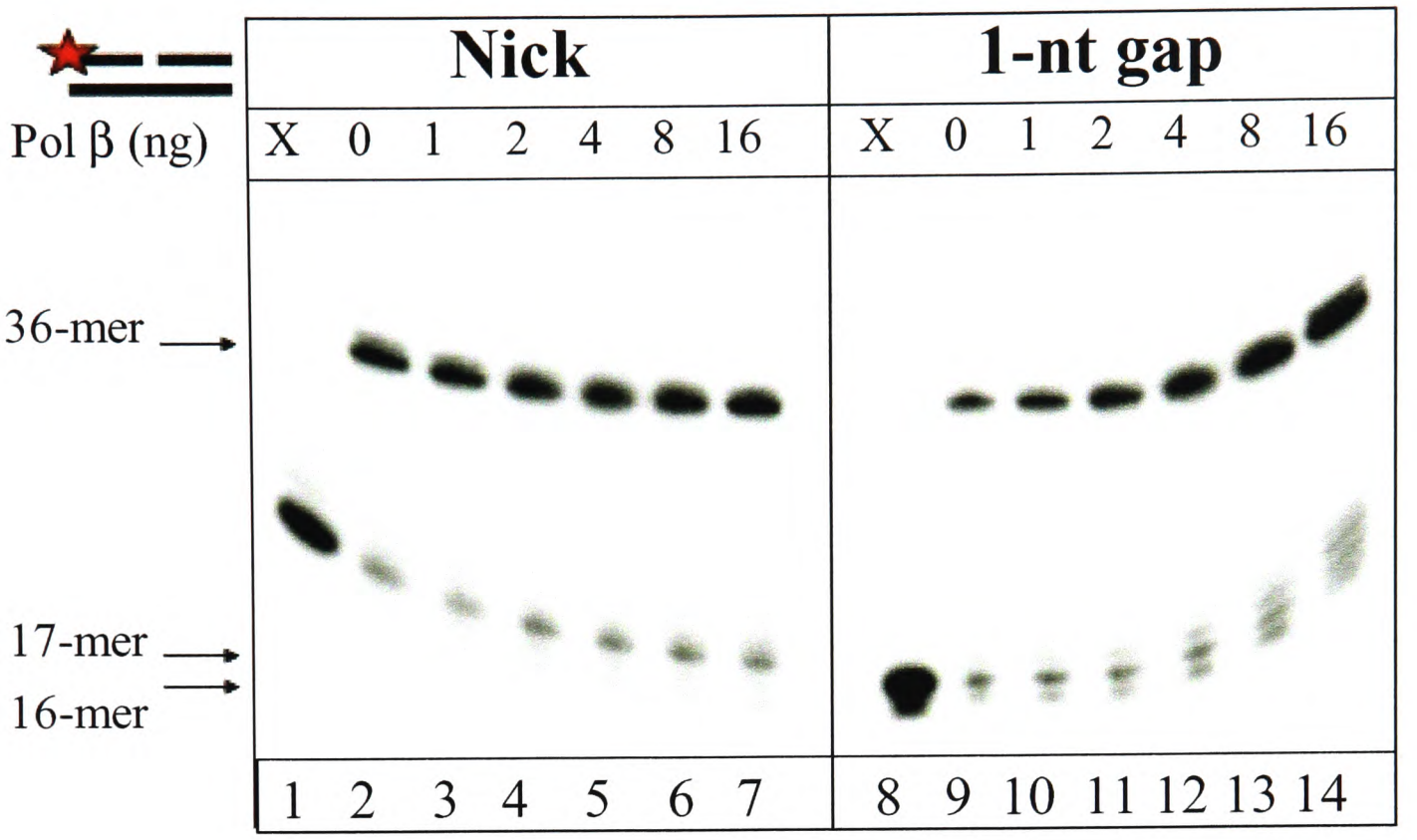

Figure 4.6 Monitoring *in vitro* repair of a nick and 1-nt gap containing oligonucleotide substrate using HeLa WCE. Reconstituted BER reactions using 8 μg HeLa WCE, dCTP only and the indicated amounts of Pol β protein were incubated at 37°C for 20 min. Reaction products were analysed on a 10% (w/v) denaturing polyacrylamide gel. Each experiment was repeated 3 times and a representative gel is shown. X; substrate only control.

4.3.4 Pol β strand displacement in Ha and Wt cells

Using HeLa WCE, I have shown that an excess of Pol β can promote processive synthesis and hence strand displacement during repair of a 1-nt gap. As Ha cells overexpress Pol β, I wanted to demonstrate whether Ha cells can also promote processive synthesis. To investigate this Wt and Ha WCEs (4 μg) were used to repair a 1-nt gap lesion using the *in vitro* assay. 3.5-fold more 1-nt gap lesions were repaired using Wt WCE compared to Ha [Fig. 4.7], however more repair intermediates (+1, +2, +3 nt added) were observed in the Ha repaired sample [Fig. 4.7, Lane 4]. Thus confirming that the Pol β overexpressing cell line, Ha, does induce more strand displacement than the wild-type (Wt) cell line.

A.

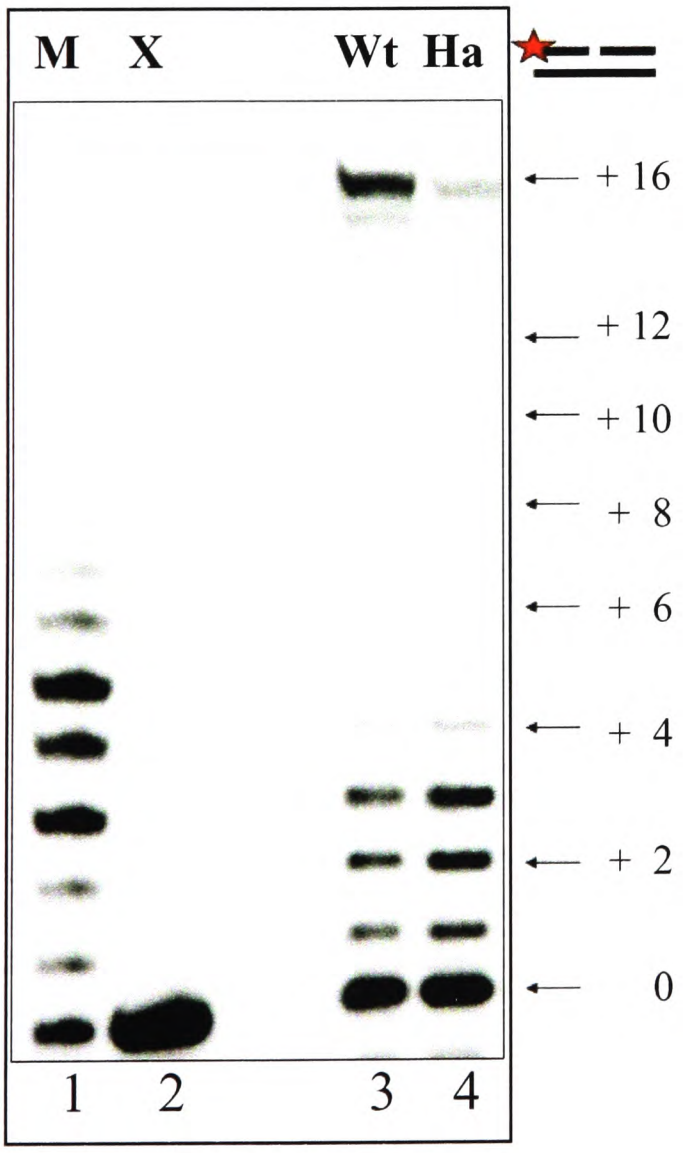

B.

Repair Product	Band Intensity (%)	
	Wt (Lane3)	**Ha** (Lane 4)
+16 nt	16.7	4.8
+ 3 nt	9.2	14.5
+ 2 nt	8.5	12.9
+ 1 nt	7.1	9.0

Figure 4.7 *In vitro* repair of a 1-nt gap containing oligonucleotide substrate using Ha and Wt WCEs. **(A)** Substrate was incubated with 4 μg of Wt (Lane 3) or Ha (Lane 4) WCE and 100 μM dNTPs. M; marker (Lane 1) represents reconstituted reaction with 8 ng Pol β and 20 μM dNTPs. X; substrate only control. All reactions were incubated at 37°C for 20 min and reaction products were analysed on a 20% (w/v) denaturing polyacrylamide gel. **(B)** Table showing percentage band intensity of Wt and Ha repair intermediates from (A).

4.4 CONCLUSIONS

In this chapter, I used *in vitro* BER assays to show that maximal repair (~90%) of abasic sites was achieved by both Ha and Wt cell lines. Although repair rates were similar, the Pol β overexpressing Ha cells showed faster initial binding to abasic sites. Interestingly, Ha cells also demonstrated faster second nucleotide addition, which may be indicative of strand displacement synthesis and subsequently more favoured progression to the long-patch BER pathway, where 2 to 6-nt are added to the repair gap.

Abasic sites can be generated by spontaneous or N-glycosidic bond cleavage by DNA glycosylases and repair of these lesions are initiated by APE1 incision of the DNA backbone, and then removal of the 5'-dRP group by Pol β through its dRP lyase activity. I showed previously that APE1 levels were equivalent between Wt and Ha cells [Fig. 3.1], thus any differences in repair can be attributed to subsequent steps conducted by DNA polymerase or DNA ligase. It was proposed by Srivastava *et al.*, that Pol β performs DNA synthesis prior to removal of the 5'-dRP moiety, and that the latter step is also the rate-limiting step in BER (Srivastava et al. 1998). Thus, perhaps in the presence of more Pol β there is faster removal of the dRP group which then shifts the rate-limiting step to the DNA ligase step. If the resulting nick is not ligated immediately, then perhaps another nucleotide is added through a strand displacement mechanism, thus pushing repair through the long-patch pathway instead.

Pol β was originally thought to be a distributive DNA polymerase but studies by Singhal *et al.* in 1993 demonstrated that Pol β fills DNA gaps of up to 6-nt by a processive rather than distributive mechanism, however a 5'-P group was required for increased activity (Singhal and Wilson 1993). Later, 1-nt gaps with 5'-P were found to be the preferred substrate for Pol β (Prasad et al. 1994). Indeed, reconstituted *in vitro* reactions of 1-nt gaps using HeLa WCE and increasing amounts of rhPol β

demonstrated that Pol β can adopt a processive mechanism of polymerisation under these conditions, and this observation was verified using the Pol β overexpressing Ha and wild-type Wt cells.

In the presence of a full dNTP pool, total repair of the 1-nt gap substrates were achieved, presumably via both processive and distributive mechanisms. However, when a mono-nucleotide dCTP pool was used, repair was limited to distributive polymerisation and subsequently the amount of repaired substrate was reduced.

In summary, Pol β overexpression increases recognition and binding of abasic sites but does not increase the repair rate. Excess Pol β appears to promotes processive or strand displacement synthesis of 1-nt gaps whereby more than one nucleotide is inserted into the repair gap. But how accurate is processive DNA synthesis and is repair fidelity compromised?

Chapter V

Results

EFFECT OF POL β OVEREXPRESSION ON REPAIR FIDELITY

5.1 INTRODUCTION

In the previous chapter I showed that excess Pol β can promote strand displacement and processive DNA synthesis during the repair of 1-nt gaps. However, it is still not known whether the fidelity of repair differs between the Ha cells compared to Wt, and if so, whether excess of Pol β may cause this. Pol β overexpression has been found in a variety of cancers, particularly uterus, ovary, prostate and stomach tumours (Srivastava, Husain et al. 1999; Bergoglio, Canitrot et al. 2001; Albertella, Lau et al. 2005; Tan, Zhao et al. 2005), and has been demonstrated to promote mutagenesis (Bergoglio, Pillaire et al. 2002), however, the type of mutations and the possible mechanisms governing mutagenesis were not identified.

Pol β plays a major role in short-patch BER and one can assume that Pol β has evolved as a distributive polymerase designed to fill 1-nt gaps containing 3'-hydroxyl and 5'-phosphate ends. Indeed, Pol β requires a phosphate group at the 5'-margin of the gap and several studies have shown that 5'-phosphorylated 1-nt gapped DNA is the preferred substrate for Pol β (Prasad, Beard et al. 1994; Chagovetz, Sweasy et al. 1997; Osheroff, Jung et al. 1999). Nucleotide misincorporation by Pol β is 10 to 100-fold lower on 5'-phosphorylated 1-nt gapped DNA compared with recessed, 6-nt gapped, 5'-phosphorylated 6-nt gapped and unphosphorylated 1-nt gapped substrates (Chagovetz, Sweasy et al. 1997). As Pol β has no proofreading activity, its incorporation accuracy results exclusively from the nucleotide selectivity of the enzyme. In the presence of excess Pol β, I observed strand displacement synthesis past 1-nt gaps, possibly attributed to multiple rounds of initiation of DNA polymerisation (Podlutsky, Dianova et al. 2001), but the accuracy of synthesis is still unknown.

The aim of this chapter is to determine whether overexpression of Pol β affects the repair fidelity of 1-nt gaps, and to elucidate what types of mutations occur.

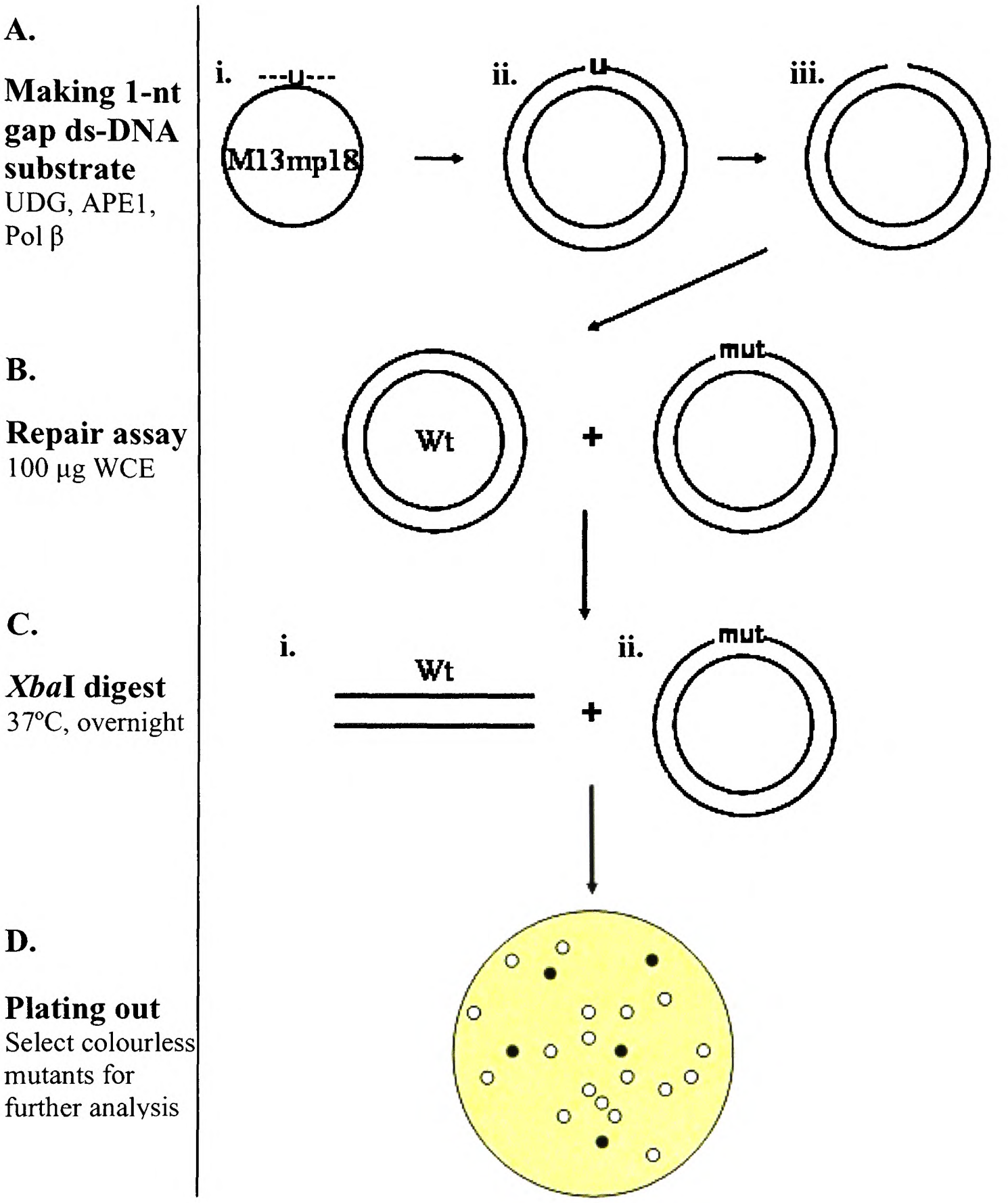

Figure 5.1 Schematic representation of the M13 mutagenesis assay. **(A)** (i) Annealing uracil-containing oligonucleotide, (ii) Synthesising double-stranded DNA, (iii) Making 1-nt gap using UDG, APE1 and Pol β in the absence of dNTPs. **(B)** Repair assay using WCE. **(C)** Restriction digest with *Xba*I, only correctly repaired substrates will be cut. **(D)** Transformation of restriction digests into XL-1 Blue *E. coli*. See Section 2.17 for more details.

5.2 OVERVIEW OF M13 MUTAGENESIS ASSAY

A scheme of the *in vitro* mutagenesis assay is outlined in Figure 5.1. Double-stranded DNA containing a 1-nt gap [Fig. 5.1A], was repaired with 100 µg of Ha or Wt WCE [Fig. 5.1B], and then digested with *Xba*I restriction enzyme overnight [Fig. 5.1C]. Substrates that have been correctly repaired will restore the *Xba*I restriction site and consequently become linearised, whereas incorrectly repaired 'mutant' substrates remain circular. DNA was collected and transformed into bacteria cells. Only circular vectors can be transformed effectively, resulting in plaques [Fig 5.1D]. The lesion is located within the lacZα region, so wild-type substrates appear blue, and mutant substrates appear colourless on X-gal plates. It should be noted however that there are limitations to this blue/white assay because not all mutations will inactivate the LacZ gene. Indeed, it may be possible for mutants to appear as blue plaques if for example insertion/deletion mutations keep the reading frame of the LacZ gene intact. Although the *Xba*I restriction digest removes a majority of the correctly repaired substrates there will inherently be some undigested substrates which also appear as blue plaques. Therefore, the frequency of mutations in this assay may be underestimated because only 'white' mutants can be measured and these certain types of 'blue' mutations can not be detected in this assay.

5.2.1 Preparation of substrate

A 1-nt gap was introduced into a double-stranded M13 bacteriophage vector [Fig. 5.1A]. Briefly, an oligonucleotide containing a site-specific uracil was annealed to single-stranded M13mp18 DNA then re-synthesised to double-stranded DNA using T4 enzymes, the fully completed double-stranded M13 DNA was isolated from a caesium chloride gradient [Fig. 5.2A], and DNA concentration was calculated using standards [Fig. 5.2B]. On the day of the experiment, the uracil lesion was converted to a 1-nt gap

using human uracil DNA glycosylase (UDG) to remove the uracil, APE1 to incise the DNA backbone, and Pol β in the absence of dNTPs to remove the residual 5-dRP group. This resulted in a 1-nt gap with 3'-hydroxyl, 5'-phosphate ends.

A.

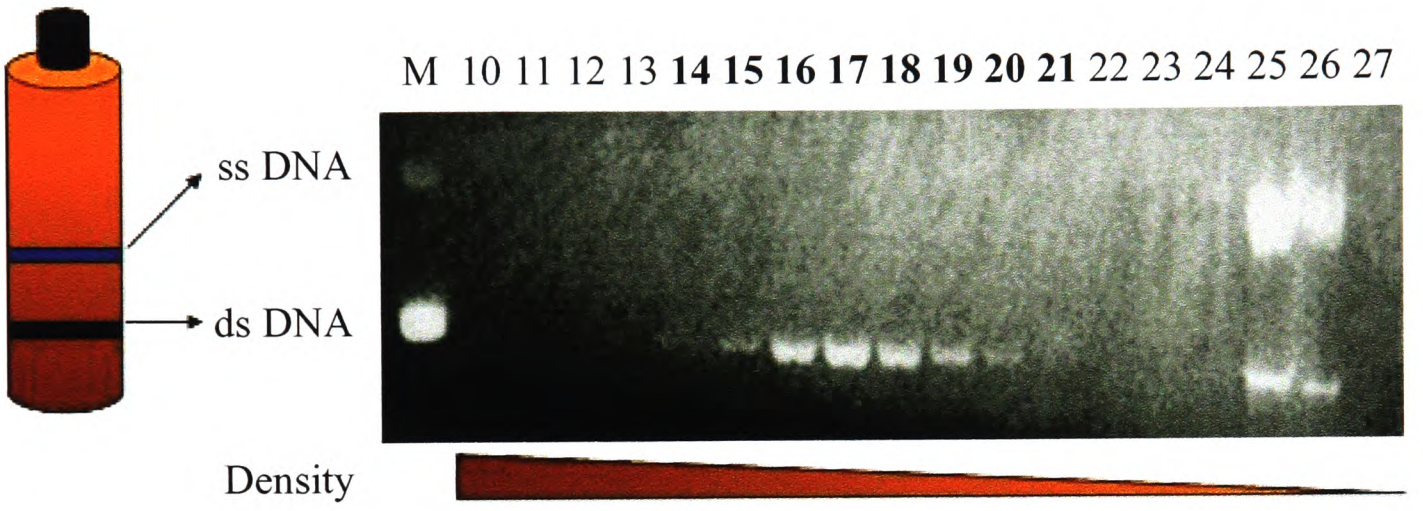

B.

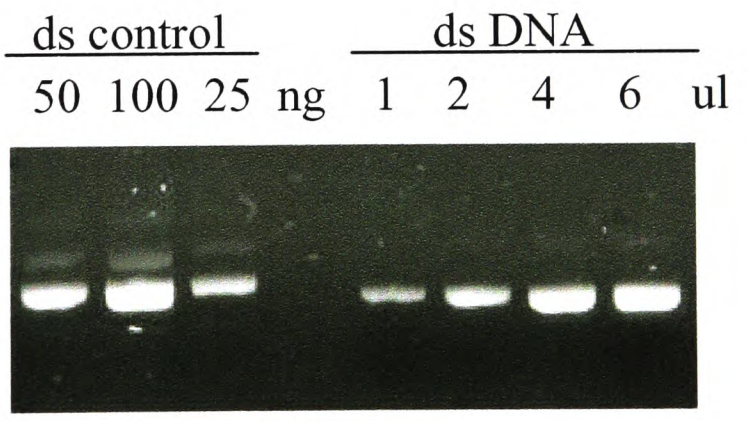

Figure 5.2 Preparation of double-stranded M13-U substrate. (A) Double-stranded M13-U DNA synthesis reaction was separated on a caesium chloride gradient (ρ = 1.55 g/ml), by high-speed centrifugation. Fractions were analysed on a 1% (w/v) agarose gel to locate the double-stranded DNA. **(B)** Estimated concentration of M13-U double-stranded DNA against a standard curve. M13-U was estimated to be 15 ng/µl.

5.2.2 Checking substrate after repair in WCEs

The M13 substrate was checked through the different stages of synthesis to check its integrity. The lesion is located within the *Xba*I restriction site, so therefore digestion with the enzyme confirms whether the site is intact or not. The substrates were electrophoresed on a 0.7% (w/v) agarose gel and compared to DNA markers for single-stranded [Fig. 5.3, Lane 1], double-stranded; open-circular and supercoiled [Fig. 5.3, Lane 2], and linear DNA {Fig. 5.3, Lane 3}. The uracil-containing M13 substrate (M13-U) was isolated mainly as covalently-closed-circular DNA with some open-circular forms {Fig. 5.3, Lane 4], and digestion with *Xba*I enzyme had no effect on the M13-U substrate because the restriction site is not intact [Fig. 5.3, Lane 5]. Most of the 1-nt gap containing substrates (M13-gap) appeared as open-circular DNA, but some linear substrates were also observed [Fig. 5.3, Lane 6], again *Xba*I digestion had no effect [Fig. 5.3, Lane 7]. M13-gap substrates were also analysed after repair in WCEs. Correctly repaired substrates have a restored *Xba*I restriction site, and thus digestion linearises the substrate. Indeed after repair and *Xba*I digestion, less open-circular and more linear DNA was observed [Fig. 5.3, Lane 9], compared to the non-digested repaired M13-gap substrate [Fig. 5.3, Lane 8]. Interestingly, there also appears to be wholesale loss of substrate when incubated with WCE.

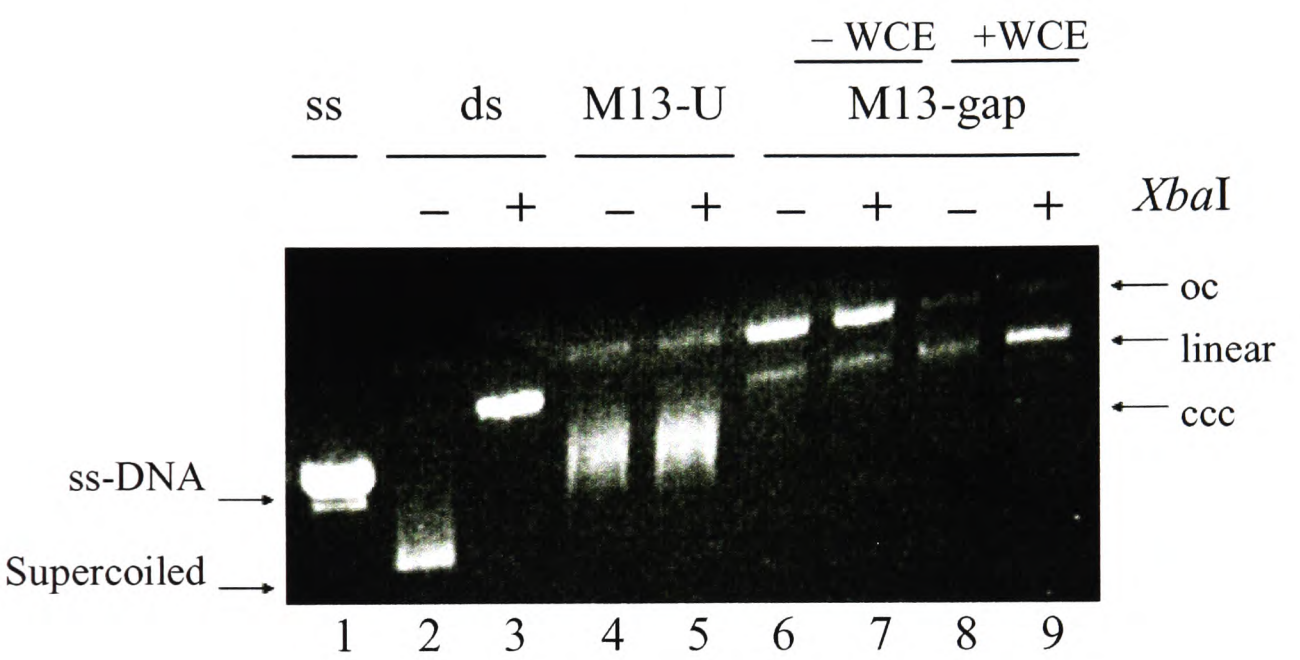

Figure 5.3 Checking M13 double-stranded substrates. DNA substrates were digested in the presence or absence of *Xba*I restriction enzyme and electrophoresed on a 0.7% (w/v) agarose gel. M13-gap was repaired in 100 μg of Wt WCE, for 20 min at 37°C [see Section 2.17.2]. There appears to be wholesale loss of substrate when incubated with WCE. M13-U: uracil-containing M13 substrate; M13-gap: 1-nt gap containing M13 substrate; ss: single-stranded M13mp18; ds: double-stranded M13mp18; oc: open-circular (nicked) DNA; ccc: covalently-closed-circular DNA.

5.3 RESULTS

5.3.1 Excess Pol β promotes mutation frequency in WCEs

Using the *in vitro* mutagenesis assay, I measured the mutation frequency during the repair of the M13-gap substrate in Wt and Pol β overexpressing Ha WCE, and showed that Ha extracts have a 9-fold higher mutation frequency than Wt extracts [Table 5.1]. The mutation frequency was calculated as the ratio of the mutant plaques obtained from digested DNA, to the total number of plaques obtained from undigested DNA. In order to verify whether the observed increased mutation frequency is caused by excess Pol β, Wt cell extracts were supplemented with 40 ng of rhPol β protein per reaction and used to repair M13-gap substrates. Addition of excess Pol β increased the mutation frequency by about 6-fold compared to the original Wt extracts [Table 5.1]. The transformation efficiency was equal for DNA treated with the three different extract/conditions.

WCE	Mutation Frequency ($x10^{-4}$)				-fold
	Exp 1	Exp 2	Exp 3	Average	
Wt	7.41	9.14	3.08	6.5 ± 3.12	1.0
Ha	50.79	61.35	63.49	58.5 ± 6.80	8.9
Wt + Pol β	37.67	47.62	25.97	37.1 ± 10.83	5.8

Table 5.1 Frequency of mutations produced by BER in human WCEs. A 1-nt gap containing substrate (M13-gap) was repaired in human WCE generated from wild type cells (Wt), Pol β overexpressing cells (Ha), or Wt extract supplemented with 40 ng rhPol β. After repair, DNA was purified and transformed into bacterial cells. The mutation frequency was calculated as described in Section 2.17.3 and the results of three independent experiments are shown with the calculated average and standard deviation.

5.3.2 Pol β induces single-nucleotide deletion mutations

The *in vitro* mutagenesis assay allows the colourless 'mutant' M13-gap substrates to be isolated. Mutant DNA was purified and then sequenced from nucleotides -15 to +50 which flank the lesion in order to characterise mutations. Interestingly, 40-65% of mutations observed in all three extracts (Ha, Wt and Wt + Pol β) were located within the repair gap [Table 5.2], and a majority of mutations were single-nucleotide deletions of the 1-nt gap [Fig. 5.4]. This data suggests that the major mutation resulting from 1-nt gap repair are single-nucleotide deletions and elevated levels of Pol β in Ha or Wt supplemented with rhPol β WCE increases the mutation rate.

Mutation Type	Wt	Ha	Wt + Pol β
Single base deletions in the repair gap	14 (41.2)	32 (65.3)	16 (53.3)
Other base deletions	3 (3.8)	0	0
Mutations outside -15/+50	17 (50.0)	17 (34.7)	14 (46.7)
Total number sequenced	34	49	30

Table 5.2 Distribution of Mutation Types generated during repair of M13-gap DNA in human WCEs. DNA from mutants generated during repair in WCEs from wild type cells (Wt), Pol β overexpressing cells (Ha), or Wt extract supplemented with 40 ng rhPol β protein was purified and sequenced. Frequencies are calculated as percentages and shown in brackets.

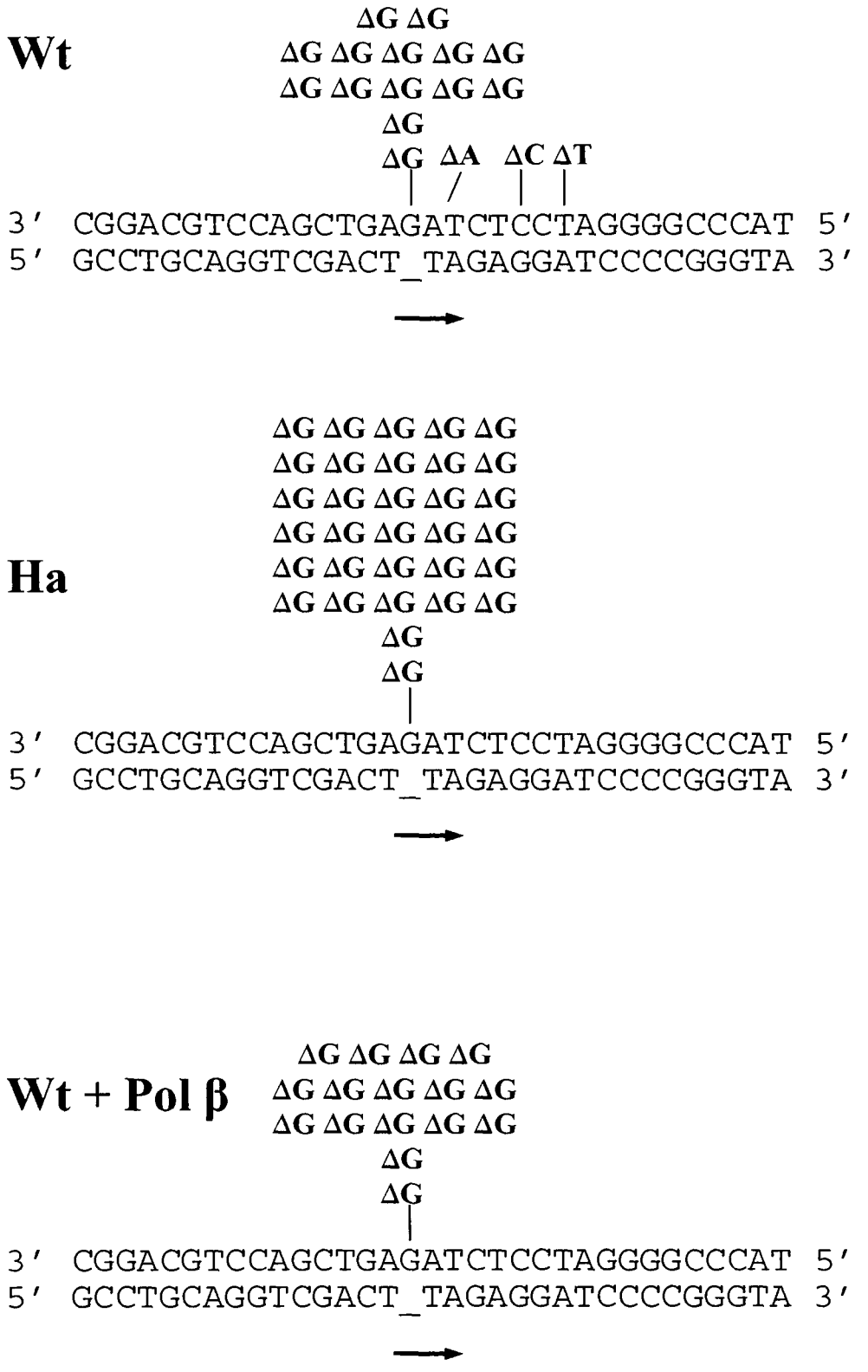

Figure 5.4 Mutation spectrum generated during repair of M13-gap DNA in human WCEs. The DNA substrate was prepared as described in Section 2.17.1, then incubated with 100 μg WCE generated from wild type cells (Wt), Pol β overexpressing cells (Ha), or Wt extract supplemented with 40 ng Pol β per reaction. After repair, DNA was purified and used for transformation of bacterial cells. Mutants were selected and the mutant phage DNA was purified and sequenced. The distribution of these mutations within the -15/+17 region is shown. Horizontal arrow shows direction of repair synthesis. Δ stands for deletion.

5.3.3 Pol β can induce template slippage during repair of 1-nt gaps

Frameshift deletions result from polymerase skipping past the templating base and nucleotide insertion opposite the next nucleotide along on the template strand. For a 1-nt gap, strand displacement would need to occur in order to access the adjacent nucleotide template. Thus, to address the mechanism of increased mutagenesis in cells overexpressing Pol β, I firstly verified that Pol β could induce strand displacement, and secondly checked whether more strand displacement occurs in Ha cell extracts during a gap filling reaction compared to Wt extracts.

Indeed, when 1-nt gap substrates were repaired using a reconstituted BER assay [see Section 2.16] whereby purified Pol β was titrated in, the efficiency of strand displacement synthesis was proportional to the amount of the enzyme used [Fig. 5.5]. Similarly, we found more strand displacement products generated during repair in Ha cell extracts which overexpress Pol β in comparison to Wt cell extracts [Fig. 4.7].

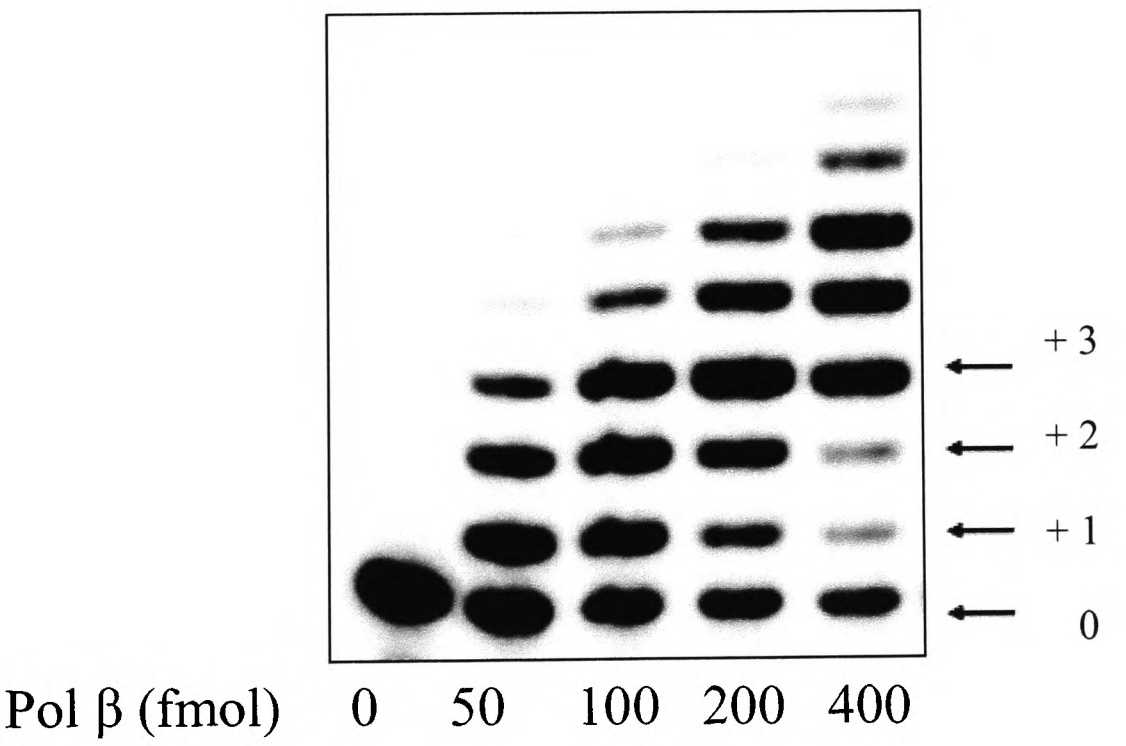

Figure 5.5 Strand displacement synthesis by Pol β. 1-nt gap oligonucleotide substrate was repaired using a reconstituted *in vitro* BER assay where the indicated amounts of rhPol β protein was titrated in. (50 fmol = 1 ng Pol β)

Following strand displacement, Pol β needs to be able to insert a nucleotide opposite the next nucleotide along on the template strand, and thus skip past the 1-nt gap. In order to demonstrate that Pol β is able to generate a 1-nt frameshift during the gap-filling reactions, I carried out DNA synthesis reactions using oligonucleotide substrates in the presence of TTP and dATP only, and in the absence of dCTP which is the templating base opposite the gap. Since the first four nucleotides on the 5'- side downstream of the gap are GATC [Fig. 5.6A], there are only three possible outcomes of the repair synthesis in the presence of TTP and dATP: misincorporation of either (a) TMP opposite to G or (b) dAMP opposite to G, followed by TMP and dAMP incorporation resulting in an extension of three nucleotides [Fig. 5.6A, product i]; (c) template slippage of Pol β and incorporation of TMP opposite to A, followed by dAMP incorporation, resulting in an extension of two nucleotides [Fig. 5.6A, product ii].

Using purified Pol β, even at low concentrations of dNTPs, I observed a small proportion of two nucleotide incorporation products that become more prominent at high TTP concentrations [Fig. 5.6B]. This result suggests that, under these conditions, slippage of Pol β dominates over misincorporation opposite to G. To demonstrate that product (ii) can be further extended to generate a stable frameshift structure [Fig. 5.6A, product iii], we carried out gap filling reactions in the presence of three dNTPs (TTP, dATP and dGTP). Pol β was able to efficiently extend the two nucleotide slippage product, thus fixing a frameshift mutation [Fig. 5.6C].

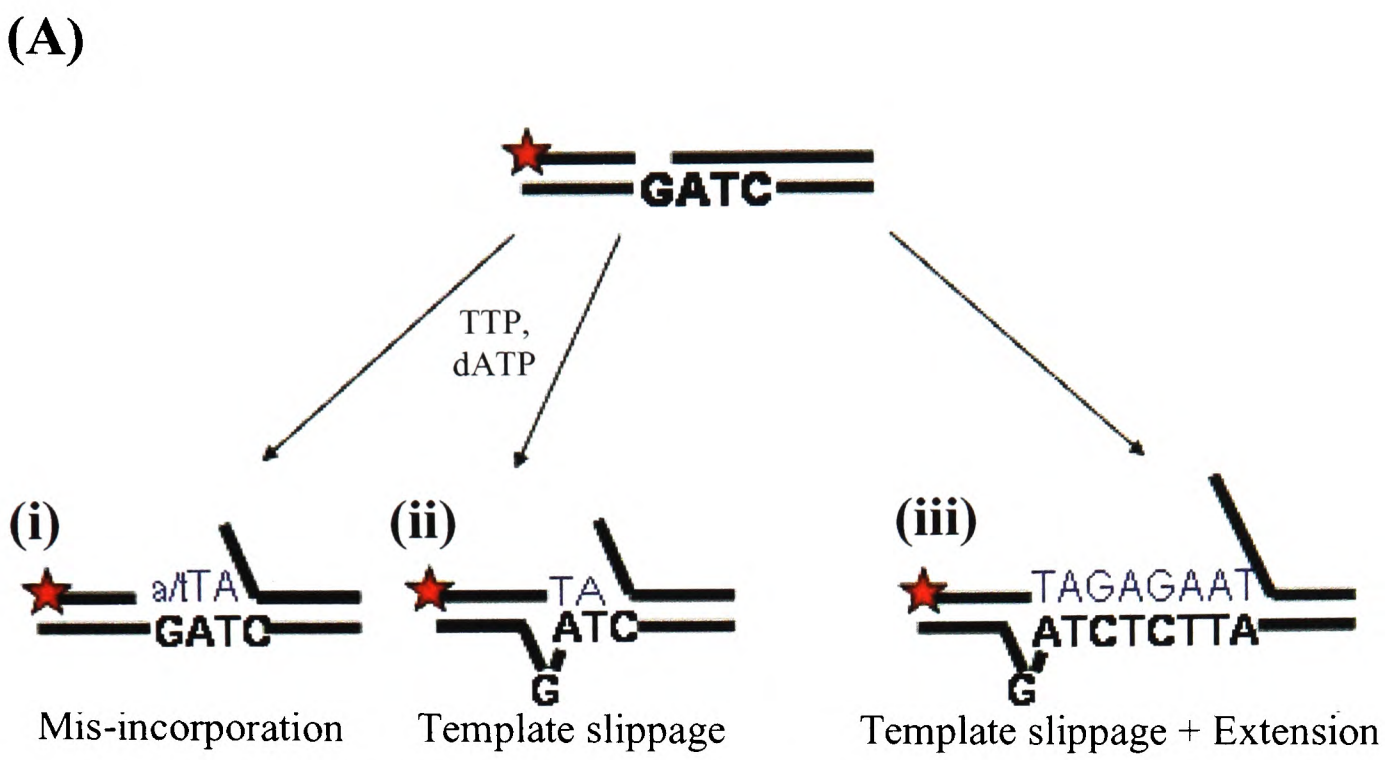

Figure 5.6 Pol β induced frameshift formation during repair of 1-nt gap containing DNA. (A) Models for 1-nt gap-filling reactions and formation of frameshift mutations. See text. Star stands for 5'-^{32}P radiolabel. **(B)** A 1-nt gap containing oligonucleotide substrate (300 fmol) was incubated with 200 fmol of purified rhPol β for 20 min at 37°C in a buffer containing the indicated amount of TTP and dATP. Reaction products were analysed by electrophoresis on a 20% denaturing polyacrylamide gel and phosphorimaging. **(C)** Lane 1, one nucleotide ladder marker. Lane 2, no dNTPs control. Lane 3, 800 μM TTP and 100 μM dATP. Lane 4, 800 μM TTP, 100 μM dATP and 100 μM dGTP.

5.3.4 Possible Model of 1-nt deletion formation by Pol β

I have been able to show that Pol β can induce strand displacement and skip past the 1-nt repair gap whereby further DNA synthesis can occur. This agrees with the 'dNTP-stabilised misalignment' model proposed by Efrati, Goodman *et al* (Efrati, Tocco et al. 1997). This model describes the misaligned incorporation of nucleotides opposite an abasic site (situated on the template strand) resulting in deletion errors (Efrati, Tocco et al. 1997). Zhang *et al.* also investigated abasic sites, but with respect to the fidelity of abasic site repair during BER. Investigations encompassed both short- and long-patch BER and showed that single-nucleotide deletions were the most abundant mutations during the repair of abasic sites (Zhang and Dianov 2005). They proposed a modified 'dNTP-stabilised' model to explain the occurrence of deletions (Zhang and Dianov 2005). Where the original 'dNTP-stabilised' model describes slippage past the lesion on the template strand, Zhang's model describes template slippage during repair of the lesion, but essentially the main principles are the same.

The 'dNTP-stabilised' model is based on two major components: (1) slippage of DNA polymerase on the template strand and (2) Stabilisation of the frameshift by further synthesis. This mode of single-nucleotide formation could be applied to the repair of 1-nt gapped DNA. Pol β can induce strand displacement, and also promote template slippage during nucleotide insertion [Fig. 5.7, ii]. To create a single-nucleotide deletion, the new nucleotide is inserted opposite the base downstream from the templating base [Fig. 5.7, iii]. The misaligned base is further stabilised by continued DNA synthesis which also extends the 5'-flap, which is later removed by FEN1 and DNA ligase I [Fig. 5.7, iv].

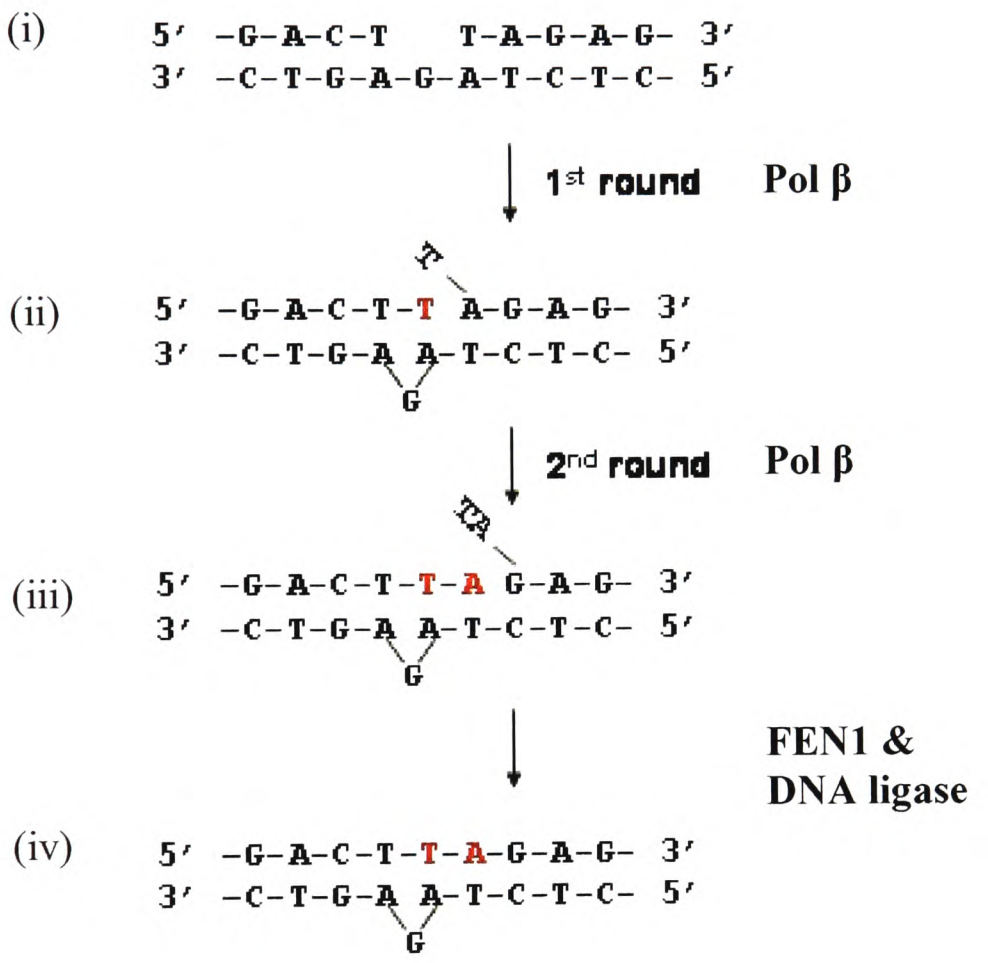

Figure 5.7 Model for the generation of 1-nt frameshift deletions. (i) DNA containing 1-nt gap. (ii) Pol β induces strand displacement and template slippage. (iii) More Pol β continues strand displacement sythesis. (iv) FEN1 and DNA ligase I cleave the 5' flap and seal the nick, respectively.

5.4 CONCLUSIONS

An excess of Pol β can increase the mutation frequency during the repair of a 1-nt gap, and the most common types of lesions observed were single-nucleotide deletions of the repair gap. A dNTP-stabilised mechanism of frameshift formation is likely to be involved, where Pol β can induce strand displacement of the double-stranded DNA downstream of the gap. Subsequently, template slippage past the templating base can occur more easily, and thus results in a single-nucleotide gap deletion after the next round of replication.

Pol β is generally considered to be a distributive enzyme, where the enzyme dissociates after nucleotide insertion, however, when there is an excess of Pol β the substrate turnover rate is increased. Nucleotide discrimination by Pol β is determined by steric exclusion against the incorrect substrate and factors such as; the precise positioning of the DNA duplex terminus, templating and incoming nucleotides and the catalytic residues within the active site of Pol β all influence Pol β fidelity (Sweasy 2003). Imprecise positioning of active site residues or DNA can result in misincorporation of nucleotides into DNA. Amino acid residues both distant and near to the Pol β active site influence its geometry and fidelity, suggesting that the movements and positioning of sub-domains of Pol β have a significant impact upon its fidelity and consequently its catalytic efficiency (Sweasy 2003). Thus, a faster turnover of substrate induced by Pol β may affect the positioning of bases, as the enzyme spends less time on the substrate, and the chances of incorrect incorporation or template slippage increases.

After template slippage, one nucleotide is displaced creating a 5'-end flap, and further strand displacement DNA synthesis by Pol β stabilises the original misaligned nucleotide. FEN1 can cleave these flaps at the single-strand, double-strand DNA

junctions. During long-patch BER, a flap of at least 2 nucleotides is removed and replaced, before ligation of the resulting nick by DNA ligase I.

It could be argued that the single-nucleotide deletion is simply a result of over-gap ligation by DNA ligase without any nucleotide insertion by DNA polymerase. DNA ligase requires 3'-hydroxyl and 5'-phosphate ends for ligation. However, repair studies with reduced abasic sites where the dRP group can not be removed to leave 5'-phosphate ends, still show single-nucleotide deletions to be the major type of mutation (Zhang and Dianov 2005). Similarly, during the repair synthesis of large gaps, single-nucleotide deletions were also shown to be the major mutations (Osheroff, Jung et al. 1999), and this also strongly argues against the involvement of DNA ligase in single-nucleotide deletion formation.

Therefore it appears that overexpression of Pol β does reduce repair fidelity by promoting strand-displacement synthesis and allowing template slippage past 1-nt gaps. Single nucleotide deletions are ultimately frameshift mutations, and if during repair synthesis an essential gene is mutated, then alternative repair mechanisms would be required to correct mistakes or cells may progress to apoptosis.

Chapter VI

General Discussion

6.1 OVERVIEW OF AIMS

The aims of this project were to investigate the Pol β overexpressing cell line, Ha, and to determine whether Pol β overexpression affects the repair capacity or fidelity of lesions associated with BER. The Ha human lymphoblastoid cell line was obtained from a head-neck cancer patient who exhibited a severe reaction to radiotherapy treatment. Preliminary data [Appendix E, Dr I. Dianova] demonstrated that the Ha cell line overexpressed the BER enzyme Pol β, and thus this cell line was selected for further investigation. A wild-type cell line, Wt, isolated from a healthy volunteer with no history of cancer was used as a control.

6.2 THE HA POL β OVEREXPRESSING CELL LINE

6.2.1 Pol β protein overexpression

My initial aim was to elucidate how Pol β was being overexpressed. Using a Western blotting technique I verified that Pol β protein was overexpressed by 5-fold using the Odyssey® (LI-COR) immunofluorescence detection method. This result was comparable to the ECL (Amersham Biosciences) enhanced chemiluminescence detection method used during the preliminary investigations which demonstrated a 6-fold level of Pol β overexpression. Thus, an overall 5 to 6-fold overexpression of Pol β protein was observed in Ha cells. Pol β protein overexpression has been observed in a variety of human tumours, such as prostate, breast and colon compared to adjacent normal tissue (Srivastava et al. 1999), however, the precise mechanism(s) causing this overexpression is still unclear.

The simplest explanation for protein overexpression would be mRNA overexpression, so I used two techniques; Northern blot and real-time RT-PCR to verify Pol β mRNA expression in Ha and Wt cells. Interestingly, only a 1.4-fold

overexpression of Pol β was observed in the Ha cells from both techniques, which only partially explains the 5 to 6-fold Pol β protein overexpression. Few studies have measured the expression levels of Pol β mRNA and protein from the same tumour sample in comparison to wild-type control, although one study has done so using *Xiphophorus* fish. Pol β mRNA and protein from tumour-bearing hybrid fishes were compared to the parental species, and although significantly different Pol β levels were observed, there was no correlation found between the amounts of mRNA and protein for each sample, regardless of whether it was from a tumour or a wild-type control (Heater et al. 2004).

There is a precedent for this absence of correlation. Indeed, when mRNA and protein levels for selected genes in yeast (*S. cerevisiae*) were compared no significant correlation was found. Moreover, while some mRNA levels were constant, the protein levels varied by more than 20-fold. Conversely, while the levels of some proteins were constant, the respective mRNA transcript levels varied by more than 30-fold (Gygi et al. 1999). The same discordant protein and mRNA expression was also found in A549 human lung cancer cells. From the 98 genes analysed, only a subset of 21 genes (21.4%) showed any significant correlation between mRNA and protein expression abundance, however this correlation was insufficient to predict the levels of protein expression from mRNA levels (Chen et al. 2002). It was proposed that the expression of this subset of 21 genes may be regulated at the transcriptional level while the remainder were regulated post-transcriptionally (Chen et al. 2002). Thus, it appears that protein overexpression may not directly correlate with mRNA overexpression, and vice versa.

6.2.2 Pol β promoter activation / transcription

Human Pol β is constitutively expressed regardless of the cell cycle or proliferation state (Zmudzka et al. 1988), however differential Pol β mRNA expression is observed in rodent tissues, with the highest and lowest abundance in testes and liver, respectively (Nowak et al. 1989). The Pol β *cis*-acting promoter contains three GC-rich Sp1 binding domains and an ATF/CRE sequence (Widen et al. 1988), and basal Pol β expression is mediated through the latter element. A study by Wilson and colleagues showed that the ATF/CRE element was responsible for Pol β promoter activation in response to MNNG treatment, a DNA alkylating agent in CHO cells (Kedar et al. 1991), and later the CRE-binding protein family member, CREB-1, was implicated in the activation of Pol β gene expression (He et al. 2003). Recent studies have shown that CREB-1 can regulate about 4000 target genes in humans, thus variations in CREB-1 levels has a genome-wide effect (Zhang et al. 2005) (see database as http://natural.salk.edu/CREB). Subsequently, I measured the levels of CREB-1 (inactive) and pCREB-1 (active) to determine whether there were transcriptional differences between the Ha and Wt cells. A Western blot method was used to measure the levels of CREB-1 and pCREB-1 (Ser 133) protein using mutually exclusive antibodies. Interestingly, a higher total amount of CREB-1 protein was observed in Wt cells however the proportion of total CREB-1 which was phosphorylated (active) was equivalent in both Wt and Ha. Therefore, a lower net amount of pCREB-1 was also found in Ha cells. This observation seems to contradict rather than support Pol β overexpression in Ha cells, but does indicate a variation in transcription factor levels between the two cell lines.

More recent studies have shown that Pol β can also be up-regulated at the GC-rich Sp1 sites by telomerase element-initiating factor (TEIF) (Zhao et al. 2005), and the

Tat HIV-regulatory protein (Srivastava et al. 2001). TEIF can bind to the promoter region of human telomerase reverse transcriptase (hTERT) and stimulates its transcription and activitt, thus suggesting a functional link between Pol β and telomerase at telomere ends (Zhao et al. 2005). The product of the Tat gene transactivates HIV-1 long terminal repeat (LTR)-directed gene expression and is essential for HIV-1 virus replication (Sodroski et al. 1985), and is also capable of inducing some inflammatory mediators (Srivastava et al. 2001). Tat induction of Pol β in HIV-1-related lymphomas suggests that deregulated Pol β may alter DNA stability in AIDS-related lymphomas (Srivastava et al. 2001).

Although I was interested in Pol β overexpression, it is noteworthy that a novel ATF2 isoform, ATF2d, which contains an internal 97-nt deletion and a unique 3' region, was shown to bind to the human Pol β ATF/CRE element and function as a repressor of the Pol β promoter. Further research needs to be done, but this may be indicative of a negative regulatory mechanism for Pol β promoter activation (Chyan et al. 2003). If so, then perhaps there may be a disruption to this negative regulatory mechanism in Ha cells thus resulting in increased activation at the Pol β promoter.

6.2.3 Pol β protein degradation

Another explanation for Pol β protein overexpression could be due to changes in protein turnover, as rates of degradation or synthesis can govern a protein's half-life *in vivo*. Thus, more protein translation and less protein degradation would result in an overall increase in a protein. To investigate Pol β protein degradation I treated Ha and Wt cells with cycloheximide, a protein synthesis inhibitor, then analysed Pol β levels at certain time points and found Pol β to be stable after 24 h in both cell lines. As mentioned previously, I found that Ha cells overexpressed Pol β mRNA and protein by 1.4- and 5 to 6-fold respectively. If it were presumed that the rate of protein translation

remains constant in Ha cells, then a slight 1.4-fold increase in mRNA level could accumulate over time to give rise to a higher 5 to 6-fold level of Pol β as the protein is still stable after 24 h and has a slow rate of protein degradation/turnover. Discrepancies between mRNA and protein levels within the same sample are often observed and it appears that protein overexpression may not directly correlate with mRNA overexpression, and vice versa. A multitude of factors may affect this, such as mRNA translation rates, mRNA or protein stability, stabilisation of the protein via alterations in the ubiquitin-proteasome pathway, and involvement of protein stabilising chaperones (Heater et al. 2004).

6.3 REPAIR OF BER LESIONS BY THE HA CELL LINE

My secondary aim was to elucidate whether Pol β overexpression affects the repair capacity or fidelity of lesions associated with BER such as abasic sites, but particularly 5'-phosphorylated 1-nt gapped DNA which is a common substrate for Pol β.

6.3.1 Abasic site repair by Ha cells

An abasic site is the main type of lesion processed by BER and can be generated spontaneously at a rate of approximately 10,000 per human genome per day (Lindahl and Andersson 1972) and also enzymatically by N-glycosidic bond cleavage. Abasic sites are highly cytotoxic as they are non-coding and may also develop into single-strand breaks. Thus failure to repair abasic sites compromises cellular viability (Loeb and Preston 1986; Guillet and Boiteux 2002). The Ha cell line showed faster initial binding to abasic sites in comparison to Wt although the overall BER repair rates were similar. Faster second nucleotide addition was also observed in Ha cells, which was indicative of more strand displacement synthesis and thus perhaps more progression to

the long-patch BER pathway. Pol β performs DNA synthesis prior to removal of the 5'-dRP moiety, and the latter step is also the rate-limiting step in BER (Srivastava et al. 1998). Thus, perhaps in the presence of more Pol β there is faster dRP group removal, and subsequently the rate-limiting step would be shifted to the DNA ligase step. If however the resulting nick is not ligated immediately, a second nucleotide may be added through a strand displacement mechanism. Indeed, the Pol β overexpressing Ha WCEs were shown to induce more strand displacement than Wt [see Section 4.3.4].

As previously described [see Section 1.4]. BER is a finely balanced and highly co-ordinated pathway involving interactions between APE1 to incise the DNA backbone, Pol β to remove the residual 5'-dRP and insert the new nucleotide, and also DNA ligase to seal the nick. In this study, no modifications were made to the abasic site and thus the majority of repair is accomplished through the short-patch BER pathway, thus utilising DNA ligase IIIα-XRCC1 BER enzymes as well. I demonstrated that Ha cells have the equivalent amount of APE1, XRCC1 (and thus DNA ligase IIIα) and PCNA protein compared to Wt, however, levels of PARP-1 were reduced. PARP-1 has been demonstrated to bind to incised abasic sites possibly to protect these single-strand break intermediates (Lindahl et al. 1995), and may also help to recruit and co-ordinate Pol β and XRCC1 BER enzymes (Caldecott et al. 1996). However, the involvement of PARP-1 appears to slow down the repair reactions and thus reduced levels of PARP-1 may increase repair reactions of abasic sites. Indeed, cell extracts deficient in PARP-1 show increased rates of abasic site repair (Allinson et al. 2003). PARP-1 has also been shown to be required in the long-patch BER pathway (Dantzer et al. 2000). PARP-1 can modify some nuclear proteins by poly(ADP-ribosyl)ation and is involved in various important cellular processes such as signalling of DNA repair initiation, DNA damage checkpoints and apoptosis (Oliver et al. 1999). Thus, perturbed

PARP-1 levels in cells may significantly affect genome integrity. Hence, if the rate-limiting step in Ha cells is shifted to the DNA ligase step then more single-strand breaks will be present, and if there is not enough PARP-1 protein to bind and protect these then potentially lethal double-strand breaks may occur resulting in genomic instability. Interestingly, more PARP-1 caspase 3 cleavage products indicative of apoptosis were observed in Ha cells.

6.3.2 1-nt gap repair by Ha cells

Initially, I used a double-stranded oligonucleotide substrate to investigate the repair of 1-nt gaps *in vitro* and showed that increasing amounts of Pol β resulted in more repair intermediates and hence promoted strand displacement [Fig. 5.5]. Furthermore, the Pol β overexpressing Ha cells where shown to cause more strand displacement than Wt cells [Fig. 4.7]. Pol β has no proof-reading ability and is more error-prone than the replicative DNA polymerases. Subsequently I used an M13 bacteriophage vector-based *in vitro* mutagenesis assay to demonstrate that excess Pol β did increase mutation frequency and that single-nucleotide (1-nt frameshift) deletions were the predominant type of lesion formed during the repair of 1-nt gaps. To explain the generation of these 1-nt frameshift deletions a dNTP-stabilised mechanism [Fig. 5.7] was suggested whereby Pol β induces strand displacement of the adjacent DNA downstream of the gap, and then template slippage past the templating base occurs thus resulting in a single-nucleotide deletion following the next round of replication. Interestingly, recent crystal structures of Pol β complexed to gapped or nicked DNA revealed that the DNA is bent approximately 90° at the site of the gap or nick (Sawaya et al. 1997), and that this bending of the helix is only permitted in one direction (Guo and Tullius 2003). This DNA kinking helps to position the Pol β enzyme and the incoming nucleotide onto the DNA correctly so that gap can be filled (Sawaya et al.

1997). Thus nucleotide discrimination by Pol β is determined by steric exclusion against the incorrect substrate, the precise positioning of the DNA duplex terminus, templating and incoming nucleotides and the catalytic residues within the active site of Pol β (Sweasy 2003). Conversely, imprecise positioning of Pol β on DNA can result in misincorporation of nucleotides into DNA. With this in mind, it may be expected that Pol β has a lower affinity for the slipped template [Fig. 5.7(ii)] because DNA kinking and hence position of DNA would be affected. Under normal conditions, this low affinity Pol β complex would be resolved before a nucleotide can be inserted to stabilise the slipped template, but perhaps in the presence of excess Pol β the probability of a Pol β molecule successfully inserting a new nucleotide increases. Thus the generation of 1-nt frameshift deletions would depend on the rate of Pol β binding on and off the slipped template and the rate of the DNA polymerisation reaction itself.

6.3.3 Pol β overexpression and frameshift deletions

Using Ha and Wt cells I have shown that 1-nt frameshift deletions are the major mutations generated during the repair of 1-nt gaps, and I also verified that excess Pol β increases the frequency of these mutations. Interestingly, 1-nt frameshifts have also previously been shown to be associated with the repair of abasic and reduced abasic sites (Zhang and Dianov 2005), and similarly mutation frequency is exacerbated by excess Pol β. During abasic site repair the new nucleotide is inserted into the repair gap before the dRP group is removed (Matsumoto and Kim 1995), and the resulting nick is ligated. Accurate processing of abasic sites by Pol β would also be determined by steric exclusion against the incorrect nucleotide, and furthermore reduced abasic sites require the addition of at least 2 nucleotides before the modified dRP group can be removed. Thus, the previously discussed model for the generation of 1-nt frameshift deletions [Fig. 5.7] can also be applied to abasic site repair

Frameshift deletions are ultimately generated by inaccurate incorporation of nucleotides onto the templating strand during DNA synthesis, usually by slippage along repeated DNA, misalignments or misligation (Ripley 1990); and in the presence of excess Pol β a dNTP-stabilised mechanism [Fig. 5.7] was proposed to explain the generation of 1-nt frameshift deletions. This mechanism involves template slippage and misalignment of the incoming nucleotide on the template strand. It is known that Pol β is an error-prone DNA polymerase because it has no proof-reading ability and it can also incorporate illegitimate dNTPs or mutagenic base analogues such as 8-oxoG during DNA synthesis (Kamath-Loeb et al. 1997). Indeed, Canitrot and colleagues suggested that excess Pol β may compete with the replicative polymerases (Pol α, Pol δ and Pol ε) during gap filling in repair, replication or recombinational pathways and promote genomic instability (Canitrot et al. 1999).

During long-patch BER a polymerase switch occurs whereby Pol β inserts the first nucleotide into the repair gap, then Pol δ/ε is recruited to continue DNA synthesis (Klungland and Lindahl 1997). If however, in the presence of excess Pol β more processive DNA synthesis occurs rather than a polymerase switch to Pol δ/ε, then potentially more errors can be incorporated into the DNA by Pol β. Pol β may also compete with Pol δ/ε during the repair of gapped DNA in NER and MMR, as well during DNA synthesis, subsequently promoting genomic instability. Indeed, Pol β has been found to be overexpressed in a variety of tumours (Canitrot et al. 1999; Srivastava et al. 1999; Bergoglio et al. 2001; Tan et al. 2005) and the patient Ha, whose lymphoblastoid cells were used in this thesis, suffered from head-neck cancer. Interestingly, although the Ha lymphoblastoid cells were not transformed from the tumour they still demonstrated Pol β overexpression, and alkaline comet assay analysis

[Appendix B, Dr I. Dianova] showed a higher basal level of DNA damage which is indicative of genome instability.

6.4 FUTURE WORK

The exact mechanisms of Pol β protein expression are still poorly understood and attempts to further elucidate these would be of great interest. In this thesis Pol β protein was found to be a highly stable protein, and I suggested that Pol β protein may accumulate in the cell. An alternative method of measuring protein degradation is the pulse-chase method. This method was not initially employed because of expense and time constraints. The 'pulse' part involves exposing cells to a radiolabeled compound such as ^{35}S-labeled methionine for a brief period of time; which allows newly synthesised proteins to be radiolabeled and tracked. Replacement with the non-radiolabeled form of the compound occurs in the 'chase' part and cells are collected at different time points allowing the rate of degradation to be measured. The main advantage to the pulse-chase labelling method over the cycloheximide method is that cellular functions are not disturbed as *de novo* synthesis of proteins is permitted rather than inhibited; however, this method is also more expensive and labour-intensive. Recent developments to the pulse-chase technique whereby proteins can be tracked *in vivo* using green-fluorescent protein (GFP) also means that analysis can be conducted on a single cell basis due to the power and sensitivity of FACS sorting (Jiang et al. 2004). The pulse-chase method can also be adapted to measure the rate of protein synthesis, and so indeed is a powerful tool (Staijen et al. 1997)

Another aspect to follow up would be to prove whether an excess of Pol β competes with Pol δ/ε making these DNA polymerases functionally redundant. Verification of Pol δ/ε protein levels as well as other DNA polymerases could be

measured to understand the comparative distribution of DNA polymerases within the Ha and Wt cells. If Pol β does compete with Pol δ/ε then it may be expected that 1-nt gaps repaired using Ha WCEs with Pol δ/ε removed (excess Pol β) would give a similar mutation rate to Ha WCEs (excess Pol β, normal Pol δ/ε), and a higher mutation rate compared to Wt WCEs (normal levels of Pol β, δ and ε). An immunodepletion method could be utilised to remove Pol δ/ε from WCEs.

6.5 SUMMARY

Pol β has been found to be overexpressed in a variety of different tumours and there is increasing evidence to suggest that Pol β overexpression can promote genomic instability. In this study, I have tried to elucidate how Pol β is overexpressed in Ha cells and have identified that Pol β promoter activation through pCREB-1 binding at the ATF/CRE element is perturbed, thus other transcriptional regulators may be involved. Pol β mRNA levels were shown to be slightly up-regulated in Ha cells (1.4-fold) whereas 5 to 6-fold more Pol β protein was observed compared to Wt. I also showed that Pol β protein is highly stable, even after 24 h, and perhaps this slight 1.4-fold increase in mRNA level could accumulate over time to contribute to the 5 to 6-fold level of Pol β protein due to the slow degradation of the protein that was observed.

I verified that an excess of Pol β does induce more strand displacement and hence is more likely to conduct processive DNA synthesis during the repair of 1-nt gaps. I also ascertained that 1-nt frameshift deletions were the major mutations arising from 1-nt gap repair. *In vivo*, 1-nt gap lesions can arise from ionising radiation damage, as a type of BER repair intermediate and also during DNA synthesis. Pol β is more error-prone than Pol δ/ε and thus repair fidelity would be compromised if Pol β competed with Pol δ/ε during long-patch BER or DNA synthesis. Thus, in summary the

data presented in this thesis suggest that Pol β overexpression may have a detrimental effect on genome stability.

References

Aas, P. A., M. Otterlei, P. O. Falnes, C. B. Vagbo, F. Skorpen, M. Akbari, O. Sundheim, M. Bjoras, G. Slupphaug, E. Seeberg and H. E. Krokan (2003). Human and bacterial oxidative demethylases repair alkylation damage in both RNA and DNA. *Nature* 421(6925): 859-63.

Affar, E. B., M. Germain, E. Winstall, M. Vodenicharov, R. G. Shah, G. S. Salvesen and G. G. Poirier (2001). Caspase-3-mediated processing of poly(ADP-ribose) glycohydrolase during apoptosis. *J Biol Chem* 276(4): 2935-42.

Albertella, M. R., A. Lau and M. J. O'Connor (2005). The overexpression of specialized DNA polymerases in cancer. *DNA Repair (Amst)* 4(5): 583-93.

Allinson, S. L., Dianova, II and G. L. Dianov (2001). DNA polymerase beta is the major dRP lyase involved in repair of oxidative base lesions in DNA by mammalian cell extracts. *EMBO J* 20(23): 6919-26.

Allinson, S. L., Dianova, II and G. L. Dianov (2003). Poly(ADP-ribose) polymerase in base excision repair: always engaged, but not essential for DNA damage processing. *Acta Biochim Pol* 50(1): 169-79.

Allinson, S. L., K. M. Sleeth, G. E. Matthewman and G. L. Dianov (2004). Orchestration of base excision repair by controlling the rates of enzymatic activities. *DNA Repair (Amst)* 3(1): 23-31.

Ames, B. N., M. K. Shigenaga and T. M. Hagen (1993). Oxidants, antioxidants, and the degenerative diseases of aging. *Proc Natl Acad Sci U S A* 90(17): 7915-22.

Aravind, L. and E. V. Koonin (2001). The DNA-repair protein AlkB, EGL-9, and leprecan define new families of 2-oxoglutarate- and iron-dependent dioxygenases. *Genome Biol* 2(3): RESEARCH0007.

Barzilay, G. and I. D. Hickson (1995). Structure and function of apurinic/apyrimidinic endonucleases. *Bioessays* 17(8): 713-9.

Baumann, P. and S. C. West (1998). DNA end-joining catalyzed by human cell-free extracts. *Proc Natl Acad Sci U S A* 95(24): 14066-70.

Beard, W. A. and S. H. Wilson (1998). Structural insights into DNA polymerase beta fidelity: hold tight if you want it right. *Chem Biol* 5(1): R7-13.

Bennett, R. A., D. M. Wilson, 3rd, D. Wong and B. Demple (1997). Interaction of human apurinic endonuclease and DNA polymerase beta in the base excision repair pathway. *Proc Natl Acad Sci U S A* 94(14): 7166-9.

Bergoglio, V., Y. Canitrot, L. Hogarth, L. Minto, S. B. Howell, C. Cazaux and J. S. Hoffmann (2001). Enhanced expression and activity of DNA polymerase beta in human ovarian tumor cells: impact on sensitivity towards antitumor agents. *Oncogene* 20(43): 6181-7.

Bergoglio, V., M. J. Pillaire, M. Lacroix-Triki, B. Raynaud-Messina, Y. Canitrot, A. Bieth, M. Gares, M. Wright, G. Delsol, L. A. Loeb, C. Cazaux and J. S. Hoffmann (2002). Deregulated DNA polymerase beta induces chromosome instability and tumorigenesis. *Cancer Res* 62(12): 3511-4.

Bradford, M. M. (1976). A rapid and sensitive method for the quantitation of microgram quantities of protein utilizing the principle of protein-dye binding. *Anal Biochem* 72: 248-54.

Bradshaw, P. S., D. J. Stavropoulos and M. S. Meyn (2005). Human telomeric protein TRF2 associates with genomic double-strand breaks as an early response to DNA damage. *Nat Genet* 37(2): 193-7.

Burgers, P. M. (1991). Saccharomyces cerevisiae replication factor C. II. Formation and activity of complexes with the proliferating cell nuclear antigen and with DNA polymerases delta and epsilon. *J Biol Chem* 266(33): 22698-706.

Cabelof, D. C., Z. Guo, J. J. Raffoul, R. W. Sobol, S. H. Wilson, A. Richardson and A. R. Heydari (2003). Base excision repair deficiency caused by polymerase beta haploinsufficiency: accelerated DNA damage and increased mutational response to carcinogens. *Cancer Res* 63(18): 5799-807.

Caldecott, K. W. (2001). Mammalian DNA single-strand break repair: an X-ra(y)ted affair. *Bioessays* 23(5): 447-55.

Caldecott, K. W., S. Aoufouchi, P. Johnson and S. Shall (1996). XRCC1 polypeptide interacts with DNA polymerase beta and possibly poly (ADP-ribose) polymerase, and DNA ligase III is a novel molecular 'nick-sensor' in vitro. *Nucleic Acids Res* 24(22): 4387-94.

Caldecott, K. W., C. K. McKeown, J. D. Tucker, S. Ljungquist and L. H. Thompson (1994). An interaction between the mammalian DNA repair protein XRCC1 and DNA ligase III. *Mol Cell Biol* 14(1): 68-76.

Caldecott, K. W., J. D. Tucker, L. H. Stanker and L. H. Thompson (1995). Characterization of the XRCC1-DNA ligase III complex in vitro and its absence from mutant hamster cells. *Nucleic Acids Res* 23(23): 4836-43.

Campalans, A., S. Marsin, Y. Nakabeppu, R. O'Connor T, S. Boiteux and J. P. Radicella (2005). XRCC1 interactions with multiple DNA glycosylases: a model for its recruitment to base excision repair. *DNA Repair (Amst)* 4(7): 826-35.

Canitrot, Y., C. Cazaux, M. Frechet, K. Bouayadi, C. Lesca, B. Salles and J. S. Hoffmann (1998). Overexpression of DNA polymerase beta in cell results in a mutator phenotype and a decreased sensitivity to anticancer drugs. *Proc Natl Acad Sci U S A* 95(21): 12586-90.

Canitrot, Y., M. Frechet, L. Servant, C. Cazaux and J. S. Hoffmann (1999). Overexpression of DNA polymerase beta: a genomic instability enhancer process. *Faseb J* 13(9): 1107-11.

Chagovetz, A. M., J. B. Sweasy and B. D. Preston (1997). Increased activity and fidelity of DNA polymerase beta on single-nucleotide gapped DNA. *J Biol Chem* 272(44): 27501-4.

Chen, D. S., T. Herman and B. Demple (1991). Two distinct human DNA diesterases that hydrolyze 3'-blocking deoxyribose fragments from oxidized DNA. *Nucleic Acids Res* 19(21): 5907-14.

Chen, G., T. G. Gharib, C. C. Huang, J. M. Taylor, D. E. Misek, S. L. Kardia, T. J. Giordano, M. D. Iannettoni, M. B. Orringer, S. M. Hanash and D. G. Beer (2002). Discordant protein and mRNA expression in lung adenocarcinomas. *Mol Cell Proteomics* 1(4): 304-13.

Cheng, K. C., D. S. Cahill, H. Kasai, S. Nishimura and L. A. Loeb (1992). 8-Hydroxyguanine, an abundant form of oxidative DNA damage, causes G----T and A----C substitutions. *J Biol Chem* 267(1): 166-72.

Chomczynski, P. and N. Sacchi (1987). Single-step method of RNA isolation by acid guanidinium thiocyanate-phenol-chloroform extraction. *Anal Biochem* 162(1): 156-9.

Chou, K. M. and Y. C. Cheng (2002). An exonucleolytic activity of human apurinic/apyrimidinic endonuclease on 3' mispaired DNA. *Nature* 415(6872): 655-9.

Chyan, Y. J., T. Y. Rawson and S. H. Wilson (2003). Cloning and characterization of a novel member of the human ATF/CREB family: ATF2 deletion, a potential regulator of the human DNA polymerase beta promoter. *Gene* 312: 117-24.

Collins, A. R. (1999). Oxidative DNA damage, antioxidants, and cancer. *Bioessays* 21(3): 238-46.

Critchlow, S. E. and S. P. Jackson (1998). DNA end-joining: from yeast to man. *Trends Biochem Sci* 23(10): 394-8.

Dalal, S., S. Hile, K. A. Eckert, K. W. Sun, D. Starcevic and J. B. Sweasy (2005). Prostate-cancer-associated I260M variant of DNA polymerase beta is a sequence-specific mutator. *Biochemistry* 44(48): 15664-73.

D'Amours, D. and S. P. Jackson (2002). The Mre11 complex: at the crossroads of dna repair and checkpoint signalling. *Nat Rev Mol Cell Biol* 3(5): 317-27.

Dantzer, F., G. de La Rubia, J. Menissier-De Murcia, Z. Hostomsky, G. de Murcia and V. Schreiber (2000). Base excision repair is impaired in mammalian cells lacking Poly(ADP-ribose) polymerase-1. *Biochemistry* 39(25): 7559-69.

Demple, B. and C. F. Amabile-Cuevas (1991). Redox redux: the control of oxidative stress responses. *Cell* 67(5): 837-9.

Demple, B. and L. Harrison (1994). Repair of oxidative damage to DNA: enzymology and biology. *Annu Rev Biochem* 63: 915-48.

Dianov, G., C. Bischoff, J. Piotrowski and V. A. Bohr (1998). Repair pathways for processing of 8-oxoguanine in DNA by mammalian cell extracts. *J Biol Chem* 273(50): 33811-6.

Dianov, G., A. Price and T. Lindahl (1992). Generation of single-nucleotide repair patches following excision of uracil residues from DNA. *Mol Cell Biol* 12(4): 1605-12.

Dianov, G. L., Allinson, S. L., Budworth, H., Sleeth, K. (2004). Mammalian Base Excision Repair. Eukaryotic DNA Damage Surveillance and Repair. K. W. Caldecott. New York, Eurekah.com and Kluwer Academic / Plenum Publishers: 27-48.

Dianov, G. L., P. O'Neill and D. T. Goodhead (2001). Securing genome stability by orchestrating DNA repair: removal of radiation-induced clustered lesions in DNA. *Bioessays* 23(8): 745-9.

Dianov, G. L., K. M. Sleeth, Dianova, II and S. L. Allinson (2003). Repair of abasic sites in DNA. *Mutat Res* 531(1-2): 157-63.

Dianova, II, V. A. Bohr and G. L. Dianov (2001). Interaction of human AP endonuclease 1 with flap endonuclease 1 and proliferating cell nuclear antigen involved in long-patch base excision repair. *Biochemistry* 40(42): 12639-44.

Dianova, II, K. M. Sleeth, S. L. Allinson, J. L. Parsons, C. Breslin, K. W. Caldecott and G. L. Dianov (2004). XRCC1-DNA polymerase beta interaction is required for efficient base excision repair. *Nucleic Acids Res* 32(8): 2550-5.

Dimitriadis, E. K., R. Prasad, M. K. Vaske, L. Chen, A. E. Tomkinson, M. S. Lewis and S. H. Wilson (1998). Thermodynamics of human DNA ligase I trimerization and association with DNA polymerase beta. *J Biol Chem* 273(32): 20540-50.

Duncan, T., S. C. Trewick, P. Koivisto, P. A. Bates, T. Lindahl and B. Sedgwick (2002). Reversal of DNA alkylation damage by two human dioxygenases. *Proc Natl Acad Sci U S A* 99(26): 16660-5.

Efrati, E., G. Tocco, R. Eritja, S. H. Wilson and M. F. Goodman (1997). Abasic translesion synthesis by DNA polymerase beta violates the "A-rule". Novel types of nucleotide incorporation by human DNA polymerase beta at an abasic lesion in different sequence contexts. *J Biol Chem* 272(4): 2559-69.

Fornace, A. J., Jr., B. Zmudzka, M. C. Hollander and S. H. Wilson (1989). Induction of beta-polymerase mRNA by DNA-damaging agents in Chinese hamster ovary cells. *Mol Cell Biol* 9(2): 851-3.

Fortini, P., B. Pascucci, E. Parlanti, R. W. Sobol, S. H. Wilson and E. Dogliotti (1998). Different DNA polymerases are involved in the short- and long-patch base excision repair in mammalian cells. *Biochemistry* 37(11): 3575-80.

Frechet, M., Y. Canitrot, C. Cazaux and J. S. Hoffmann (2001). DNA polymerase beta imbalance increases apoptosis and mutagenesis induced by oxidative stress. *FEBS Lett* 505(2): 229-32.

Friedberg, E. C., Walker G. C., Siede, W., Wood, R. D., Schulz, R. A., Ellenberger, T. (1995). DNA Repair and Mutagenesis. Washington D.C., ASM Press.

Frosina, G. (2000). Overexpression of enzymes that repair endogenous damage to DNA. *Eur J Biochem* 267(8): 2135-49.

Gu, H., J. D. Marth, P. C. Orban, H. Mossmann and K. Rajewsky (1994). Deletion of a DNA polymerase beta gene segment in T cells using cell type-specific gene targeting. *Science* 265(5168): 103-6.

Guillet, M. and S. Boiteux (2002). Endogenous DNA abasic sites cause cell death in the absence of Apn1, Apn2 and Rad1/Rad10 in Saccharomyces cerevisiae. *EMBO J* 21(11): 2833-41.

Guo, H. and T. D. Tullius (2003). Gapped DNA is anisotropically bent. *Proc Natl Acad Sci U S A* 100(7): 3743-7.

Gygi, S. P., Y. Rochon, B. R. Franza and R. Aebersold (1999). Correlation between protein and mRNA abundance in yeast. *Mol Cell Biol* 19(3): 1720-30.

He, F., X. P. Yang, D. K. Srivastava and S. H. Wilson (2003). DNA polymerase beta gene expression: the promoter activator CREB-1 is upregulated in Chinese hamster ovary cells by DNA alkylating agent-induced stress. *Biol Chem* 384(1): 19-23.

Heater, S. J., L. P. Oehlers, Jr., J. D. Rains and R. B. Walter (2004). DNA polymerase beta mRNA and protein expression in Xiphophorus fish. *Comp Biochem Physiol C Toxicol Pharmacol* 138(3): 325-34.

Helleday, T. (2003). Pathways for mitotic homologous recombination in mammalian cells. *Mutat Res* 532(1-2): 103-15.

Hofseth, L. J., M. A. Khan, M. Ambrose, O. Nikolayeva, M. Xu-Welliver, M. Kartalou, S. P. Hussain, R. B. Roth, X. Zhou, L. E. Mechanic, I. Zurer, V. Rotter, L. D. Samson and C. C. Harris (2003). The adaptive imbalance in base excision-repair enzymes generates microsatellite instability in chronic inflammation. *J Clin Invest* 112(12): 1887-94.

Hubscher, U., G. Maga and S. Spadari (2002). Eukaryotic DNA polymerases. *Annu Rev Biochem* 71: 133-63.

Jiang, X., P. Coffino and X. Li (2004). Development of a method for screening short-lived proteins using green fluorescent protein. *Genome Biol* 5(10): R81.

Jonsson, Z. O. and U. Hubscher (1997). Proliferating cell nuclear antigen: more than a clamp for DNA polymerases. *Bioessays* 19(11): 967-75.

Kamath-Loeb, A. S., A. Hizi, H. Kasai and L. A. Loeb (1997). Incorporation of the guanosine triphosphate analogs 8-oxo-dGTP and 8-NH2-dGTP by reverse transcriptases and mammalian DNA polymerases. *J Biol Chem* 272(9): 5892-8.

Kaufmann, S. H., S. Desnoyers, Y. Ottaviano, N. E. Davidson and G. G. Poirier (1993). Specific proteolytic cleavage of poly(ADP-ribose) polymerase: an early marker of chemotherapy-induced apoptosis. *Cancer Res* 53(17): 3976-85.

Kedar, P. S., S. G. Widen, E. W. Englander, A. J. Fornace, Jr. and S. H. Wilson (1991). The ATF/CREB transcription factor-binding site in the polymerase beta promoter mediates the positive effect of N-methyl-N'-nitro-N-nitrosoguanidine on transcription. *Proc Natl Acad Sci U S A* 88(9): 3729-33.

Kesti, T. and J. E. Syvaoja (1991). Identification and tryptic cleavage of the catalytic core of HeLa and calf thymus DNA polymerase epsilon. *J Biol Chem* 266(10): 6336-41.

Kim, K., S. Biade and Y. Matsumoto (1998). Involvement of flap endonuclease 1 in base excision DNA repair. *J Biol Chem* 273(15): 8842-8.

Kirby, K. S. (1956). A new method for the isolation of ribonucleic acids from mammalian tissues. *Biochem J* 64(3): 405-8.

Klungland, A. and T. Lindahl (1997). Second pathway for completion of human DNA base excision-repair: reconstitution with purified proteins and requirement for DNase IV (FEN1). *EMBO J* 16(11): 3341-8.

Klungland, A., I. Rosewell, S. Hollenbach, E. Larsen, G. Daly, B. Epe, E. Seeberg, T. Lindahl and D. E. Barnes (1999). Accumulation of premutagenic DNA lesions in mice defective in removal of oxidative base damage. *Proc Natl Acad Sci U S A* 96(23): 13300-5.

Krokan, H. E., R. Standal and G. Slupphaug (1997). DNA glycosylases in the base excision repair of DNA. *Biochem J* 325 (Pt 1): 1-16.

Kubota, Y., R. A. Nash, A. Klungland, P. Schar, D. E. Barnes and T. Lindahl (1996). Reconstitution of DNA base excision-repair with purified human proteins: interaction between DNA polymerase beta and the XRCC1 protein. *EMBO J* 15(23): 6662-70.

Kunkel, T. A. (1992). DNA replication fidelity. *J Biol Chem* 267(26): 18251-4.

Kunkel, T. A. (1999). The high cost of living. American Association for Cancer Research Special Conference: endogenous sources of mutations, Fort Myers, Florida, USA, 11-15 November 1998. *Trends Genet* 15(3): 93-4.

Kunkel, T. A. and K. Bebenek (2000). DNA replication fidelity. *Annu Rev Biochem* 69: 497-529.

Kunkel, T. A., J. D. Roberts and R. A. Zakour (1987). Rapid and efficient site-specific mutagenesis without phenotypic selection. *Methods Enzymol* 154: 367-82.

Li, X., J. Li, J. Harrington, M. R. Lieber and P. M. Burgers (1995). Lagging strand DNA synthesis at the eukaryotic replication fork involves binding and stimulation of FEN-1 by proliferating cell nuclear antigen. *J Biol Chem* 270(38): 22109-12.

Lindahl, T. (1974). An N-glycosidase from Escherichia coli that releases free uracil from DNA containing deaminated cytosine residues. *Proc Natl Acad Sci U S A* 71(9): 3649-53.

Lindahl, T. (1993). Instability and decay of the primary structure of DNA. *Nature* 362(6422): 709-15.

Lindahl, T. and A. Andersson (1972). Rate of chain breakage at apurinic sites in double-stranded deoxyribonucleic acid. *Biochemistry* 11(19): 3618-23.

Lindahl, T., M. S. Satoh and G. Dianov (1995). Enzymes acting at strand interruptions in DNA. *Philos Trans R Soc Lond B Biol Sci* 347(1319): 57-62.

Lindahl, T. and R. D. Wood (1999). Quality control by DNA repair. *Science* 286(5446): 1897-905.

Livak, K. (1997). ABI Prism 7700 Sequence Detection System, User Bulletin 2. PE Applied Biosystems. Foster City, CA.

Loeb, L. A. and B. D. Preston (1986). Mutagenesis by apurinic/apyrimidinic sites. *Annu Rev Genet* 20: 201-30.

Marintchev, A., M. R. Gryk and G. P. Mullen (2003). Site-directed mutagenesis analysis of the structural interaction of the single-strand-break repair protein, X-

ray cross-complementing group 1, with DNA polymerase beta. *Nucleic Acids Res* 31(2): 580-8.

Matsumoto, Y. and K. Kim (1995). Excision of deoxyribose phosphate residues by DNA polymerase beta during DNA repair. *Science* 269(5224): 699-702.

Matsuzaki, J., Y. Dobashi, H. Miyamoto, I. Ikeda, K. Fujinami, T. Shuin and Y. Kubota (1996). DNA polymerase beta gene mutations in human bladder cancer. *Mol Carcinog* 15(1): 38-43.

McCullough, A. K., M. L. Dodson and R. S. Lloyd (1999). Initiation of base excision repair: glycosylase mechanisms and structures. *Annu Rev Biochem* 68: 255-85.

Meira, L. B., S. Devaraj, G. E. Kisby, D. K. Burns, R. L. Daniel, R. E. Hammer, S. Grundy, I. Jialal and E. C. Friedberg (2001). Heterozygosity for the mouse Apex gene results in phenotypes associated with oxidative stress. *Cancer Res* 61(14): 5552-7.

Minowa, O., T. Arai, M. Hirano, Y. Monden, S. Nakai, M. Fukuda, M. Itoh, H. Takano, Y. Hippou, H. Aburatani, K. Masumura, T. Nohmi, S. Nishimura and T. Noda (2000). Mmh/Ogg1 gene inactivation results in accumulation of 8-hydroxyguanine in mice. *Proc Natl Acad Sci U S A* 97(8): 4156-61.

Mishina, Y., E. M. Duguid and C. He (2006). Direct reversal of DNA alkylation damage. *Chem Rev* 106(2): 215-32.

Mol, C. D., T. Izumi, S. Mitra and J. A. Tainer (2000). DNA-bound structures and mutants reveal abasic DNA binding by APE1 and DNA repair coordination [corrected]. *Nature* 403(6768): 451-6.

Montecucco, A., R. Rossi, D. S. Levin, R. Gary, M. S. Park, T. A. Motycka, G. Ciarrocchi, A. Villa, G. Biamonti and A. E. Tomkinson (1998). DNA ligase I is recruited to sites of DNA replication by an interaction with proliferating cell nuclear antigen: identification of a common targeting mechanism for the assembly of replication factories. *EMBO J* 17(13): 3786-95.

Nakamura, J., D. K. La and J. A. Swenberg (2000). 5'-nicked apurinic/apyrimidinic sites are resistant to beta-elimination by beta-polymerase and are persistent in human cultured cells after oxidative stress. *J Biol Chem* 275(8): 5323-8.

Narayan, S., F. He and S. H. Wilson (1996). Activation of the human DNA polymerase beta promoter by a DNA-alkylating agent through induced phosphorylation of cAMP response element-binding protein-1. *J Biol Chem* 271(31): 18508-13.

Nowak, R., J. A. Siedlecki, L. Kaczmarek, B. Z. Zmudzka and S. H. Wilson (1989). Levels and size complexity of DNA polymerase beta mRNA in rat regenerating liver and other organs. *Biochim Biophys Acta* 1008(2): 203-7.

Oliver, F. J., J. Menissier-de Murcia, C. Nacci, P. Decker, R. Andriantsitohaina, S. Muller, G. de la Rubia, J. C. Stoclet and G. de Murcia (1999). Resistance to endotoxic shock as a consequence of defective NF-kappaB activation in poly (ADP-ribose) polymerase-1 deficient mice. *EMBO J* 18(16): 4446-54.

Osheroff, W. P., H. K. Jung, W. A. Beard, S. H. Wilson and T. A. Kunkel (1999). The fidelity of DNA polymerase beta during distributive and processive DNA synthesis. *J Biol Chem* 274(6): 3642-50.

Parsons, J. L., Dianova, II and G. L. Dianov (2004). APE1 is the major 3'-phosphoglycolate activity in human cell extracts. *Nucleic Acids Res* 32(12): 3531-6.

Parsons, J. L. and R. H. Elder (2003). DNA N-glycosylase deficient mice: a tale of redundancy. *Mutat Res* 531(1-2): 165-75.

Pelletier, H., M. R. Sawaya, W. Wolfle, S. H. Wilson and J. Kraut (1996). Crystal structures of human DNA polymerase beta complexed with DNA: implications

for catalytic mechanism, processivity, and fidelity. *Biochemistry* 35(39): 12742-61.

Pescini, R., W. Kaszubska, J. Whelan, J. F. DeLamarter and R. Hooft van Huijsduijnen (1994). ATF-a0, a novel variant of the ATF/CREB transcription factor family, forms a dominant transcription inhibitor in ATF-a heterodimers. *J Biol Chem* 269(2): 1159-65.

Podlutsky, A. J., Dianova, II, V. N. Podust, V. A. Bohr and G. L. Dianov (2001). Human DNA polymerase beta initiates DNA synthesis during long-patch repair of reduced AP sites in DNA. *EMBO J* 20(6): 1477-82.

Podust, V. N., L. S. Chang, R. Ott, G. L. Dianov and E. Fanning (2002). Reconstitution of human DNA polymerase delta using recombinant baculoviruses: the p12 subunit potentiates DNA polymerizing activity of the four-subunit enzyme. *J Biol Chem* 277(6): 3894-901.

Podust, V. N. and U. Hubscher (1993). Lagging strand DNA synthesis by calf thymus DNA polymerases alpha, beta, delta and epsilon in the presence of auxiliary proteins. *Nucleic Acids Res* 21(4): 841-6.

Posnick, L. M. and L. D. Samson (1999). Imbalanced base excision repair increases spontaneous mutation and alkylation sensitivity in Escherichia coli. *J Bacteriol* 181(21): 6763-71.

Prasad, R., W. A. Beard, P. R. Strauss and S. H. Wilson (1998). Human DNA polymerase beta deoxyribose phosphate lyase. Substrate specificity and catalytic mechanism. *J Biol Chem* 273(24): 15263-70.

Prasad, R., W. A. Beard and S. H. Wilson (1994). Studies of gapped DNA substrate binding by mammalian DNA polymerase beta. Dependence on 5'-phosphate group. *J Biol Chem* 269(27): 18096-101.

Prasad, R., R. K. Singhal, D. K. Srivastava, J. T. Molina, A. E. Tomkinson and S. H. Wilson (1996). Specific interaction of DNA polymerase beta and DNA ligase I in a multiprotein base excision repair complex from bovine testis. *J Biol Chem* 271(27): 16000-7.

Puebla-Osorio, N., D. B. Lacey, F. W. Alt and C. Zhu (2006). Early embryonic lethality due to targeted inactivation of DNA ligase III. *Mol Cell Biol* 26(10): 3935-41.

Rasouli-Nia, A., F. Karimi-Busheri and M. Weinfeld (2004). Stable down-regulation of human polynucleotide kinase enhances spontaneous mutation frequency and sensitizes cells to genotoxic agents. *Proc Natl Acad Sci U S A* 101(18): 6905-10.

Rice, N. R. and M. K. Ernst (1993). In vivo control of NF-kappa B activation by I kappa B alpha. *EMBO J* 12(12): 4685-95.

Ripley, L. S. (1990). Frameshift mutation: determinants of specificity. *Annu Rev Genet* 24: 189-213.

Roesler, W. J., E. A. Park and P. J. McFie (1998). Characterization of CCAAT/enhancer-binding protein alpha as a cyclic AMP-responsive nuclear regulator. *J Biol Chem* 273(24): 14950-7.

Rydberg, B. and T. Lindahl (1982). Nonenzymatic methylation of DNA by the intracellular methyl group donor S-adenosyl-L-methionine is a potentially mutagenic reaction. *EMBO J* 1(2): 211-6.

Sambrook, J., Fritsch, E.F., Maniatis, T. (1989). Molecular Cloning: A Laboratory Manual. Cold Spring Harbor, Cold Spring Harbor Laboratory Press.

Sanger, F., S. Nicklen and A. R. Coulson (1977). DNA sequencing with chain-terminating inhibitors. *Proc Natl Acad Sci U S A* 74(12): 5463-7.

Sawaya, M. R., R. Prasad, S. H. Wilson, J. Kraut and H. Pelletier (1997). Crystal structures of human DNA polymerase beta complexed with gapped and nicked DNA: evidence for an induced fit mechanism. *Biochemistry* 36(37): 11205-15.

Scharer, O. D. and J. Jiricny (2001). Recent progress in the biology, chemistry and structural biology of DNA glycosylases. *Bioessays* 23(3): 270-81.

Sedgwick, B. (2004). Repairing DNA-methylation damage. *Nat Rev Mol Cell Biol* 5(2): 148-57.

SenGupta, D. N., B. Z. Zmudzka, P. Kumar, F. Cobianchi, J. Skowronski and S. H. Wilson (1986). Sequence of human DNA polymerase beta mRNA obtained through cDNA cloning. *Biochem Biophys Res Commun* 136(1): 341-7.

Sheng, M., M. A. Thompson and M. E. Greenberg (1991). CREB: a Ca(2+)-regulated transcription factor phosphorylated by calmodulin-dependent kinases. *Science* 252(5011): 1427-30.

Simonelli, V., L. Narciso, E. Dogliotti and P. Fortini (2005). Base excision repair intermediates are mutagenic in mammalian cells. *Nucleic Acids Res* 33(14): 4404-11.

Singhal, R. K., R. Prasad and S. H. Wilson (1995). DNA polymerase beta conducts the gap-filling step in uracil-initiated base excision repair in a bovine testis nuclear extract. *J Biol Chem* 270(2): 949-57.

Singhal, R. K. and S. H. Wilson (1993). Short gap-filling synthesis by DNA polymerase beta is processive. *J Biol Chem* 268(21): 15906-11.

Sleeth, K. M., R. L. Robson and G. L. Dianov (2004). Exchangeability of mammalian DNA ligases between base excision repair pathways. *Biochemistry* 43(40): 12924-30.

Slupphaug, G., I. Eftedal, B. Kavli, S. Bharati, N. M. Helle, T. Haug, D. W. Levine and H. E. Krokan (1995). Properties of a recombinant human uracil-DNA glycosylase from the UNG gene and evidence that UNG encodes the major uracil-DNA glycosylase. *Biochemistry* 34(1): 128-38.

Slupphaug, G., C. D. Mol, B. Kavli, A. S. Arvai, H. E. Krokan and J. A. Tainer (1996). A nucleotide-flipping mechanism from the structure of human uracil-DNA glycosylase bound to DNA. *Nature* 384(6604): 87-92.

Sobol, R. W., J. F. Foley, A. Nyska, M. G. Davidson and S. H. Wilson (2003). Regulated over-expression of DNA polymerase beta mediates early onset cataract in mice. *DNA Repair (Amst)* 2(5): 609-22.

Sobol, R. W., J. K. Horton, R. Kuhn, H. Gu, R. K. Singhal, R. Prasad, K. Rajewsky and S. H. Wilson (1996). Requirement of mammalian DNA polymerase-beta in base-excision repair. *Nature* 379(6561): 183-6.

Sodroski, J., R. Patarca, C. Rosen, F. Wong-Staal and W. Haseltine (1985). Location of the trans-activating region on the genome of human T-cell lymphotropic virus type III. *Science* 229(4708): 74-7.

Srivastava, D. K., B. J. Berg, R. Prasad, J. T. Molina, W. A. Beard, A. E. Tomkinson and S. H. Wilson (1998). Mammalian abasic site base excision repair. Identification of the reaction sequence and rate-determining steps. *J Biol Chem* 273(33): 21203-9.

Srivastava, D. K., I. Husain, C. L. Arteaga and S. H. Wilson (1999). DNA polymerase beta expression differences in selected human tumors and cell lines. *Carcinogenesis* 20(6): 1049-54.

Srivastava, D. K., C. L. Tendler, D. Milani, M. A. English, J. D. Licht and S. H. Wilson (2001). The HIV-1 transactivator protein Tat is a potent inducer of the human DNA repair enzyme beta-polymerase. *Aids* 15(4): 433-40.

Staijen, I. E., V. Hatzimanikatis and B. Witholt (1997). The AlkB monooxygenase of Pseudomonas oleovorans--synthesis, stability and level in recombinant Escherichia coli and the native host. *Eur J Biochem* 244(2): 462-70.

Stucki, M., B. Pascucci, E. Parlanti, P. Fortini, S. H. Wilson, U. Hubscher and E. Dogliotti (1998). Mammalian base excision repair by DNA polymerases delta and epsilon. *Oncogene* 17(7): 835-43.

Sweasy, J. B. (2003). Fidelity mechanisms of DNA polymerase beta. *Prog Nucleic Acid Res Mol Biol* 73: 137-69.

Sweasy, J. B., T. Lang, D. Starcevic, K. W. Sun, C. C. Lai, D. Dimaio and S. Dalal (2005). Expression of DNA polymerase {beta} cancer-associated variants in mouse cells results in cellular transformation. *Proc Natl Acad Sci U S A* 102(40): 14350-5.

Tan, X. H., M. Zhao, K. F. Pan, Y. Dong, B. Dong, G. J. Feng, G. Jia and Y. Y. Lu (2005). Frequent mutation related with overexpression of DNA polymerase beta in primary tumors and precancerous lesions of human stomach. *Cancer Lett* 220(1): 101-14.

Tanaka, M., J. S. Lai and W. Herr (1992). Promoter-selective activation domains in Oct-1 and Oct-2 direct differential activation of an snRNA and mRNA promoter. *Cell* 68(4): 755-67.

Tebbs, R. S., M. L. Flannery, J. J. Meneses, A. Hartmann, J. D. Tucker, L. H. Thompson, J. E. Cleaver and R. A. Pedersen (1999). Requirement for the Xrcc1 DNA base excision repair gene during early mouse development. *Dev Biol* 208(2): 513-29.

Tom, S., L. A. Henricksen and R. A. Bambara (2000). Mechanism whereby proliferating cell nuclear antigen stimulates flap endonuclease 1. *J Biol Chem* 275(14): 10498-505.

Tsuchimoto, D., Y. Sakai, K. Sakumi, K. Nishioka, M. Sasaki, T. Fujiwara and Y. Nakabeppu (2001). Human APE2 protein is mostly localized in the nuclei and to some extent in the mitochondria, while nuclear APE2 is partly associated with proliferating cell nuclear antigen. *Nucleic Acids Res* 29(11): 2349-60.

Turchi, J. J., G. Siegal and R. A. Bambara (1992). DNA helicase E and DNA polymerase epsilon functionally interact for displacement synthesis. *Biochemistry* 31(37): 9008-15.

Van Dyck, E., A. Z. Stasiak, A. Stasiak and S. C. West (1999). Binding of double-strand breaks in DNA by human Rad52 protein. *Nature* 398(6729): 728-31.

Vodenicharov, M. D., F. R. Sallmann, M. S. Satoh and G. G. Poirier (2000). Base excision repair is efficient in cells lacking poly(ADP-ribose) polymerase 1. *Nucleic Acids Res* 28(20): 3887-96.

Wang, G., Y. Yu, X. Chen and H. Xie (2001). Low concentration N-methyl-N'-nitro-N-nitrosoguanidine activates DNA polymerase-beta expression via cyclic-AMP-protein kinase A-cAMP response element binding protein pathway. *Mutat Res* 478(1-2): 177-84.

Ward, J. F. (1988). DNA damage produced by ionizing radiation in mammalian cells: identities, mechanisms of formation, and reparability. *Progress In Nucleic Acid Research And Molecular Biology* 35: 95-125.

Watson, J. D. and F. H. Crick (1953). Molecular structure of nucleic acids; a structure for deoxyribose nucleic acid. *Nature* 171(4356): 737-8.

Weiser, T., M. Gassmann, P. Thommes, E. Ferrari, P. Hafkemeyer and U. Hubscher (1991). Biochemical and functional comparison of DNA polymerases alpha, delta, and epsilon from calf thymus. *J Biol Chem* 266(16): 10420-8.

Widen, S. G., P. Kedar and S. H. Wilson (1988). Human beta-polymerase gene. Structure of the 5'-flanking region and active promoter. *J Biol Chem* 263(32): 16992-8.

Wiederhold, L., J. B. Leppard, P. Kedar, F. Karimi-Busheri, A. Rasouli-Nia, M. Weinfeld, A. E. Tomkinson, T. Izumi, R. Prasad, S. H. Wilson, S. Mitra and T. K. Hazra (2004). AP endonuclease-independent DNA base excision repair in human cells. *Mol Cell* 15(2): 209-20.

Wilson, S. H. (1998). Mammalian base excision repair and DNA polymerase beta. *Mutat Res* 407(3): 203-15.

Wilson, S. H. and T. A. Kunkel (2000). Passing the baton in base excision repair. *Nat Struct Biol* 7(3): 176-8.

Wood, R. D., M. Mitchell and T. Lindahl (2005). Human DNA repair genes, 2005. *Mutat Res* 577(1-2): 275-83.

Xanthoudakis, S., R. J. Smeyne, J. D. Wallace and T. Curran (1996). The redox/DNA repair protein, Ref-1, is essential for early embryonic development in mice. *Proc Natl Acad Sci U S A* 93(17): 8919-23.

Zhang, Q. M. and G. L. Dianov (2005). DNA repair fidelity of base excision repair pathways in human cell extracts. *DNA Repair (Amst)* 4(2): 263-70.

Zhang, X., D. T. Odom, S. H. Koo, M. D. Conkright, G. Canettieri, J. Best, H. Chen, R. Jenner, E. Herbolsheimer, E. Jacobsen, S. Kadam, J. R. Ecker, B. Emerson, J. B. Hogenesch, T. Unterman, R. A. Young and M. Montminy (2005). Genome-wide analysis of cAMP-response element binding protein occupancy, phosphorylation, and target gene activation in human tissues. *Proc Natl Acad Sci U S A* 102(12): 4459-64.

Zhao, Y., J. Zheng, Y. Ling, L. Hou and B. Zhang (2005). Transcriptional upregulation of DNA polymerase beta by TEIF. *Biochem Biophys Res Commun* 333(3): 908-16.

Zmudzka, B. Z., A. Fornace, J. Collins and S. H. Wilson (1988). Characterization of DNA polymerase beta mRNA: cell-cycle and growth response in cultured human cells. *Nucleic Acids Res* 16(20): 9587-96.

Publications

Redacted journal article "Base excision repair fidelity in normal and cancer cells" can be found at http://dx.doi.org/10.1093/mutage/gel020

Appendices

i.

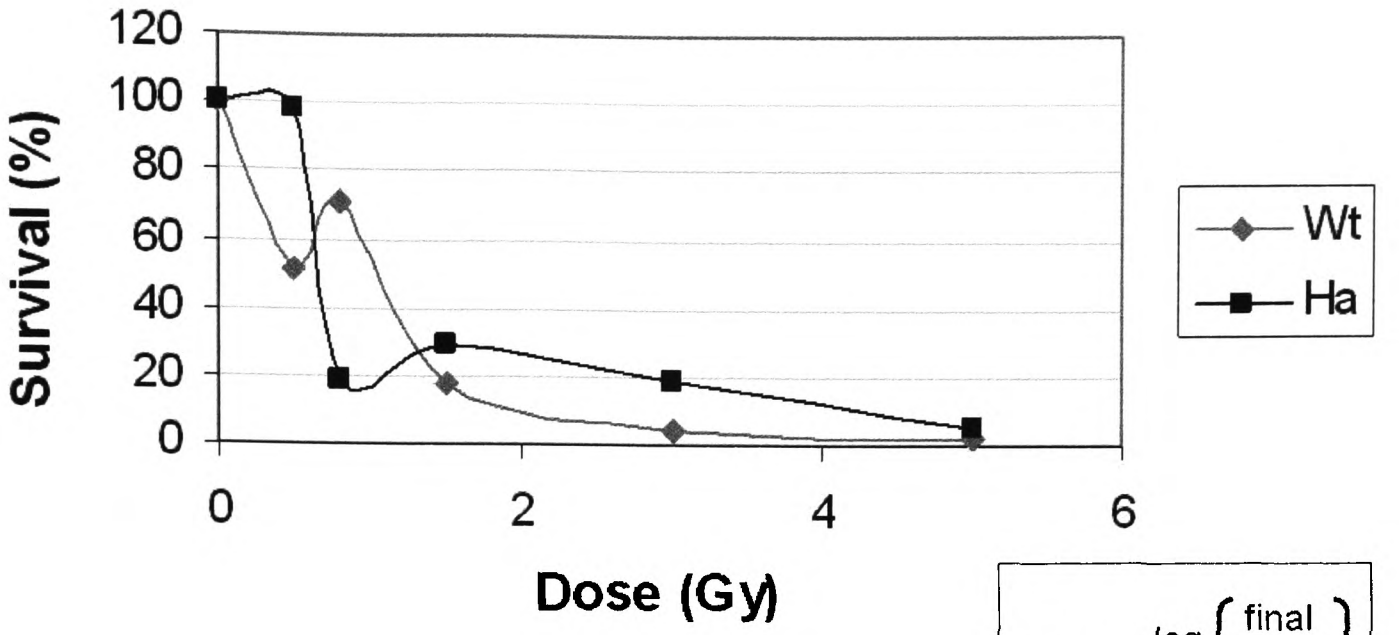

$$PD = \frac{\log\left(\frac{final}{initial}\right)}{\log 2}$$

ii.

Wt

Dose (Gy)	Average population doubling (PD)	Ave. PD relative to 0Gy	PD control – PD sample	Starting no. of living cells after irradiation	Survival (%)
0	5.95	1	0	5000	100
0.5	5.63	0.95	0.32	4005	80
0.8	5.46	0.92	0.49	3560	71
1.5	3.48	0.58	2.47	902	18
3.0	1.32	0.22	4.63	202	4
5.0	0	0	5.95	81	1.6

Ha

Dose (Gy)	Average population doubling (PD)	Ave. PD relative to 0Gy	PD control – PD sample	Starting no. of living cells after irradiation	Survival (%)
0	4.29	1	0	5000	100
0.5	4.25	0.99	0.04	4863	97
0.8	1.86	0.43	2.43	928	19
1.5	2.49	0.58	1.80	1436	29
3.0	1.86	0.43	2.43	928	19
5.0	0	0	4.29	256	5

Population survival curves for Ha and Wt cells. **(i)** The Ha and Wt human lymphoblastoid cells were irradiated with the indicated dose (Gy) of gamma radiation and allowed to recover for 10 days. Cell survival was measured using erythosin B stain

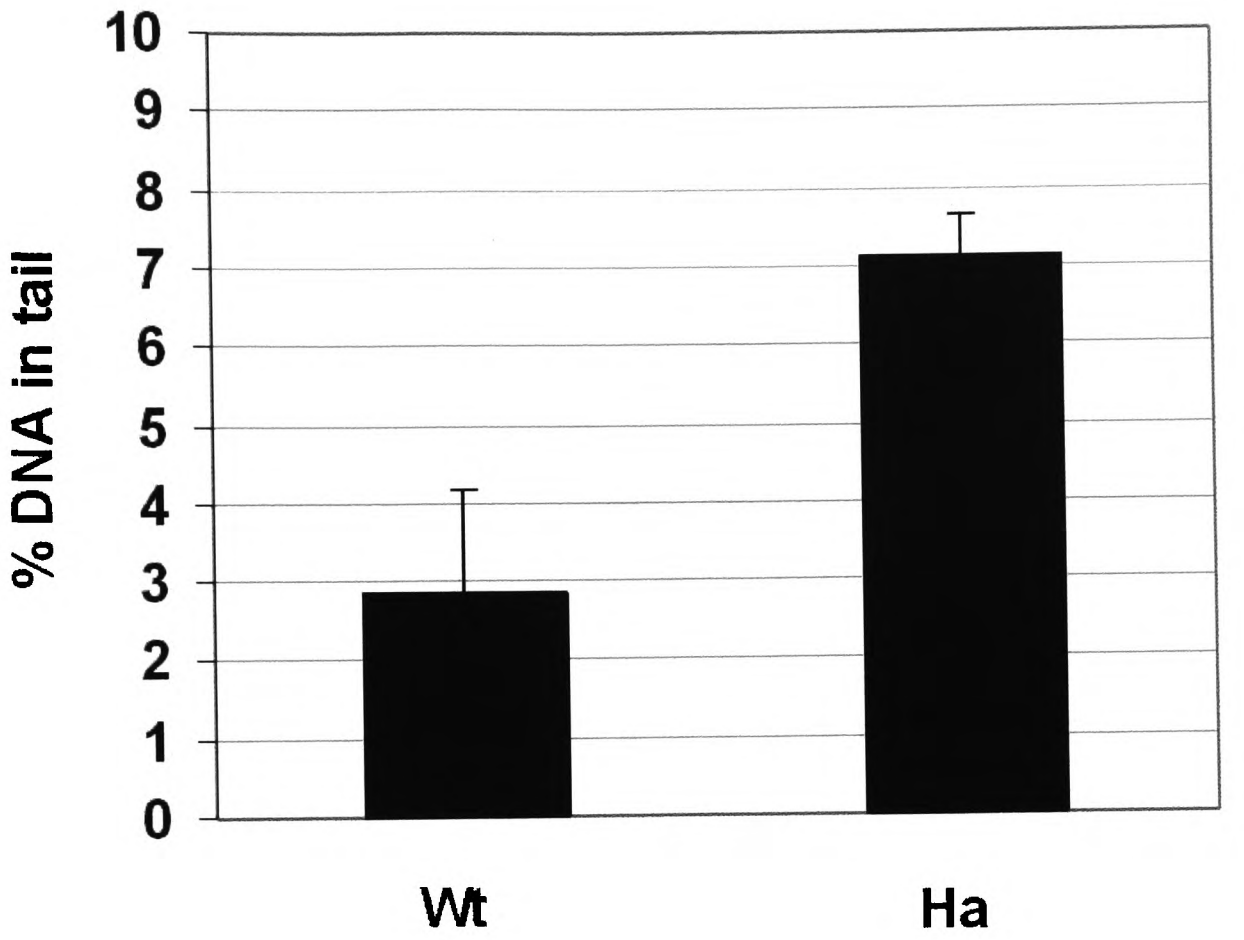

Experiment no.	% DNA in tail	
	Wt	**Ha**
1	1.9	6.8
2	3.8	7.5
Average	**2.85**	**7.15**
St. dev	1.344	0.495
Fold-	**1.0**	**2.5**

Alkaline comet assay of untreated Ha and Wt cells - showing that Ha cells have a higher basal level of DNA damage compared to Wt cells. (Data provided by Dr. I. Dianova).

i.

Wt

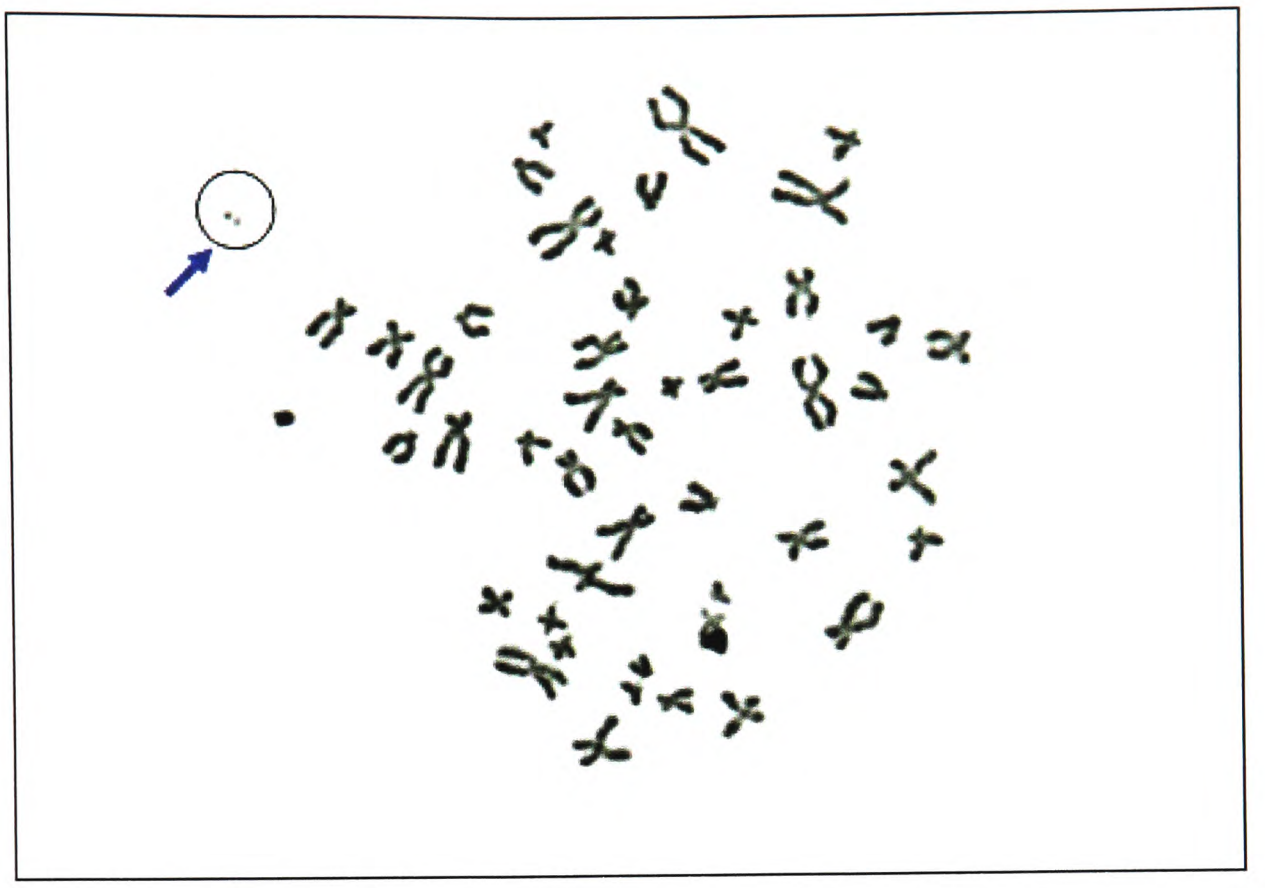

ii.

Ha

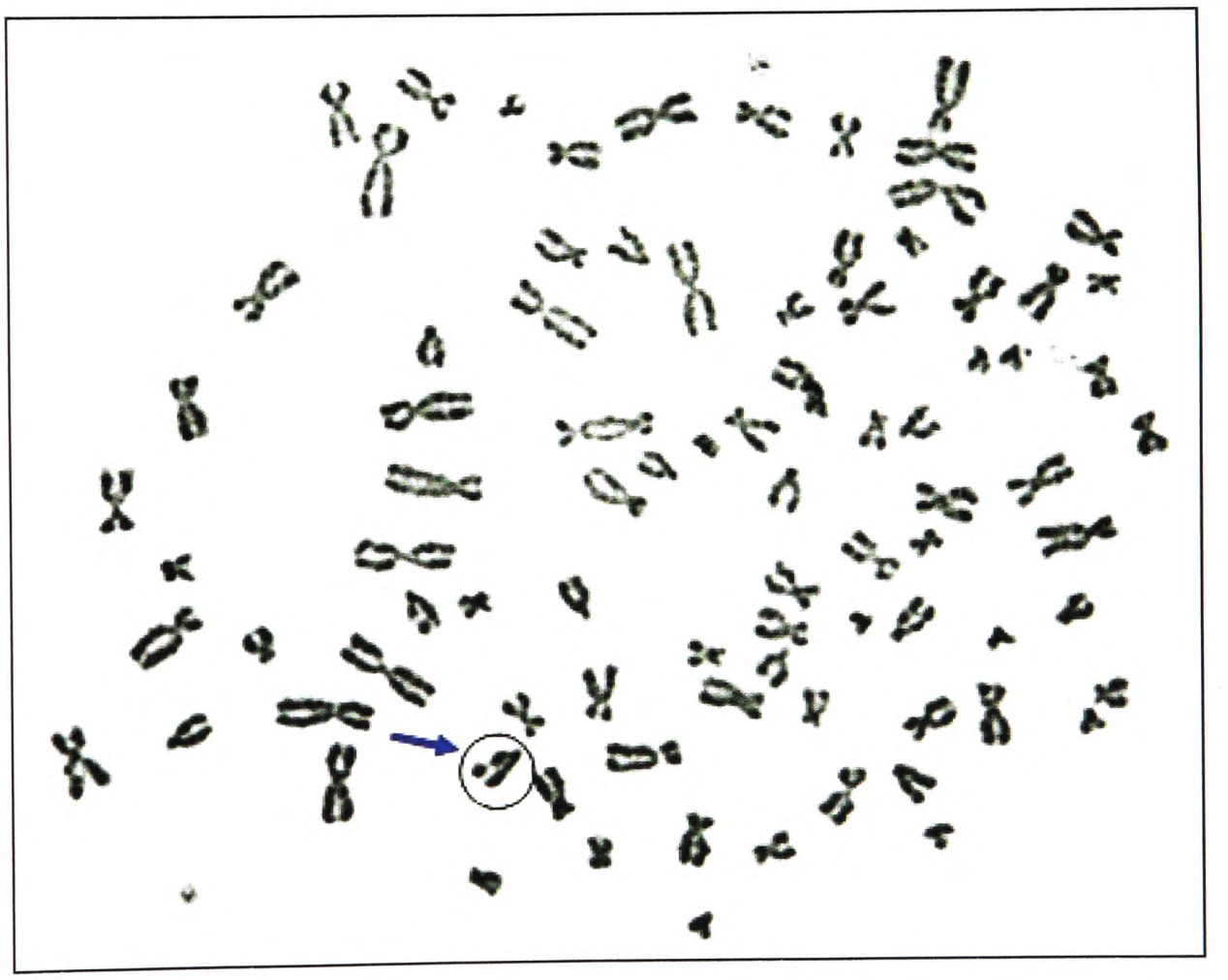

Ha cells are aneuploid. Solid metaphase staining demonstrated that Ha cells are tetraploid rather than diploid. **(i)** Wt diploid chromosome, arrow showing a double minute chromosomal break. **(ii)** Ha tetraploid chromosome, arrow showing a chromatid break.

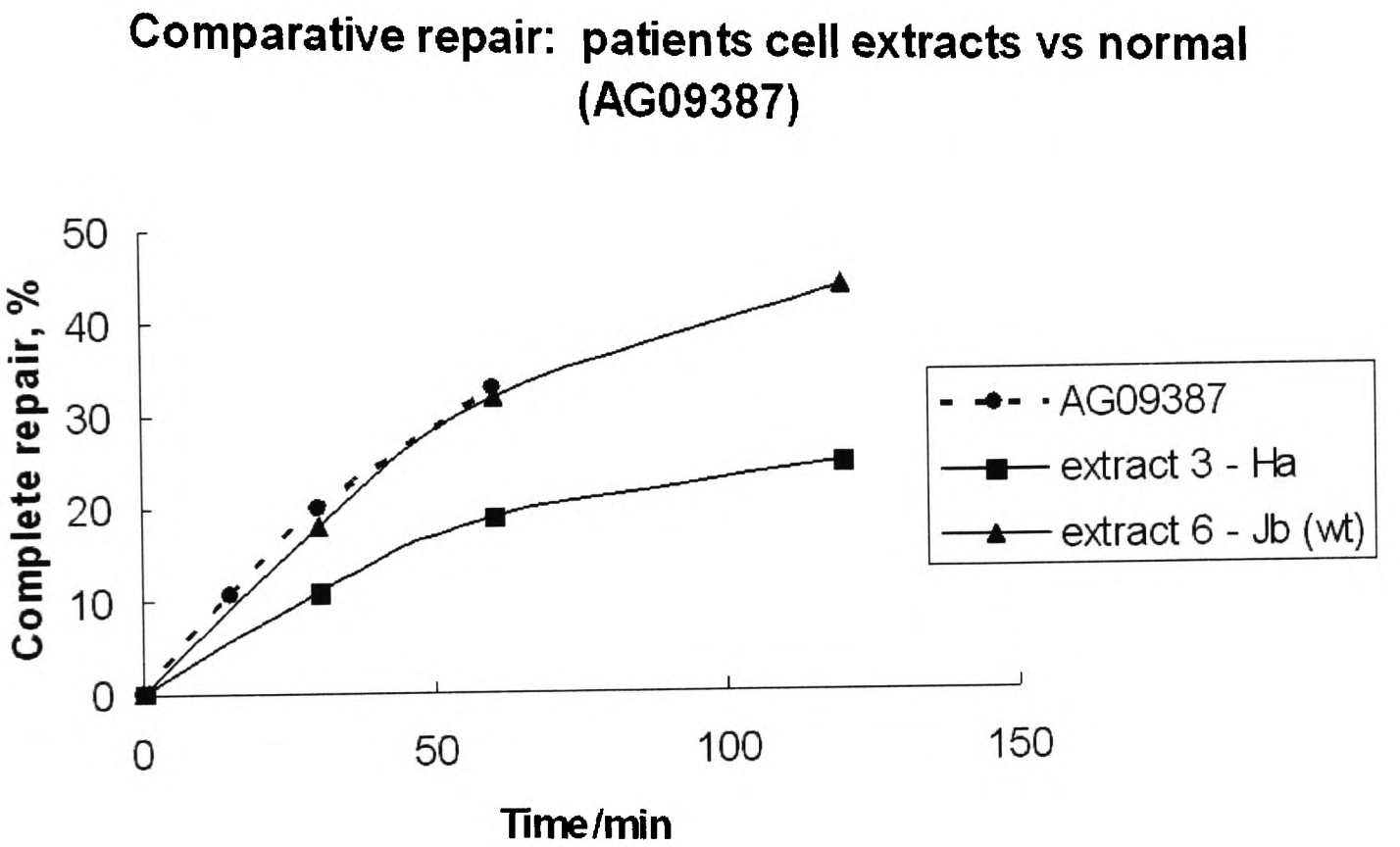

Comparative repair of an 8-oxoG lesion using human WCE. Using an *in vitro* BER repair assay [Section 2.15.1], an 8-oxoG-containing substrate was incubated with 100 μg of human WCE and dNTPs at 37°C for the indicated times. The repair profiles of patient extract 3 (Ha)(■) and extract 6 (Wt)(▲) were compared to the normal extract (AG09387)(●). Extract 6 (Wt) was shown to be comparable, whereas extract 3 (Ha) showed reduced 8-oxoG repair capacity compared to the normal AG09387 extract. Data was kindly provided by Dr. Sarah Allinson.

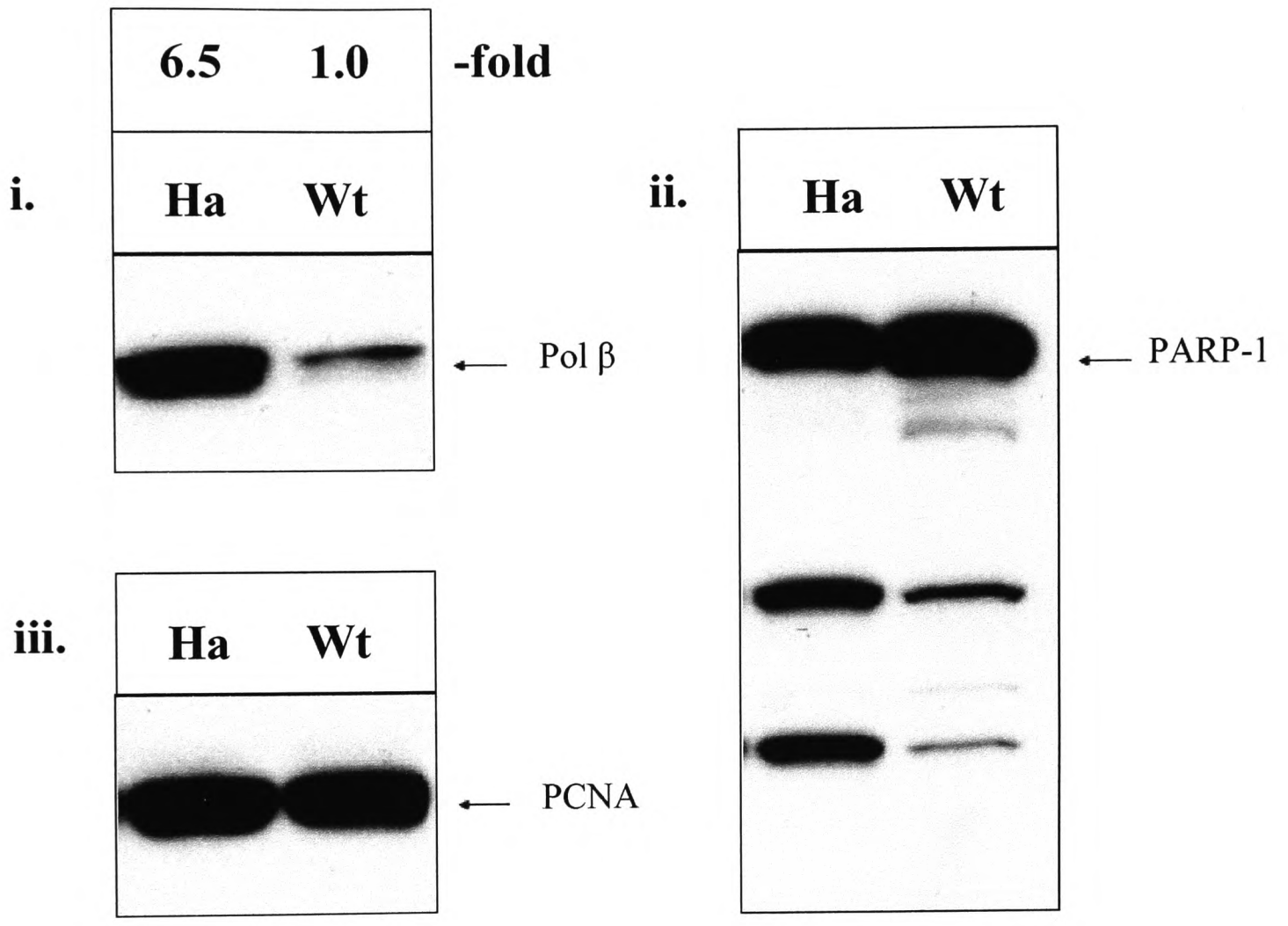

Western blot analysis of Ha and Wt WCE using ECL detection method. WCE was separated by 12% SDS-PAGE, transferred onto a PVDF membrane and immunoblotted with the indicated antibodies using the ECL™ detection method [see Section 2.8.2]. **(i)** anti-Pol β, 39 kDa band. **(ii)** anti-PARP-1 band, 113 kDa. **(iii)** anti-PCNA, 29 kDa band. (Data provided by Dr I. Dianova)

i.

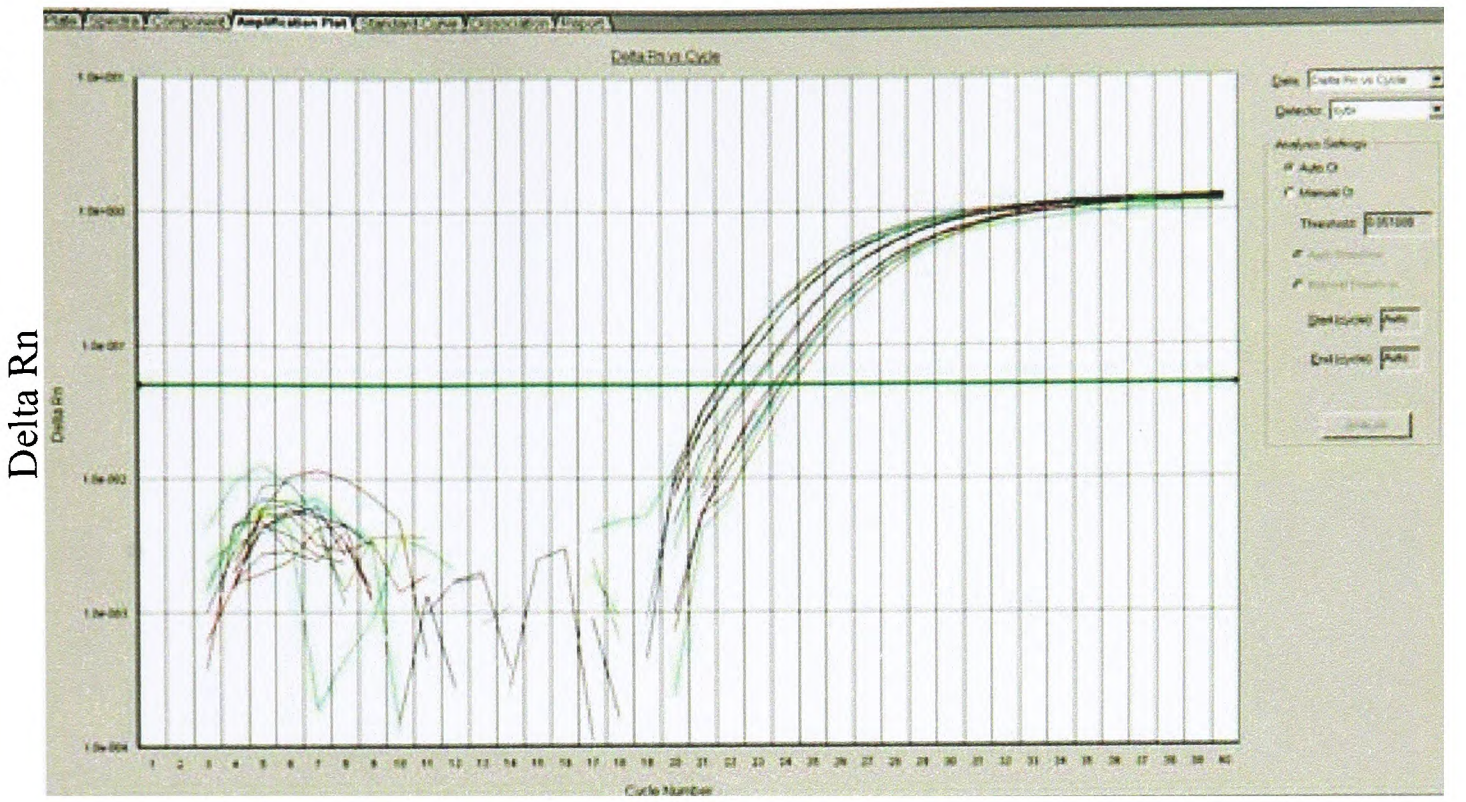

ii.

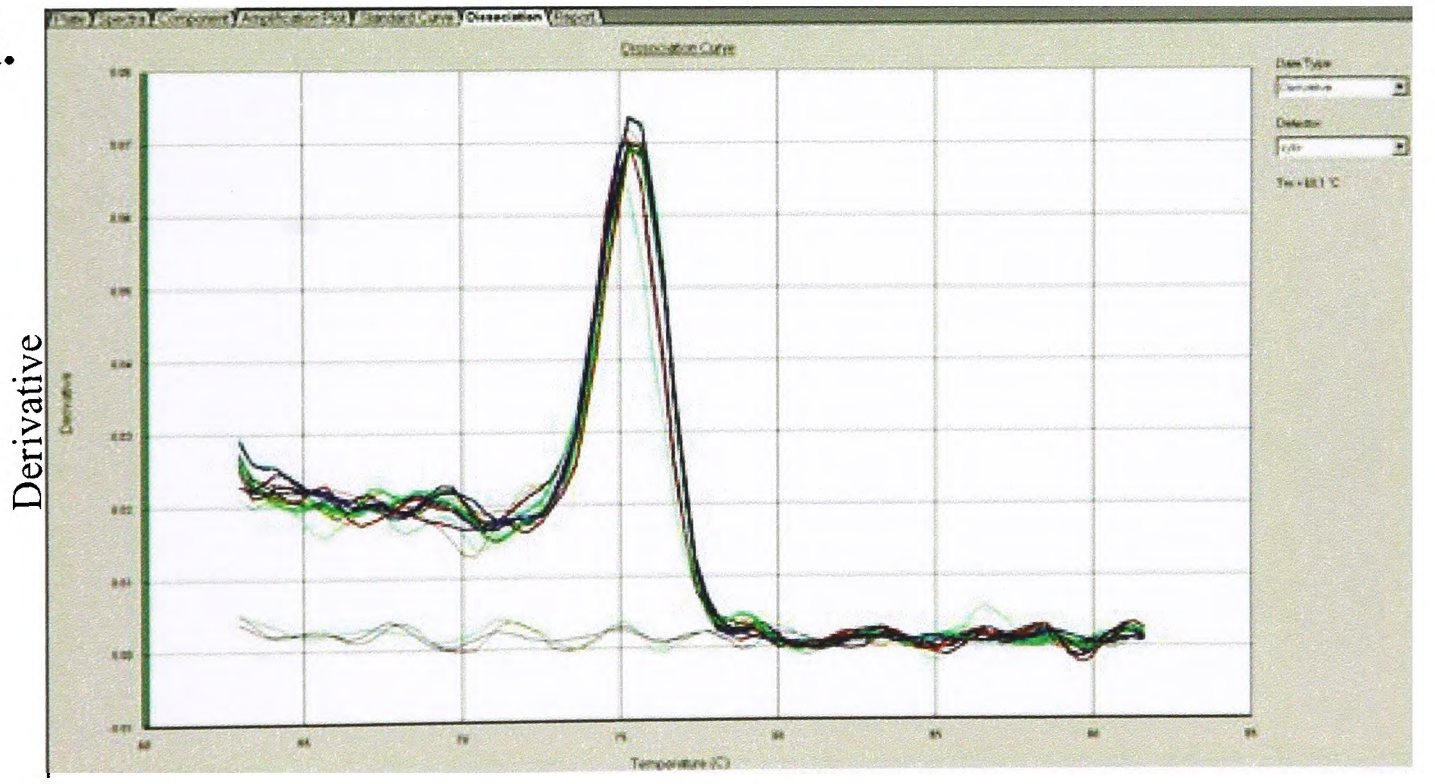

Example of raw real-time quantitative PCR data

(i) PCR amplification Curves

(ii) Melting (Dissociation) Curves